Electrochemical performance improvement and its mechanism analyses on Li-ion battery cathode $LiNi_{1/3}Co_{1/3}Mn_{1/3}O_2$ by surface coating

March 2014

Xizheng Liu

Electrochemical performance improvement and its mechanism analyses on Li-ion battery cathode $LiNi_{1/3}Co_{1/3}Mn_{1/3}O_2$ by surface coating

Graduate School of Systems and Information Engineering
University of Tsukuba

March 2014

Xizheng Liu

ABSTRACT

Layered cathode $LiNi_{1/3}Co_{1/3}Mn_{1/3}O_2$ is one of the most promising candidates to replace the commercial $LiCoO_2$ for lithium ion battery because of its low cost and moderate electrochemical performance. However, it still remains necessary for increasing of the cycle life and rate capability for its more widely feasible application. Until now, it has been reported that many ways can enhance battery performance such as dopping and surface coating. By a proper coating layer, it not only effectively stabilize of the electrode/electrolyte interface, but also improve the rate performance by facilitating the Li^+ and electron transfer between the electrode and electrolyte. However, looking for a suitable coating material to improve the cathode performance is still a formidable task for the materials scientists. In this doctor thesis, the effects of different surface coating materials on the electrochemical behaviors of $LiNi_{1/3}Co_{1/3}Mn_{1/3}O_2$ were detailed studied.

Three kinds of materials (organic conductive compound poly(3,4-dioxyethylenethiophene) PEDOT, metal oxide V_2O_5 and metal phosphates $FePO_4$) were coated on layered cathode $LiNi_{1/3}Co_{1/3}Mn_{1/3}O_2$ to investigate the coating effects. All of the three kinds of coating materials showed positive effects on battery performances. Metal oxide V_2O_5 coated $LiNi_{1/3}Co_{1/3}Mn_{1/3}O_2$ showed a moderate improved effects of cycle and rate performance which mainly originated from the enhancement of surface electronic/ionic transport. PEDOT coated $LiNi_{1/3}Co_{1/3}Mn_{1/3}O_2$ exhibited a improved rate performance, at a charge/discharge current of 1500 mA/g, the discharge capacity was improved from 44.3 to 73.9 mAh/g. Metal phosphates $FePO_4$ coated $LiNi_{1/3}Co_{1/3}Mn_{1/3}O_2$ showed the best cycle and thermal stability among the three coating materials.

$FePO_4$ coated $LiNi_{1/3}Co_{1/3}Mn_{1/3}O_2$ was chosen as the model to studied the internal mechanism of improvement by surface coating. GITT, EIS and CV on different cycled cells were conducted and diffusion coefficients after different charge-discharge cycles were calculated. The results show that Li^+ diffusion coefficients decreased upon charge-discharge cycles. It is mainly aroused by the changes of internal structures

which originated from the cation mixing between the transition metal layer and the lithium layer. Meanwhile, the coated samples showed an enhanced Li^+ diffusion coefficients at the corresponding number of charge-discharge cycles. Magnetic studies of the fresh and cycled samples confirmed the occurrence migration of Ni^{2+} to the lithium layer and there is an inhibition trend for the $FePO_4$ coated samples.

TABLE OF CONTENTS

LIST OF FIGURES

LIST OF TABLES

Chapter 1. General Introduction

1.1 Lithium ion battery

1.1.1 Brief introduction of lithium ion battery

The progress of modern civilization have encountered bottleneck because of excessive consumption of fossil energy, air pollution and global warming. One of the implemented strategies is appeal to the develop and effective use of renewable energy sources. The urgency for energy renewal requires in a larger extent applications than that of presently in force. Accordingly, the worldwide use of wind and solar power energy plants are mature technologies which draw particular attentions. The effective use of these intermittence resources highly dependent on the energy storage systems. Moreover, the rapid development of portable electronics and electric vehicles (EV), hybrid electric vehicles (HEVs) requires more excellent energy storage systems [1-3]. Recently, several progress have been made in order to improve the existed energy storage systems to meet the commercial demands. Lithium ion batteries is one of the main focus by considering its advantages in specific energy, energy density (in both cases, the larger the better), cost (the lower the better) and safety [4] as shown in Fig.1.1.

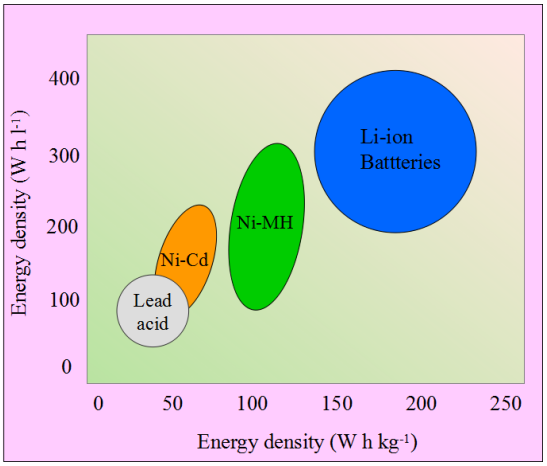

Fig. 1.1. Energy density comparison of all rechargeable storage batteries available

In the initial stage of lithium battery research, lithium metal directly used as anode

material. The lithium dendrite generated during the recharge of battery can penetrate the separator, make the short circuit and fires, leading to the withdrawal of lithium metal/MoS_2 batteries from the market in the late 1980s [5]. The concept of lithium ion batteries is combination of two Li storage compounds capable of reversible Li-ion insertion and de-insertion at different potentials to form a Li-ion transfer cell, which was first proposed in the late 1970s by Armand and co-workers. It got seriously attentions and great success until it was introduced in the market in 1991 by Sony Corporation [6]. The first commercialized lithium ion battery composed by a $LiCoO_2$ cathode and graphite as the anode. Since 1991, graphite has no challenge as the optimum anode material because of its advantages as lower work potential, higher capacity, stability and low cost. Whereas, many novel insertion materials have been investigated as cathode materials, with varied compositions as $LiMO_2$ (M= Mn, Co, Ni) or new stabilized structures as $LiMn_2O_4$ (spinel) and $LiFePO_4$ (olivine). During the recent 5 years, composite materials (1-x) Li_2MnO_3 x $Li(MnNiCo)O_2$ have been studied extensively because of its higher specific capacity above 250 mAh/g [7].

Bellcore patented the plastic lithium ion batteries used polymer electrolyte instead of the liquid electrolyte in 1994. After 3 years, the commercialization of polymer lithium-ion battery was introduced to the market and rapidly entered the cell phone and laptop computer market [8]. Lithium-sulfur and Lithium-air batteries are other two kinds of new batteries systems which are drawing extensive attentions due to its ultrahigh reversible charge/discharge capacities [9-10].

1.1.2 Composites and Working principle of lithium ion battery

The schematic illustration of lithium ion battery and working principles was shown in Fig.1.2. The inner components are composed of cathode, anode, separator and electrolyte. Electrode materials of the two Li storage compounds capable of reversible Li-ion insertion and de-insertion at different potential and that permit the Li ion shuttled between the cathode and anode during the charge/discharge process.

Cells are usually assembled with a lithiated cathode and a delithiated anode in the

discharged state. When charging the cells, lithium ions migrate from the cathode to the anode through the electrolyte, and the electrons from the cathode to the anode through the external circuit. As charging, there are increasing of cathode potential and decreasing of anode potential, leading to a higher cell voltage and storage of electrical energy. In discharge, a load is placed between the positive and negative electrodes in the external circuit and the movements of lithium ions and electrons are reversed.

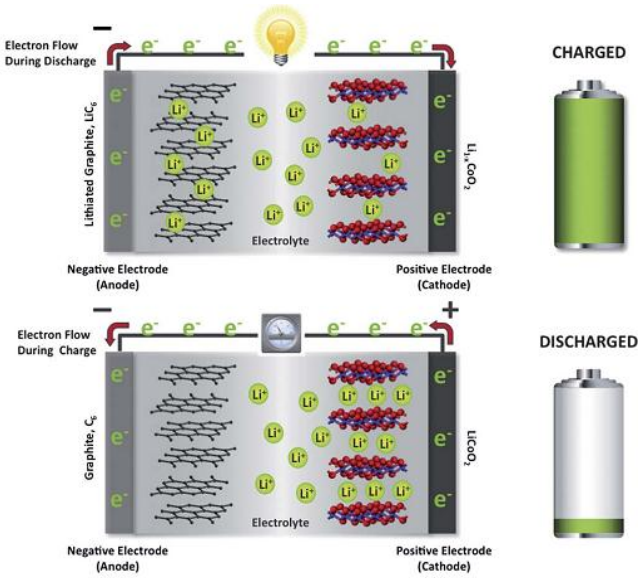

Fig. 1.2. A schematic illustration of working principles of lithium ion batteries [6].

1.2 Cathode materials for lithium ion battery

Materials with the three kinds of structures dominate the cathode market in the near future, although they are not in advance, which mainly include layered materials ($LiCoO_2$, $LiNi_xCo_yMn_zO_2$...), spinel ($LiMn_2O_4$, $LiNi_{0.5}Mn_{1.5}O_4$) and polyanionic ($LiFePO_4$) as shown in Fig.1.3 [2].

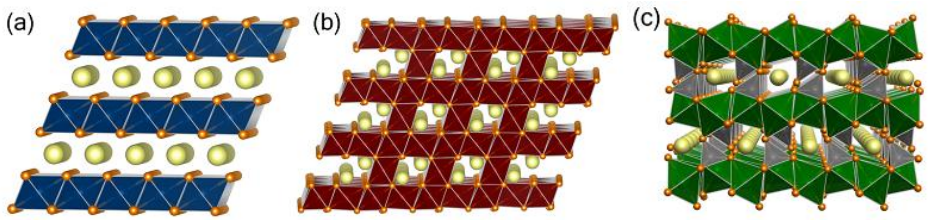

Fig. 1.3. Illustration of the crystal structures of typical cathode materials a: $LiCoO_2$, b: $LiMn_2O_4$, c: $LiFePO_4$ [2].

1.2.1 Layered $LiNi_xCo_yMn_zO_2$ and Li-excess cathode materials

In 1980s, Prof. J. B. Goodenough et al. started studying the oxide cathode material $LiCoO_2$ for lithium ion battery [11]. Layered cathode materials have the same α-$NaFeO_2$ structure as $LiCoO_2$ with a space group of *R-3m* [12]. Take $LiCoO_2$ as example as shown in Fig. 1.3a, Co locate at octahedral center in a cubic close-packed oxygen array, connect to a layer by edge-share linkers. The lithium layers lie between slabs of Co-O. The layered structure provide a 2-dimensional interstitial space which can facilitate the mobility of Li ion in the host materials.

Layered $LiNi_xCo_yMn_zO_2$ series compounds have been synthesized using relatively non-toxic and cheap resource Ni and Mn instead of Co, which is scarcity of resources and high toxicity. Ideally, all the transition metals cation Ni, Co and Mn uniformly distributed in the transition metal layers and lithium ion located in the lithium layers.

$LiNi_{1/3}Co_{1/3}Mn_{1/3}O_2$ draw many attentions in layered $LiNiCoMnO_2$ compounds. The valence states are Ni^{2+}, Co^{3+} and Mn^{4+}, respectively. During charge/discharge process, the mainly electrochemical redox reactions is Ni^{2+}/Ni^{4+} along with the desertion/insertion of Li ions. In this case, the average oxidation state of Mn is tetravalent so that the electrochemical inactive Mn^{4+} provides significant structural stability during electrochemical cycling, even at a high cutoff voltage of 4.6 V. The Mn^{4+} can stabilize the whole structure and show no redox activities during charge/discharge process. It is inevitable that there is a Li/Ni disorder during the synthesis which can damage the battery performance [2]. The introduce of Co^{3+} can obviously decrease the Li/Ni disorder and improve the rate capability [13]. This material deliver a discharge capacity of 150 mAh/g at a cutoff voltage of 2.5-4.2 V which is comparable with $LiCoO_2$ but cheap and safe than $LiCoO_2$.

A Li_2MnO_3-stabilized $LiMO_2$ (M= Mn, Ni, Co) electrodes for lithium ion batteries with a high capacity (>200 mAh/g) have been designed and investigated in last several years [7]. Their capacity outperform that of conventional layered $LiCoO_2$, spinel $LiMn_2O_4$ and olivine $LiFePO_4$. It is comprised of two layered components Li_2MnO_3 and $LiMO_2$ (M= Mn, Ni, Co) which the Li_2MnO_3 composite can be

considered as $Li(Li_{1/3}Mn_{2/3})O_2$ and the excess Li located in the Mn layer. Although the Li_2MnO_3 itself showed no electrochemical activity because of Mn^{4+} in this compound can not oxide to a higher valence state. However, in composite Li_2MnO_3-$LiMO_2$, the Li_2MnO_3 component can be activated by extracting Li_2O in a controlled manner, either chemically of electrochemically, to form a MnO_2 component as a electrochemical active part and present reversible charge/discharge capacities in the following cycles. The initial Li_2MnO_3 component activation, which is a dynamics determined process, is very important for the capacities of the initial cycles. The lower rate and voltage fading with prolonged cycles is obstacle for the commercialization of this kind of materials.

1.2.2 Spinel $LiMn_2O_4$ and its derivative

M. M. Thackeray et al. first investigated the Li ion reversible insertion/deinsertion in manganese spinels [14]. The structure of spinel framework $LiMn_2O_4$ is shown in Fig.1.3b. The MnO_6 octahedra are edge-sharing and connect to a 3-dimensional channel for lithium diffusion. Spinel structures with cubic symmetry show a higher Li ion conductivity than other intercalation materials because of the isotropically multidirectional Li ion diffusion. It delivers a capacity of 110 mAh/g with a average voltage about 4 V. This material attracted wide attentions because of its abound resource of manganese. The disproportionation reaction and Jahn-Teller effects of Mn^{3+} lead to a dissolution of Mn^{2+} from the electrode material, especially at elevated temperature, which prohibited its more extensive practical applications.

Part of the manganese ios can be substituted by other metal ions, and showed a modified electronic properties but a maintained spinel structure [15]. In the divalent or trivalent metal cations replaced samples, there is an increase of average Mn ion valency which not only suppresses Jahn-Teller distortions and phase transitions, but also may decrease Mn dissolution. A typical example for substituted spinel materials is $LiNi_{0.5}Mn_{1.5}O_4$ which is a true high-voltage cathode material. It is composed by divalent Ni^{2+} and tetravalent Mn^{4+}. Only Ni^{2+} showed electrochemical activities at a

high voltage of 4.8 V and Mn^{4+} appeared as stabilizing the whole spinel structure. It is now commonly accepted that $LiNi_{0.5}Mn_{1.5}O_4$ is a more promising candidate for commercial high voltage cathode material.

1.2.3 Polyanionic materials

Different from the above simple oxides, polyanionic material which build on transition metals and polyanions $(XO_4)^{n-}$, have attracted extensive attentions in the last 15 years since the discovery of electrochemical active $LiFePO_4$ by J. B. Goodenough and co-workers [16]. $LiFePO_4$ showed a well-reversible Li ions insertion/deinsertion reactions at about 3.5 V (vs. Li/Li^+) and a typical two-phase reactions. The following work by Armand found that carbon coating of $LiFePO_4$ provides a safe cathode of good rate capability despite only 1 D channels for Li ion cpnduction and a poor electronic conductivity of the oxide. The structure of $LiFePO_4$ as shown in Fig.1.3c, the LiO_6 octahedra are edge-shared parallel to b-axis and formed a Li tunnel in this orientation. The FeO_6 octahedra and PO_4 tetrahedral built on distorted oxygen hexagonal formed the typical olivine structure. Although this structure type had been first investigated as magnetic studies, it is now a popular cathode materials which showed better reversible charge/discharge properties [17]. Also many other polyanionic materials, with a heter-atom center XO_4 (X=P, S, Si, Mo, W), have been heavily investigated by many groups worldwide. The particularly stable open 3D framework guaranteed the long-term cycling and fast ion motion.

1.3 Modification of $LiNi_{1/3}Co_{1/3}Mn_{1/3}O_2$ for lithium ion battery

Cathode materials with any of the three main structures witnessed a great progress in the last several years. Table 1.1 summarized the main features of the typical cathode materials currently still active in the market. All of the listed materials have made great success in portable electronic, however, further improvement should be made in consideration of its applications as storing wind and solar energy in smart grids and Electric Vehicles (EV). Besides the design and synthesis of materials with

new structures as cathode materials, ion doping and surface coating are two main facile but feasible strategies to improve the electrochemical performance of existed typical materials. In this study, $LiNi_{1/3}Co_{1/3}Mn_{1/3}O_2$, as one of the most promising cathode materials for their advantages in electrochemical performance and cost, was take as the object of study. Herein, the research progress of ion doping and surface coating for cathode materials have been summarized.

Table 1.1. Advantages and Disadvantages of the three mainstreaming cathode materials

Electrode materials	Voltage (V)	Capacity (mAh/g)	Specific energy (mWh/g)	Advantages	Disadvantages
Layered $LiCoO_2$ (2d structure)	～4	140	560	High electronic and Li ion conductivity; revolutionized the portable electronics market	Expensive and toxic Co, safety concerns, only 50% of the theoretical capacity can be utilized
Spinel $LiMn_2O_4$ (3d structure)	～4	120	480	Environmentally benign and cheap Mn, high electronic and Li ion conductivity, excellent rate capability and safety	Dissolution of Mn^{2+} and Jahn-Teller effects of Mn^{3+}; severe capacity fade at elevated temperature (55 ℃)
Olivine $LiFePO_4$ (1d tunnel)	～3.5	160	560	Environmentally benign and cheap Fe, covalently bonded PO4 groups lead to excellent safety	Low electronic and Li ion conductivity, Carbon coating is indispensable and low tap density
Layered $LiNi_{1/3}Co_{1/3}Mn_{1/3}O_2$	～4	>150	>600	Low cost than $LiCoO_2$ but comparable electrochemical performance	Capacity fading and voltage decay upon cycling

1.3.1 Dopping for layered cathode materials $LiNi_{1/3}Co_{1/3}Mn_{1/3}O_2$

Cationic or ionic doping have been proved to be an effective way in modifying the electronic structure, enhancing the stability of structure and improving the electrochemical performance of cathode materials [18]. Normally, ion doping include non-transition metal cation doping, transition metal doping, and anion doping. Ceder's group in MIT and other researchers in the world have reported the theoretical calculation results that the rational doping can modify the electronic structure and change the lithium diffusion barriers [19-20].

By doping non-transition metals into the layered structure, structure integrity, electronic conductivity and safety of the electrode are greatly enhanced. However, the Li diffusion was deteriorated by doping with non-transition metal ions. Compared the Al or Mg doped samples and bare $LiCoO_2$, Al doped system showed a activation barrier 100 meV higher, and for Mg-doped samples of 30 meV higher than that of the bare $LiCoO_2$ [19]. For transition metal ion doping, the early transition metals tend to induce less electron density around oxygen than the late transition metals leaving the oxygen ions with less screening power. This phenomena lead to a relatively low activation barriers for Li migration of the late transition metals doped samples. Anion doping for oxygen in cathode materials, it can effectively reducing the impedance and lattice changes during cycling [21].

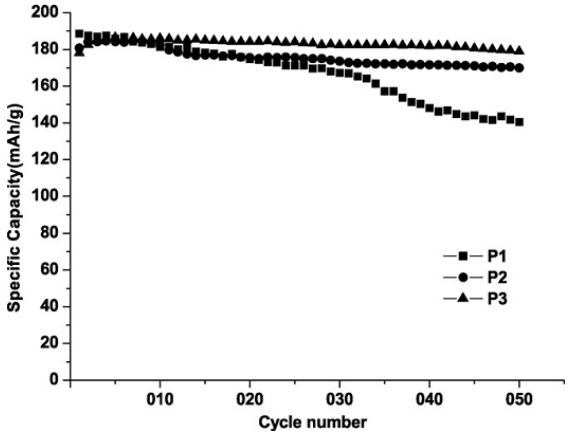

Fig. 1.4. Cyclic performances of P1: $Li(Ni_{1/3}Co_{1/3}Mn_{1/3})O_2$, P2: $Li(Ni_{1/3}Co_{1/3}Mn_{1/3})O_{1.98}F_{0.02}$, P3: $Li(Ni_{1/3}Co_{1/3}Mn_{1/3})O_{1.96}F_{0.04}$ in the voltage range of 2.8-4.6 V [24].

Many research group gave their contributions on optimization and synthesis of doped $LiNi_{1/3}Co_{1/3}Mn_{1/3}O_2$ by using different doping ions. D. Liu et al. reported the comparison of two typical elements, Fe^{3+} and Al^{3+} (Fe^{3+} doping lowers the delithiation voltage while the Al^{3+} doping raises the delithiation voltage), on the electrochemical performances and structure of $LiNi_{1/3}Co_{1/3}Mn_{1/3}O_2$ [18]. Both of the Al and Fe doped samples show similar discharge capacities and rather good reversibility. For the Al doped samples, only the samples with low-dose doping show a improved electrochemical performance, high-dose doping sample (x>1/6) show poor capacity retention.

Zr-doped $LiNi_{1/3}Co_{1/3}Mn_{1/3}O_2$ have been synthesized by a thermal polymerization method [22]. The Zr doping results in higher lithium diffusion coefficient and more stable resistance during the electrochemical cycling so that the Zr doped samples show notable improvement of cycling performance and rate capability. Sun et al. synthesized the Mg, Cr and Al doped sample and got a good doping effects by Cr. The capacity retention of $Li(Ni_{1/3}Co_{1/3-0.05}Mn_{1/3}Cr_{0.05})O_2$ is 97% after 50 cycles [23].

Anion F^- doped uniform and spherical $Li(Ni_{1/3}Co_{1/3}Mn_{1/3})O_{(2-\delta)}F_\delta$ powders were synthesized via NH_3 and F^- coordination hydroxide co-precipitation. The F doped samples exhibited a improved layered characteristics of the lattice and the cyclic performance. As shown in Fig. 1-4, the doped samples showed almost no capacity fading even after 50 cycles [24]. Anion-cation doubly doped $Li(Ni_{1/3}Co_{1/3}Mn_{1/3})_{0.96}Si_{0.04}O_{1.96}F_{0.04}$ have been synthesized by using co-precipitated method in oxygen atmosphere. The doubly substituted exhibits a large capacity, enhanced electrochemical performance, and good stability in the delithiated state.

1.3.2 Surface coating techniques

More recently, researchers have considered the surface properties of electrodes as critical factors for optimizing electrochemical performance of lithium ion batteries. In particular, the electrolyte decomposition on the electrode surface, the side-reactions at the interface of electrode and electrolyte, the charge transfer between the electrolyte

and electrode can all profoundly influence the electrochemical performance and safety of batteries. With the progress of knowledge of electrode materials, it has been found that surface coating on cathode by an appropriate coating layer material is a facile but feasible way to improve the electrochemical performance. Fig.1.5 illustrate the schematic of surface coating. A proper coating layer can prevent the electrode directly contact with the electrolyte, and thus suppress the side-reactions at the interface of electrolyte/electrode which lead to the deterioration of the cell properties. Meanwhile, a coating material, with high ionic/electronic conductivity, can improve the rate capacity by decreasing the charge barriers of the electrode surface. In addition, a passivated coating layer can stabilize the electrode surface and decrease the surface reaction activity, which enhance the thermal stability and safety.

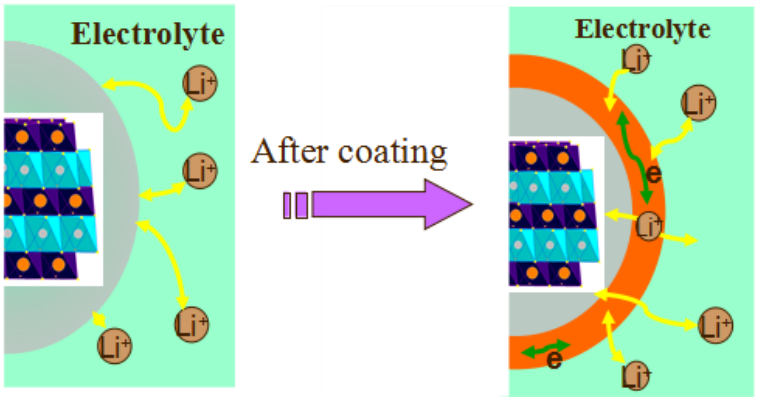

Fig. 1.5. Schematic of surface coating

Many scientists in the world express their great enthusiasm in improving the electrochemical performance of cathode by surface coating. The techniques applied to surface coating are mainly include: normally surface coating, core-shell structure material synthesis and ultrathin film coating [50]. Different surface morphologies can be obtained with different techniques as shown in Fig.1.6.

Rough coating Core-shell ultra thin film coating

Fig. 1.6. Schematic of three types of surface coating with different techniques.

Most of the normally surface coating are conducted in wet-process, mixing of the cathode materials with coating layer materials and followed by a heat treatment. The coated samples usually show a rough surface, some areas are heavily coated and other areas are only barely coated. However, the advantages of this technique ensure its long enduring vitality, such as, it is easy to operation and convenient to design, get rid of complicated equipment and reducing production costs, easy to realize industrialization production.

Synthesis of core-shell materials were first reported by Amine and Sun et al [51]. The core-shell structure materials were usually composed by a core material with high voltage, high capacity but high reactivity toward electrolyte and, a shell material with low reactivity toward electrolyte. By regulating the ratio of core to shell, a core-shell material with concentration gradient can be successfully synthesized and excellent electrochemical performance have been obtained. The precisely controlling of the synthesis process is vital for the obtaining of core-shell materials.

Ultra-thin film coating techniques are usually conducted by atomic layer deposition (ALD). It is a mature technique which has been widely used in semiconductor industry. It can accurately control the thickness of coating layer at a nano meter scale by controlling the deposition time [52]. Dramatic electrochemical performance improvement can be obtained by a fully thin film protection for cathode materials with high power and long life.

1.3.3 Surface coating for layered cathode materials $LiNi_{1/3}Co_{1/3}Mn_{1/3}O_2$

Improve the electrochemical performance of $LiNi_{1/3}Co_{1/3}Mn_{1/3}O_2$ have initiated extensive enthusiasm during the last decade because it is one of the most promising cathode materials for widespread commercial applications. Tremendous efforts have focused on the surface coating techniques with different coating materials and different experiment process. Some of the research progress about surface coating of $LiNi_{1/3}Co_{1/3}Mn_{1/3}O_2$ have been summarized in Table 1.2.

Table 1.2. Different coating layer on $LiNi_{1/3}Co_{1/3}Mn_{1/3}O_2$ with their synthetic details and resulting features

Coating layer	Synthesis procedure	Optimized coating amount	Improvement	Interpretation	ref.
Al_2O_3	Atomic layer deposition	4 layers coating	65%-91% at 100^{th} cycles (4.5V, 0.2C)	This layer decrease the surface resistance	25
Al_2O_3	Co-precipitation on cathode surface before and after lithiation	1 wt.%	78.8%-93% at 100 cycles (4.5V, 0.5C)	Improve the Li diffusion coefficient and decrease the activation energy of charge transfer	26
$LiAlO_2$	Decomposed from $C_9H_{21}O_3Al$ and mixed with LiOH calcined at 600 ℃ (sol-gel)	3 wt.%	Capacity retention of 96.7% at the 50^{th} cycle 1C rate 2.5-4.5 V	The formation of Li-Al-O solid solution and higher ionic conductivity	27
AlF_3	Pristine were immersed into $Al(NO_3)_3$ and NH_4F was added. calcined at 400 ℃ for 5 h	2 mol%	Capacity retention of 92-93% at the 50^{th} cycle (4.5V, 0.5C)	Stable charge transfer resistance regardless of the cycle number	28
$(B,Al)_2O_3$	Aluminum isopropoxide and boron trifluoridediethylet herate in ethanol, mixed with pristine, calcined at 700 ℃ for 10h (sol-gel)	Very thick coating layer	Capacity retention of 93% at the 40^{th} cycle (3.0-4.5V, 1C)	Improvement in the charge transfer kinetics and the stability in electrolyte	29
$AlPO_4$	$Al(NO_3)_3$ and $(NH_4)_2HPO_4$ were added into H_2O, stirred until a white suspension was formed and pristine was added. Calcined at 400 ℃ or 700 ℃ for 5 h.	1 wt.%	Nearly 90% capacity retention at the 50^{th} cycles (2.7-4.2V, 0.5C)	The high surface content of aluminum is in favor of forming a stable solid electrolyte film	30

ZrO_2	Mixed pristine and $Zr(OC_3H_7)_4$ in 1-propanol. Sintered at 450 ℃ for 6h	10-25nm coating layer	161 mAh/g at the 40^{th} cycle (4.5V, 0.1C)	Stable cell resistance regardless of cycle number, decrease of electrolyte decomposition reactions	31
ZrO_2 /$LiZrO_3$	Coating ZrO_2 on the pristine before lithiation, calcined at 900 ℃ for 24 h.	1% in (Zr/Ni+Co +Mn)	About 99% capacity retention at the 100^{th} cycle (4.5V, 0.5C)	The incorporation of Zr in the crystal lattice modified the rate capability by increasing the lattice parameters.	32
ZrF_x	Mixed $Zr(CH_3CO_2)_2(OH)_2$ and NH_4F in water, then added pristine, processed in hydrothermal process 120 ℃ for 15 h , finally calcined at 400 ℃ for 5 h.	0.5 wt.%	From 86.4% to 90.5% at the 100^{th} cycle. (60 ℃, 3.0-4.3V, 1C)	Coating layer protected the vulnerable surface, enhance the thermal stability, effectively suppress reactions between electrode and electrolyte in the fully charged state.	33
CaF_2	$Ca(NO_3)_2$ and NH4F dissolved in water, pristine was added, calcined at 500 ℃ for 2 h.	4-8 nm coating layer (1%)	Capacity retention of 98.1% at the 50^{th} cycle (4.5V, 0.1C) Over 85% at 5C	Stabilize the surface structure and reduce the charge transfer resistance	34
CaF_2	Wet coating process, similar to ref.34, calcined at 650 ℃ for 6 h	1 wt.%	Capacity retention from 67.9% to 93.5% at the 65^{th} cycle(2.5-4.6V, 0.15C)	Coating layer benefit the cycle performance	35
SrF_2	Wet coating process in $Sr(NO_3)_2$ and NH_4F solution, calcined at 400 ℃ for 5 h in N_2	2.0 mol%	Capacity retention of 86.9% at the 50^{th} cycle (2.5-4.6V)	The coating leads to the slight decrease of both initial capacity and rate capability but it improves the cycling performance by suppress the increase of total resistance.	36

TiO_2	Dispersed pristine in ethanol, then added $C_{16}H_{36}O_4Ti$, calcined at 500 ℃ for 6 h.	1 wt.% coated sample	Good rate capacities. More than 99.0% retention at the 12^{th} cycle at 3.0V (2.8-4.5V)	The coated TiO_2 layer stabilized the layered structure by suppressing the dissolution of metal ions, increase the diffusion coefficient of Li ions.	37
$Li_4Ti_5O_{12}$	Mixed lithium ethoxide and tera-iso-propoxy titanium in ethanol, sprayed on the pristine powder. calcined at 700 ℃ for 0.5 h	0.3 mol.% coated sample	91% retention at the 100^{th} cycle 80 ℃. (full cell vs. SiO)	The LTO coating layer prevented the oxidative dissolution of the electrolyte on the surface of electrode.	38
Ag	Mixed $AgNO_3$ and pristine in solution, calcined at 500 ℃ for 1 h	9:1 $AgNO_3$ /pristine	Capacity retention of 94.7% at the 50^{th} cycle. (2.8-4.4V, 20 mA/g)	Enhanced the surface electrical conductivity, lower the cell polarization and reduce the resistance.	39
Y_2O_3	Wet-coating process, $Y(NO_3)_3$ in water, calcined at 650 ℃ for 5.5 h	1 wt.% coated sample	Capacity retention from 97.2% to 99.7% at the 20^{th} cycle. (2.8-4.5V, 2.0mA cm^{-2})	The coating layer could protect the electrode from being corroded by the electrolyte and benefit to decrease the resistance at delithiated state.	40
CeO_2	Wet-coating process, $Ce(NO_3)_3$ in water, calcined at 700 ℃ for 5 h	1 wt.% coated sample	Capacity retention from 86.6% to 93.2% at the 12^{th} cycle. (2.8-4.5V, 3C)	The coating layer protected the surface of cathode material from harmful reaction with the electrolyte	41
ZnO	$Zn(CH_3COO)_2$ dissolved in water, added pristine, calcined at 500 ℃ for 3 h	Several to 20 nm	Capacity retention from 91.6% to 99.9% at the 20^{th} cycle. (2.5-4.3V, 70mA/g)	Surface coating increase the initial resistance but provide a stable interface of electrode/electrolyte.	42

LiF	Dispersed the pristine in $LiNO_3$ solution, added NH_4F, calcined at 500 ℃ for 2 h		Capacity retention of 97.5% at 0.1C at room temperature and 93.5% at 1C at 60 ℃	Reduce the dissolution of metal ions and enhance the conductivity of the oxide surface. Part of F^- doped in the surface lattice.	43
Carbon	Carbon coating was conducted in an inverse microemulsion medium in the presence of glucose, finally calcined at 900 ℃ in air for 6 h .	0.9 g pristine raw materials with 0.3 g glucose	A capacity retention of 83.3% at the 20^{th} cycle (2.5-4.4V, C/7)	Increase of the grain connectivity and protected the metal oxide from chemical reaction.	44
Carbon	Decompose of gel-like PVA at 400 ℃ for 30 min.	1.0 wt.% coated	Capacity retention of 96.3% at the 40^{th} cycle (2.8-4.4V, C/8)	Decrease the charge transfer resistance.	45
Graphene	Microemulsion and ball milling techniques.	With 10 wt.% in the composite.	Obviously improved the high rate capacity.	Increase the grain connectivity and high electronic conductivity.	46
Polypyrrole PPy	In-situ chemical oxidation polymerization method. Only dried at 70 ℃ for 24 h.	2 wt.% coated sample	Higher discharge capacity of 149 mAh/g (120 mAh/g bare) at the 50^{th} cycle (2.8-4.6V, 0.1C)	The PPy coating significantly decrease the charge-transfer resistance.	47
Polyimide (PI)	Pristine powder were added to the PI coating solution, a programme heat treating to 400 ℃ in N_2.	About 10 nm coating layer.	Capacity retention were 58% vs. 71% (4.6V, 1C) and 52% vs. 66% (4.8V, 1C).	The coating layer severed as an anomalous ion-conductive protection skin suppressing the undesired side reactions on the delithiated electrode surface.	48

PTAEP	Direct UV-assisted conformal coating of PTAEP gel polymer electrolyte on pristine surface.	About 20 nm coating layer.	Capacity retention from 73% to 84% at the 50^{th} cycle (2.8-4.6V, 1C).	The PTAEP coating layer effectively mitigates undesired interfacial side reactions and suppressed the exothermic reaction.	49

1.4 Target and outline of this dissertation

1.4.1 Motivation of this research

Research and development of lithium ion batteries with higher capacities, longer cycle life and low cost is an achievable way to realize the low carbon society and solve the problems about energy crisis and environmental pollutions. One of the determinants is the cathode materials because it makes up about 15% of the total battery cost. $LiNi_{1/3}Co_{1/3}Mn_{1/3}O_2$ is a promising material for replacing the $LiCoO_2$ in the cathode market for its integrating of advantages in electrochemical performance and cost. However, the gradually capacity fading with prolonged cycles, limited rate performance and safety still remains to improve.

The inadequate electrochemical performance of $LiNi_{1/3}Co_{1/3}Mn_{1/3}O_2$ can be ascribed to the following possible factors: first, side-reactions between the electrode and electrolyte which consume some of the Li^+ ion and lead to a decrease of efficiency; second, the accumulation of by-products on the electrode surface which will lead to an increase of cell polarization and resistance; third, the inevitable Li/Ni disorder; fourth, the inadequate electronic and ionic transfer ability which lead to a limited rate capability. To solve these problems, besides the optimization of the synthesis conditions, many researchers have put forward some methods to overcome the drawbacks by surface coating with lower reactivity toward electrolyte to enhance the electrochemical performance.

By summarizing the surface coating of $LiNi_{1/3}Co_{1/3}Mn_{1/3}O_2$, the coating layer are mainly include metal oxide, metal fluoride, conductive polymer and also some other

materials. Much of the studied materials are electrochemical inactive. For the metal contained coating layer, there is a common feature is that the metal center has only one stable valence state at normal conditions for battery operations. One of the fatal flaws for these materials is that they are generally inactive to lithium ion and have low lithium ion conductivity. Thus, excess coating of such materials is at the expense of capacities and efficiency. The reported carbon coated samples is different from the carbon coating layer in C-coated $LiFePO_4$. Because the high temperature inert gas atmosphere lead to much oxygen-deficient sites and damaged electrochemical performance. Thus, the most acceptable carbon coating is not the most optimal choice as coating layer for $LiNi_{1/3}Co_{1/3}Mn_{1/3}O_2$. It is highly urgent to explore new materials as coating layer to improve the electrochemical performance of $LiNi_{1/3}Co_{1/3}Mn_{1/3}O_2$, with which have certain Li^+ ion conductivity, both chemical stability and thermal stability, and also low cost and be possible to realize industry production. Thus, we chose improve the electrochemical performance of $LiNi_{1/3}Co_{1/3}Mn_{1/3}O_2$ by surface coating technique as my doctor research topic, explored different coating material, especially the material which can be inserted by Li^+ ions. I also try to give a detailed analysis about the mechanism of improved electrochemical performance by surface coating.

1.4.2 Targets of this research

The targets of this study on surface coating of $LiNi_{1/3}Co_{1/3}Mn_{1/3}O_2$ are as follows:

- To enhance the electrochemical performance of $LiNi_{1/3}Co_{1/3}Mn_{1/3}O_2$ by different surface coating materials
- To study the effects of coating amount and heat treated temperature on electrochemical performance, acquire the optimized coating conditions and coating layer material
- To investigate the different coating effects in different coating materials and mechanism analyses
- Detailed study the performance degradation mechanism of pristine and coated

$LiNi_{1/3}Co_{1/3}Mn_{1/3}O_2$ by different techniques and, get the finial conclusions which can give help to the future designing of superior coating layers for layer cathode materials

1.4.3 Outline of this thesis

There are six chapters in this dissertation.

Chapter 1 is a comprehensive review of lithium ion battery. It mainly include a a brief introduction about lithium ion batteries, cathode materials and surface modification about cathode materials. The research motivation and targets have also been introduced.

In chapter 2, electronic and ionic double conductive materials V_2O_5 coated $LiNi_{1/3}Co_{1/3}Mn_{1/3}O_2$ have been synthesized and characterized by a variety of techniques. Cycle and rate performance were tested to study the V_2O_5 coating effects. EIS and CV measurements were carried out to understand the difference of battery polarization and resistance by V_2O_5 coating.

In chapter 3, mechanical flexibility of organic conductive polymer PEDOT was used to modify the surface of $LiNi_{1/3}Co_{1/3}Mn_{1/3}O_2$. Similar techniques were applied to study the electrochemical performance. The mechanism of improved rate performance was detailed investigated by GITT and CV.

In chapter 4, thermal and chemical stable $FePO_4$ coated $LiNi_{1/3}Co_{1/3}Mn_{1/3}O_2$ was synthesized by a simple method. Coating conditions have been carefully studied. The capacity fading and voltage decay of pristine and coated samples have been examined and its mechanism have been primitively studied.

Chapter 5 focuses on the detailed study of performance degradation mechanism of $LiNi_{1/3}Co_{1/3}Mn_{1/3}O_2$ and its improvement by surface coating. A combination of electrochemical and magnetical techniques were used to investigate the gradually evolutions of electrode surface and internal structure and also its improvement by surface coating.

Chapter 6 is the general conclusion and avenues for future work of this research.

1.5 References

[1] B. Dunn, H. Kamath and J. M. Tarascon: "Electrical Energy Storage for the Grid: A Battery of Choices", *Science*, Vol. 334, pp. 928-935, 2011

[2] B. C. Melot and J. M. Tarascon: "Design and Preparation of Materials for Advanced Electrochemical Storage", *Accounts of Chem. Res.*, Vol. 46, pp. 1226-1238, 2013

[3] B. Scrosati and J. Garche: "Lithium batteries: Status, prospects and future", *J. Power Source*, Vol. 195, 2419-2430, 2010

[4] J. B. Goodenough and K. S. Park: "The Li-Ion Rechargeable Battery: A perspective", *J. A. Chem. Soc.*, Vol. 135, pp. 1167-1176, 2013

[5] D. Fouchard and L. Lechner: "Analysis of Safety and Reliability in Secondary Lithium Batteries", *Electrochim. Acta*, Vol. 38, pp. 1193-1198, 1993

[6] M. M. Thackeray, C. Wolverton and E. D. Isaacs: "Electrical energy storage for transportation-approaching the limits of, and going beyond, lithium-ion batteries", *Energy Environ. Sci.*, Vol. 5, pp. 7854-7863, 2012

[7] M. M. Thackeray, S. H. Kang, C. S. Johnson, J. T. Vaughey, R. Benedek and S. A. Hackney: "Li_2MnO_3-stabilized $LiMO_2$ (M = Mn, Ni, Co) electrodes for lithium-ion batteries", *J. Mater. Chem.*, Vol. 17, pp. 3112-3125, 2007

[8] T. Janoschka, M. D. Hager and U. S. Schubert: "Powering up the Future: Radical Polymers for Battery Applications", *Adv. Mater.*, Vol. 24, pp. 6397-6409, 2012

[9] Y. X. Yin, S. Xin, Y. G. Guo and L. J. Wan: "Lithium–Sulfur Batteries: Electrochemistry, Materials, and Prospects", *Angew. Chem. Int. Ed.*, Vol. 52, pp. 13186-13200, 2013

[10] F. J. Li, T. Zhang and H. S. Zhou: "Challenges of non-aqueous Li-O_2 batteries: electrolytes, catalysts, and anodes", *Energy Environ. Sci.*, Vol. 6, pp. 1125-1141, 2013

[11] K. Mizushima, P. C. Jones, P. J. Wiseman and J. B. Goodenough: "Lixcoo2 "(Oless-Thanxless-Than-or-Equal-To1) - a New Cathode Material for Batteries of High-Energy Density", *Mater. Res. Bull.*, Vol. 15, pp. 783-789, 1980

[12] P. He, H. J. Yu, D. Li and H. S. Zhou: "Layered lithium transition metal oxide

cathodes towards high energy lithium-ion batteries", *J. Mater. Chem.*, Vol. 22, pp. 3680-3695, 2012

[13] N. A. Chernova, M. Ma, J. Xiao, M. S. Whittingham, J. Breger and C. P. Grey, "Layered $Li_xNi_yMn_yCo_{1-2y}O_2$ cathodes for lithium ion batteries: Understanding local structure via magnetic properties", *Chem. Mater.*, Vol. 19, pp. 4682-4693, 2007

[14] M. M. Thackeray, W. I. F. David, P. G. Bruce and J. B. Goodenough: "Lithium Insertion into Manganese Spinels", *Mater. Res. Bull.*, Vol. 18, pp. 461-472, 1983

[15] A. Kraytsberg and Y. Ein-Eli: "Higher, Stronger, Better...A review of 5 Volt Cathode Materials for Advanced Lithium-Ion Batteries", *Adv. Energy Mater.*, Vol. 2, pp. 922-939, 2012

[16] A. K. Padhi, K. S. Nanjundaswamy and J. B. Goodenough: "Phospho-olivines as positive-electrode materials for rechargeable lithium batteries", *J. Electrochem. Soc.*, Vol. 144, pp. 1188-1194, 1997

[17] C. Masquelier and L. Croguennec: "Polyanionic (Phosphates, Silicates, Sulfates) Frameworks as Electrode Materials for Rechargeable Li (or Na) Batteries", *Chem. Rev.*, Vol. 113, pp. 6552-6591, 2013

[18] D. T. Liu, Z. X. Wang and L. Q. Chen: "Comparison of structure and electrochemistry of Al- and Fe-doped $LiNi_{1/3}Co_{1/3}Mn_{1/3}O_2$", *Electrochimica Acta*, Vol. 51, pp. 4199-4203, 2006

[19] K. Kang and G. Ceder: "Factors that affect Li mobility in layered lithium transition metal oxides", *Phy. Rev. B.*, Vol. 74, pp. 094105, 2006

[20] K. Kang, Y. S. Meng, J. Breger, C. P. Grey and G. Ceder: "Electrodes with high power and high capacity for rechargeable lithium batteries", *Science*, Vol. 311 , pp. 977-980, 2006

[21] S. W. Cho, G. O. Kim and K. S. Ryu: "Sulfur anion doping and surface modification with $LiNiPO_4$ of a $Li[Co_{0.1}Ni_{0.15}Li_{0.2}Mn_{0.55}]O_2$ cathode material for Li-ion batteries", *Solid State Ionics*, Vol. 206, pp. 84-90, 2012

[22] C. X. Ding, Y. C. Bai, X. Y. Feng and C. H. Chen: "Improvement of electrochemical properties of layered $LiNi_{1/3}Co_{1/3}Mn_{1/3}O_2$ positive electrode material by zirconium doping", *Solid State Ionics*, Vol. 189 , pp. 69-73, 2011

[23] L. Liu, K. N. Sun, N. Q. Zhang and T. Y. Yang: "Improvement of high-voltage cycling behavior of $LiNi_{1/3}Co_{1/3}Mn_{1/3}O_2$ cathodes by Mg, Cr, and Al substitution", *J. Solid State Electrochem.*, Vol. 13 , pp. 1381-1386, 2009

[24] K. H. Dai, Y. T. Xie, Y. J. Wang, Z. S. Song and Q. Lu: "Effect of fluorine in the preparation of $LiNi_{1/3}Co_{1/3}Mn_{1/3}O_2$ via hydroxide co-precipitation", *Electrochimica Acta*, Vol. 53, pp. 3257-3261, 2008

[25] L. A. Riley, S. Van Ana., A. S. Cavanagh, Y. Yan, S. M. George, P. Liu, A. C. Dillon and S. H. Lee: "Electrochemical effects of ALD surface modification on combustion synthesized $LiNi_{1/3}Co_{1/3}Mn_{1/3}O_2$ as a layered-cathode material", *J. Power Source*, Vol. 196, pp. 3317-3324, 2011

[26] Y. Huang, J. Chen, F. Cheng, W. Wan, W. Liu, H. Zhou and X. Zhang: "A modified Al_2O_3 coating process to enhance the electrochemical performance of $LiNi_{1/3}Co_{1/3}Mn_{1/3}O_2$ and its comparison with traditional Al_2O_3 coating process", *J. Power Source*, Vol. 195, pp. 8267-8274, 2010

[27] H. S. Kim, Y. Kim, S. I. Kim and S. W. Martin: "Enhanced electrochemical properties of $LiNi_{1/3}Co_{1/3}Mn_{1/3}O_2$ cathode material by coating with $LiAlO_2$ nanoparticles", *J. Power Source*, Vol. 161, pp. 623-627, 2006

[28] Y. K. Sun, S. W. Cho, S. W. Lee, C. S. Yoon and K. Amine: "AlF3-coating to improve high voltage cycling performance of $LiNi_{1/3}Co_{1/3}Mn_{1/3}O_2$ cathode materials for lithium secondary batteries", *J. Electro. Soc.*, Vol. 154, pp. A168-A172, 2007

[29] T. E. Hong, E. D. Jeong, S. R. Baek, M. R. Byeon, Y. S. Lee, F. N. Khan and H. S. Yang: "Nano SIMS characterization of boron- and aluminum-coated $LiNi_{1/3}Co_{1/3}Mn_{1/3}O_2$ cathode materials for lithium secondary ion batteries", *J. Appl. Electrochem.*, Vol. 42, pp. 41-46, 2012

[30] J. H. Wang, Y. Wang, Y. Z. Guo, Z. Y. Ren and C. W. Liu: "Effect of heat-treatment on the surface structure and electrochemical behavior of $AlPO_4$-coated $LiNi_{1/3}Co_{1/3}Mn_{1/3}O_2$ cathode materials", *J. Mater. Chem. A.*, Vol. 1, pp. 4879-4884, 2013

[31] S. K. Hu, G. H. Cheng, M. Y. Cheng, B. J. Hwang and R. Santhanam: "Cycle life improvement of ZrO_2-coated spherical $LiNi_{1/3}Co_{1/3}Mn_{1/3}O_2$ cathode material for

lithium ion batteries", *J. Power Source*, Vol. 188, pp. 564-569, 2009

[32] Y. Huang, J. Chen, J. Ni, H. Zhou and X. Zhang: "A modified ZrO_2-coating process to improve electrochemical performance of $LiNi_{1/3}Co_{1/3}Mn_{1/3}O_2$", *J. Power Source*, Vol. 188, pp. 538-545, 2009

[33] S. H. Yun, K. S. Park and Y. J. Park: "The electrochemical property of ZrF_x-coated $LiNi_{1/3}Co_{1/3}Mn_{1/3}O_2$ cathode material", *J. Power Source*, Vol. 195, pp. 6108-6115, 2010

[34] S. J. Shi, J. P. Tu, Y. J. Mai, Y. Q. Zhang, Y. Y. Tang and X. L. Wang: "Structure and electrochemical performance of CaF_2 coated $LiNi_{1/3}Co_{1/3}Mn_{1/3}O_2$ cathode material for Li-ion batteries", *Electrochimica Acta*, Vol. 83, pp. 105-112, 2012

[35] K. Xu, Z. Jie, R. Li, Z. Chen, S. Wu, J. Gu and J. Chen: "Synthesis and electrochemical properties of CaF_2-coated for long-cycling $LiNi_{1/3}Co_{1/3}Mn_{1/3}O_2$ cathode materials", *Electrochimica Acta*, Vol. 60 , pp. 130-133, 2012

[36] J. Li, L. Wang, Q. Zhang and X. He: "Electrochemical performance of SrF_2-coated $LiNi_{1/3}Co_{1/3}Mn_{1/3}O_2$ cathode materials for Li-ion batteries", *J. Power Source*, Vol. 190, pp. 149-153, 2009

[37] F. Wu, M. Wang, Y. Su, S. Chen and B. Xu: "Effect of TiO_2-coating on the electrochemical performances of $LiNi_{1/3}Co_{1/3}Mn_{1/3}O_2$", *J. Power Source*, Vol. 191, pp. 628-632, 2009

[38] M. Morishita, T. Mukai, T. Sakamoto, M. Yanagida and T. Sakai: "Improvement of Cycling Stability at 80 degrees C for 4 V-Class Lithium-Ion Batteries and Safety Evaluation", *J. Electro. Soc.*, Vol. 154, pp. A1311-A1318, 2013

[39] R. Guo, P. Shi, X. Cheng and Y. Ma, Z. Tan: "Effect of Ag additive on the performance of $LiNi_{1/3}Co_{1/3}Mn_{1/3}O_2$ cathode material for lithium ion battery", *J. Power Source*, Vol. 189, pp. 2-8, 2009

[40] F. Wu, M. Wang, Y. Su and S. Chen: "Surface modification of $LiNi_{1/3}Co_{1/3}Mn_{1/3}O_2$ with Y_2O_3 for lithium-ion battery", *J. Power Source*, Vol. 189, pp. 743-747, 2009

[41] M. Wang, F. Wu, Y. Su and S. Chen: "Modification of $LiNi_{1/3}Co_{1/3}Mn_{1/3}O_2$ cathode material by CeO_2-coating", *Sci. China Ser E-Tech. Sci.*, Vol. 52, pp.

2737-2741, 2009

[42] L. Tan and H. Liu: "Influence of ZnO coating on the structure, morphology and electrochemical performances for $LiNi_{1/3}Co_{1/3}Mn_{1/3}O_2$ material", *Russian J. Electro.*, Vol. 47, pp. 156-160, 2011

[43] S. J. Shi, J. P. Tu, Y. Y. Tang, Y. Q. Zhang, X. Y. Liu, X. L. Wang and C. D. Gu: "Enhanced electrochemical performance of LiF-modified $LiNi_{1/3}Co_{1/3}Mn_{1/3}O_2$ cathode materials for Li-ion batteries", *J. Power Source*, Vol. 225, pp. 338-346, 2013

[44] N. N. Sinha and N. Munichandraiah: "Synthesis and Characterization of Carbon-Coated $LiNi_{1/3}Co_{1/3}Mn_{1/3}O_2$ in a Single Step by an Inverse Microemulsion Route", *ACS App. Mater. Inter.*, Vol. 1, pp. 1241-1249, 2009

[45] R. Guo, P. Shi, X. Cheng and C. Du: "Synthesis and characterization of carbon-coated $LiNi_{1/3}Co_{1/3}Mn_{1/3}O_2$ cathode material prepared by polyvinyl alcohol pyrolysis route", *J. Alloys and Com.*, Vol. 473, pp. 53-59, 2009

[46] C. V. Rao, A. L. M. Reddy, Y. Ishikawa and P. M. Ajayan: "$LiNi_{1/3}Co_{1/3}Mn_{1/3}O_2$-Graphene Composite as a Promising Cathode for Lithium-Ion Batteries", *ACS App. Mater. Inter.*, Vol. 3, pp. 2966-2972, 2011

[47] P. Zhang, L. Zhang, X. Ren, Q. Yuan, J. Liu and Q. Zhang: "Preparation and electrochemical properties of $LiNi_{1/3}Co_{1/3}Mn_{1/3}O_2$-PPy composites cathode materials for lithium-ion battery", *Syn. Metal*, Vol. 161 , pp. 1092-1097, 2011

[48] J. H. Park, J. H. Cho, S. B. Kim, W. S. Kim, S. Y. Lee and S. Y. Lee: "A novel ion-conductive protection skin based on polyimide gel polymer electrolyte: application to nanoscale coating layer of high voltage $LiNi_{1/3}Co_{1/3}Mn_{1/3}O_2$ cathode materials for lithium-ion batteries", *J. Mater. Chem.*, Vol. 22, pp. 12574-12581, 2012

[49] E. H. Lee, J. H. Park, J. H. Cho, S. J. Cho, D. W. Kim, H. Dan, Y. Kang and S. Y. Lee: "Direct ultraviolet-assisted conformal coating of nanometer-thick poly(tris(2-(acryloyloxy)ethyl) phosphate) gel polymer electrolytes on high-voltage $LiNi_{1/3}Co_{1/3}Mn_{1/3}O_2$ cathodes", *J. Power Source*, Vol. 244, pp. 389-394, 2013

[50] Z. H. Chen, Y. Qin, K. Amine and Y. K. Sun: "Role of surface coating on cathode materials for lithium-ion batteries", *J. Mater. Chem.*, Vol. 20, pp. 7606-7612, 2010

[51] Y. K. Sun, S. T. Myung, M. H. Kim, J. Prakash and K. Amine: "Synthesis and

characterization of $Li[(Ni_{0.8}Co_{0.1}Mn_{0.1})_{0.8}(Ni_{0.5}Mn_{0.5})_{0.2}]O_2$ with the microscale core-shell structure as the positive electrode material for lithium batteries", *J. Am. Chem. Soc.*, Vol. 127, pp. 13411-13418, 2005

[52] X. B. Meng, X. Q. Yang and X. L. Sun: "Emerging Applications of Atomic Layer Deposition for Lithium-Ion Battery Studies", *Adv. Mater.*, Vol. 24, pp. 3589-3615, 2012

Chapter 2. Improvement of electrochemical properties of $LiNi_{1/3}Co_{1/3}Mn_{1/3}O_2$ by coating with V_2O_5 layer

2.1 Introduction

Surface coating have been proved to be a facile but feasible way to strengthen the electrochemical performance of layered cathode materials [1-3]. A variety of materials have been investigated as coating layer materials [4-12]. Most of the reported metal contained coating layer materials have a common feature that the metal center has only one stable valence state at a normal redox conditions of battery operations. One of the fatal flaws for these materials is that they are generally inactive to lithium ions and have low lithium ion conductivity. The excess coating of such materials is at the expense of capacities and efficiency. Thus, the exploration of new material as coating layer for layered cathode is still a challenge.

Recent research progresses prove that amorphous vanadium oxide have became one of the most attractive candidates as coating material for it acts as an ion and electrons double conductive materials [13-16]. K. S. Park et al. reported that VO_x impregnated $LiFePO_4$ with improved rate capacities [13]. They also synthesized VO_x impregnated $0.5Li_2MnO_3$-$0.5LiNi_{0.4}Co_{0.2}Mn_{0.4}O_2$ cathode materials which showed an improved electrochemical performance for the vanadium ions in $3d^0$ electronic states during high voltage charging state could reduce the surface catalytic activities and stabilize the surface oxide ions during their electrochemical oxidation [14]. J. W. Lee et al. reported that a vanadium oxide coating layer on $LiCoO_2$ improved the cycleability at a high-charge cut-off voltage [15]. A suppression of dissolution of Mn from spinel $LiMn_2O_4$ by coating with VO_x layer have also been reported by J.Cho [17]. However, the effects of the VO_x coating layer on $Li[Ni_{1/3}Co_{1/3}Mn_{1/3}]O_2$ have still not been investigated.

In this chapter, we have explored the possibility of coating the $LiNi_{1/3}Co_{1/3}Mn_{1/3}O_2$ particles by a V_2O_5 layer. We adopted the sol-gel method to get a uniform V_2O_5 coating layer. The effect of the V_2O_5 coating layer on the structure and morphology have also been studied. The charge-discharge properties at a high rate and also the rate

performance have been explored. Cyclic voltammetry (CV) and electrochemical impedance spectroscopy (EIS) on cycled cells with different times were used to investigate the mechanism of the improvement in the electrochemical properties of the V_2O_5 coated $LiNi_{1/3}Co_{1/3}Mn_{1/3}O_2$ material.

2.2 Experimental and Characterization

2.2.1 Preparation of V_2O_5 coated $LiNi_{1/3}Co_{1/3}Mn_{1/3}O_2$

Pristine $LiNi_{1/3}Co_{1/3}Mn_{1/3}O_2$ powder was synthesized by carbonate precipitation method according the reference [18]. The coating process was conducted by sol-gel method. The V_2O_5 hydrosol was first obtained by adding of certain amount of V_2O_5 and H_2O_2 to 5 ml deionized water with vigorously stirring. And then $LiNi_{1/3}Co_{1/3}Mn_{1/3}O_2$ (1 g) was added to the hydrosol, kept on stirring for 2 h at room temperature. After ultrasonic treatment for 10 minutes, the suspension was dried at 80 ℃. The final powder was heat-treated in a furnace at 350 ℃ for 5 h in air. For comparing, the pristine samples had also been heat-treated under the same conditions.

2.2.2 Characterization

The structure of the powder samples of pristine and coated samples were analyzed using a Bruker D8 Advance X-Ray powder Diffractometer (XRD) with Cu *K*α radiation. The morphology of all the samples were examined using Scanning Electronic Microscope (SEM) on a JSM-6700F instrument and Transmission electron microscope (TEM) on a JEOL 3100F with a voltage of 300 KV.

2.2.3 Fabrication of batteries and electrochemical test

The electrochemical performance of the pristine and V_2O_5 coated $Li[Ni_{1/3}Co_{1/3}Mn_{1/3}]O_2$ cathodes were conducted by coin cells (CR 2032) consisting of a cathode, metallic lithium anode, polypropylene separator, and an electrolyte of 1M $LiPF_6$ in EC/DEC (1:1 vol%). The cathode contained 80 wt% active materials, 15

wt% acetylene black, and 5 wt% polytetrafluoroethylene (PTFE) binder. The above mixture were mixed and ground in a agate mortar and then pressed onto a aluminum mesh which served as a current collector and dried at 80 ℃ for 12 h under vacuum. The cells were assembled in an Ar-filled glove box and subjected to galvanostatic cycling using a Hokuto Denko in a potential range of 2.8-4.5 V (versus Li^+/Li) at currents of 150 mAh/g and 300 mAh/g. The specific capacity and current density are base on the synthesized cathode materials, for the coated materials, the coating layer have been included. The Cyclic Voltammetry (CV) were done with coin cells on a Solartron Instrument Model 1287 in the voltage range of 2.8-4.5 V (versus Li^+/Li) with a scan rate of 0.2 mV/s. The electrochemical impedance spectroscopy (EIS) were also done with coin cells on a Solartron Instrument Model 1287 electrochemical interface and a 1255 B frequency response analyzer controlled by Z-plot. The measurements were performed in the frequency range 0.5 MHz to 0.05 Hz with an AC signal of 5 mV. Data analysis used the software Zview 2.70. (Scribner Associates Inc., USA)

2.3 Results and Discussion

2.3.1 Confirmation of surface coating layer

XRD patterns of the pristine $LiNi_{1/3}Co_{1/3}Mn_{1/3}O_2$ and 3 wt%-V_2O_5-coated $LiNi_{1/3}Co_{1/3}Mn_{1/3}O_2$ are presented in Fig.2.1a. The patterns showed that the synthesized materials have highly crystalline and all the diffraction peaks could be indexed as a layered oxide structure which based on a hexagonal α-$NaFeO_2$ structure with a space group of *R*-3m. The splitting of the peaks (108), (110) and (006), (102) in the XRD patterns indicated that the materials had a well ordered α-$NaFeO_2$ structure, $I_{003}/I_{104}>1.2$ was an indication of desirable cation mixing [19]. The lattice parameters of pristine and V_2O_5 coated sample were summarized in Table 2.1. It is clear that there is no significant difference before and after surface coating by V_2O_5. The relatively low heat treatment temperature of the V_2O_5 coating layer seemed not allow for the formation of a solid solution between the V_2O_5 coating layer and the pristine

$LiNi_{1/3}Co_{1/3}Mn_{1/3}O_2$ materials. It demonstrated that the layered structure of $LiNi_{1/3}Co_{1/3}Mn_{1/3}O_2$ had not been affected by coating. No impurities or secondary phases was observed in this figure. In order to confirm the contents of coating layer, we also synthesized the V_2O_5 powder using the same synthesis route without adding of layered material $LiNi_{1/3}Co_{1/3}Mn_{1/3}O_2$. The XRD patterns (in Fig.2.1b) showed that it can be indexed as compound V_2O_5 with space group of P_{mmn} and the JCPDS card 41-1462. So the coating layer can be considered as V_2O_5.

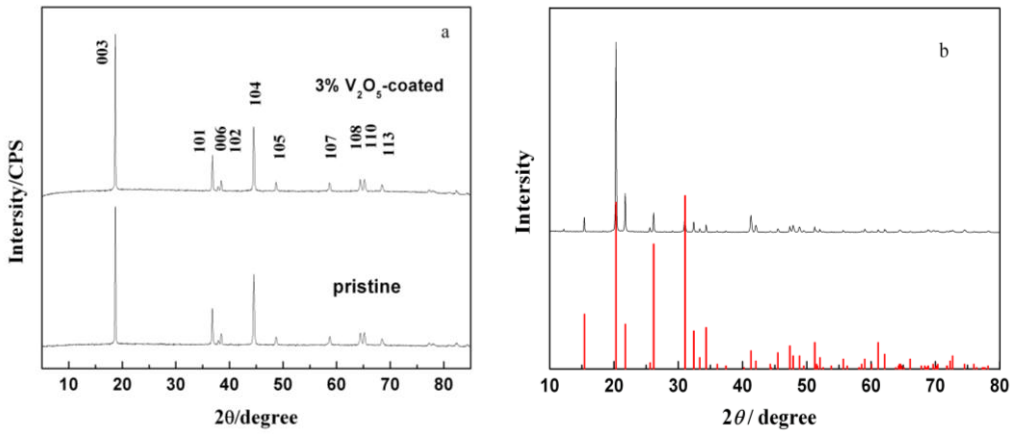

Fig. 2.1. XRD of patterns of (a) $LiNi_{1/3}Co_{1/3}Mn_{1/3}O_2$ and 3 wt% V_2O_5-coated $LiNi_{1/3}Co_{1/3}Mn_{1/3}O_2$; (b) V_2O_5 powder

Table 2.1 Lattice parameters of Pristine $LiNi_{1/3}Co_{1/3}Mn_{1/3}O_2$ and 3% V_2O_5-coated $LiNi_{1/3}Co_{1/3}Mn_{1/3}O_2$

Sample	a (Å)	c (Å)	V ($Å^3$)
Pristine $LiNi_{1/3}Co_{1/3}Mn_{1/3}O_2$	2.8608(6)	14.2334(50)	100.88(5)
3 wt% V_2O_5-coated	2.8584(8)	14.2295(69)	100.68(8)

The surface morphologies of the pristine and 3 wt%-V_2O_5-coated samples were observed by SEM and TEM. As shown in Fig.2.2a and 2.2c, the secondary particles of pristine $LiNi_{1/3}Co_{1/3}Mn_{1/3}O_2$ (from 2 μm to several μm) consisted of primary particles (300-500 nm in size). We can see clearly that the surface and edge of the particles are smooth and clean from TEM image in Fig. 2.2e. In contrast, after coating with V_2O_5, the particle is almost no changes in size (Fig. 2.2b and 2.2d), but the surface became considerably rough and ambiguous (as shown in Fig.2.2f), the coating layer is about

5-8 nm. These figures revealed that the V_2O_5 was successfully coating on the pristine $LiNi_{1/3}Co_{1/3}Mn_{1/3}O_2$.

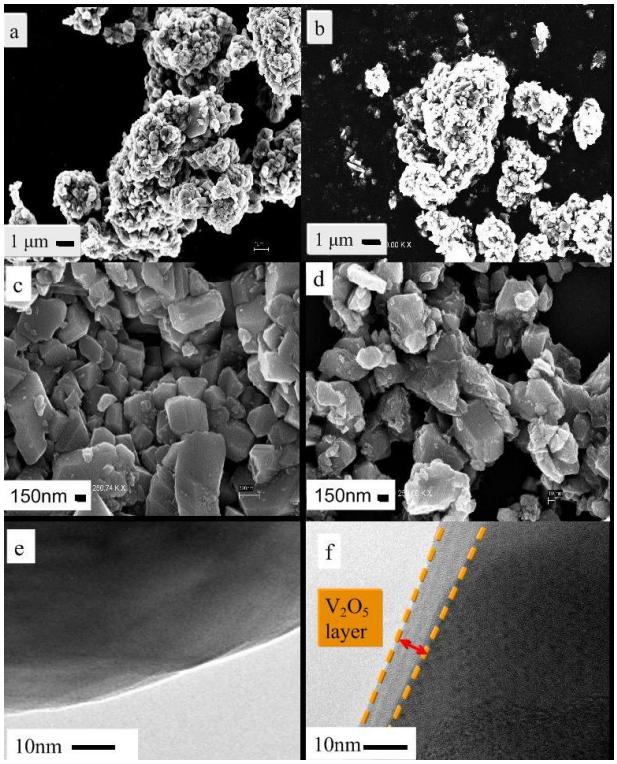

Fig. 2.2. SEM and TEM of pristine $LiNi_{1/3}Co_{1/3}Mn_{1/3}O_2$ (a), (c) and (e); 3 wt% V_2O_5-coated $LiNi_{1/3}Co_{1/3}Mn_{1/3}O_2$ (b), (d) and (f).

The SEM-energy dispersive spectrometry (EDS) measurements have been conducted to get the directly evidence of the composition and distribution of vanadium in 3 wt% V_2O_5-coated $LiNi_{1/3}Co_{1/3}Mn_{1/3}O_2$ as shown in Fig.2.3a-2.3c. Based on the mapping, V in the sample is homogeneously distributed in the composite, indicating uniform distribution of vanadium oxide on the surface of $LiNi_{1/3}Co_{1/3}Mn_{1/3}O_2$. X-ray photoelectron spectroscopy (XPS) were employed to reveal subtle information of the surface structure. Fig.2.3d shows that the binding energies of electrons in V $2p^3$ are located at 516.9 and 515.8 eV. These two peaks related to the formal oxidation degrees of +5 and +4, corresponding to the vanadium oxides V_2O_5 and VO_2, respectively [14]. The peak intensity for V^{4+} is less than 10% compared with the peak intensity for V^{5+}. Therefore, the major component in the coating layer is V_2O_5.

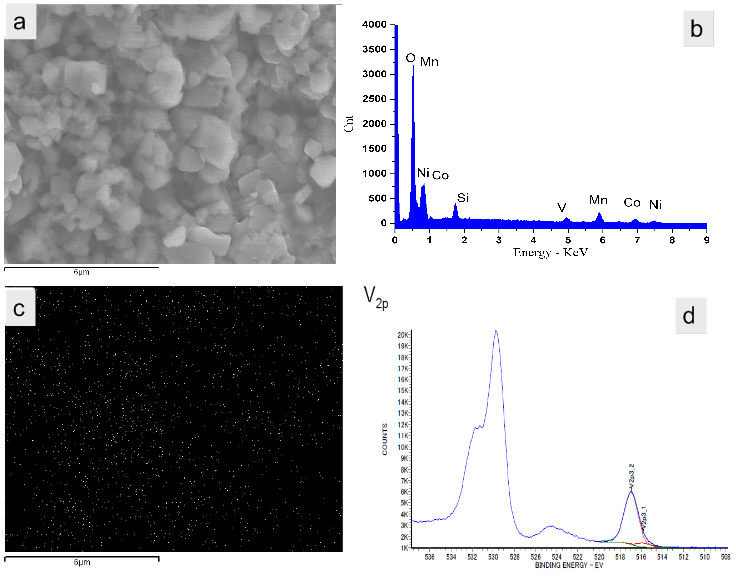

Fig. 2.3. (a) SEM image of 3 wt% V_2O_5-coated $LiNi_{1/3}Co_{1/3}Mn_{1/3}O_2$; (b) EDS spectrum of 3 wt% V_2O_5-coated $LiNi_{1/3}Co_{1/3}Mn_{1/3}O_2$; (c) EDS dot-mapping for V; (d) XPS analysis of V 2p core peaks for 3 wt% V_2O_5-coated $LiNi_{1/3}Co_{1/3}Mn_{1/3}O_2$.

2.3.2 Electrochemical performance

The capacity, cycle performance and rate capability of pristine and coated $Li[Ni_{1/3}Co_{1/3}Mn_{1/3}]O_2$ electrode were characterized to investigate the coating effects. The cycle performance of the pristine and coated samples with different V_2O_5 coating contents are shown in Fig.2.4a. The charge-discharge were conducted between 2.8-4.5 V at a current of 150 mA/g. With 1 wt%, 2 wt%, 3 wt%, 4 wt% and 5 wt% V_2O_5 coating, the discharge capacities are 111.5, 118.7, 140.1, 128.0 and 124.8 mAh/g at the 100^{th} cycle, respectively. Meanwhile, the discharge capacity is 103.2 mAh/g for the pristine $Li[Ni_{1/3}Co_{1/3}Mn_{1/3}]O_2$ at the 100^{th} cycle. It is clearly indicated that the cycle performance have been improved by V_2O_5 coating. The optimal coating amount is 3 wt% according the capacity retention.

The cycle performance at a relatively high charge-discharge current of 300 mA/g was also examined on pristine and 3 wt% V_2O_5-coated $Li[Ni_{1/3}Co_{1/3}Mn_{1/3}]O_2$ as shown in Fig.2.4b. The pristine sample showed a higher initial discharge capacity than the coated samples, but it suffered a serious capacity fading upon cycling. In contrast,

the coated samples showed a relatively smaller initial discharge capacity, there is a slight capacity fading upon cycling.

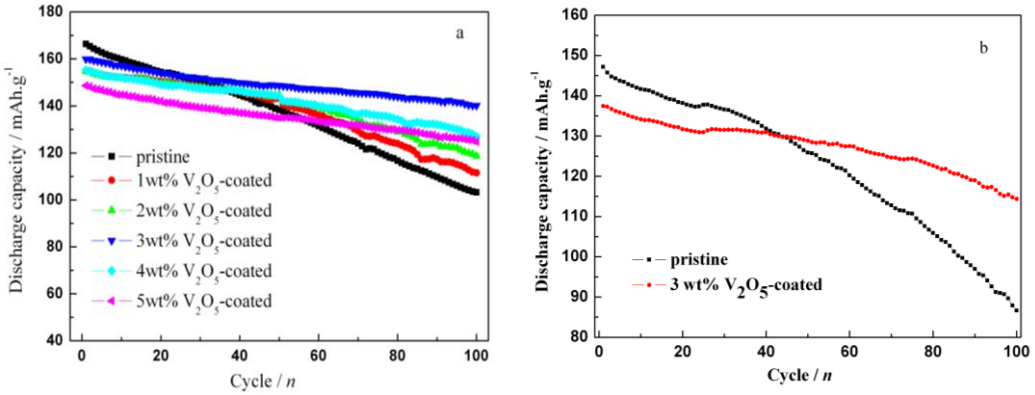

Fig. 2.4. (a) Cycle performance of pristine and different amount of V_2O_5-coated $LiNi_{1/3}Co_{1/3}Mn_{1/3}O_2$ in the voltage range of 2.8-4.5 V at a current of 150 mA/g; (b) Cycle performance of pristine and 3 wt% V_2O_5-coated and $LiNi_{1/3}Co_{1/3}Mn_{1/3}O_2$ at 300 mA/g in the voltage range of 2.8-4.5 V.

Table 2.2. Discharge capacities of pristine and V_2O_5-coated $LiNi_{1/3}Co_{1/3}Mn_{1/3}O_2$ electrodes during 100 cycles in the voltage range of 4.5-2.8 V

	1^{st} (mAh/g)	50^{th} (mAh/g)	100^{th} (mAh/g)
Pristine	147	126	87
3 wt% coated	137	129	114

Table 2.2 summarized the discharge capacity for the 1^{st}, 50^{th} and 100^{th} cycles of the pristine and coated electrodes. At the 50^{th} cycle, the two samples showed similar discharge capacities of 126 mAh/g (pristine samples) and 129 mAh/g (3 wt% V_2O_5-coated samples). But at the 100^{th} cycle, the pristine only showed a discharge capacity of 87 mAh/g and retained 59.2% of its original capacity of approximately. However, the 3 wt% V_2O_5-coated materials showed higher capacities of 114 mAh/g and displayed 83.2% retention of the initial discharge capacity. It can be clearly concluded that the capacity fading has been suppressed by surface coating of V_2O_5. The most possible reason for the capacity fading is side-reaction between electrode and electrolyte during extensive cycling. For the coated samples, the V_2O_5 coating

layer acted as a protective layer, it prevented the directly contact between the active electrode material and electrolyte, therefore, it impeded the side reactions at the interface upon charge-discharge cycles.

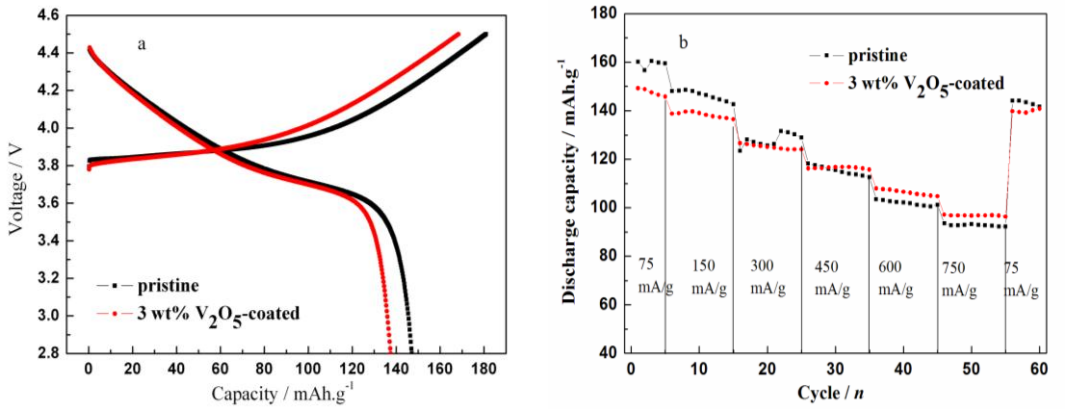

Fig. 2.5. (a) Comparison of the initial charge/discharge curves of pristine (black) and 3 wt% V_2O_5-coated $LiNi_{1/3}Co_{1/3}Mn_{1/3}O_2$ (red); (b) Rate capabilities of pristine and 3 wt% V_2O_5-coated $LiNi_{1/3}Co_{1/3}Mn_{1/3}O_2$ in the voltage range of 2.8-4.5 V.

Fig.2.5a shows the first charge/discharge profiles of the pristine and 3 wt% V_2O_5 coated materials between 2.8-4.5 V at a current of 300 mA/g. The charge-discharge curves showed typical potential plateaus of layered compounds at 3.9 V region, which originating from the Ni^{2+}/Ni^{4+} redox couples [20]. The pristine $Li[Ni_{1/3}Co_{1/3}Mn_{1/3}]O_2$ presented a charge capacity of 180.9 mAh/g and discharge capacity of 147 mAh/g at the first cycle, however, there were a little lower charge-discharge capacities for coated samples. For the 3 wt% V_2O_5-coated sample, the charge capacity was 168.3 mAh/g and discharge capacity was 137 mAh/g at the first cycle. The reason for lower initial capacities of the coated materials is that the V_2O_5 coating layer showed no capacity contribution at the voltage above 2.8 V. It can also be explained by the V^{5+}/V^{4+} redox not occurred in the experiment condition according cyclic voltammetry measurements as shown in the following results. Fig.2.5b presents the discharge capacity retentions of the pristine and coated samples at different rates in a range of 2.8-4.5 V. The coated samples clearly shows a better discharge capacity than the pristine when the rate is larger than 450 mA/g. This result indicates that a V_2O_5

coating layer assist the lithium ions and electrons transport at the electrode surface. This effects are more obvious at high rates. The capacity recovery of the coated sample, when took the charge-discharge at 75 mA/g rate again after high rate cycling, were better (93.6% for 3 wt% V_2O_5 coated sample) than the pristine samples (90%). This result also confirm that the coating layer can impede the capacity fading.

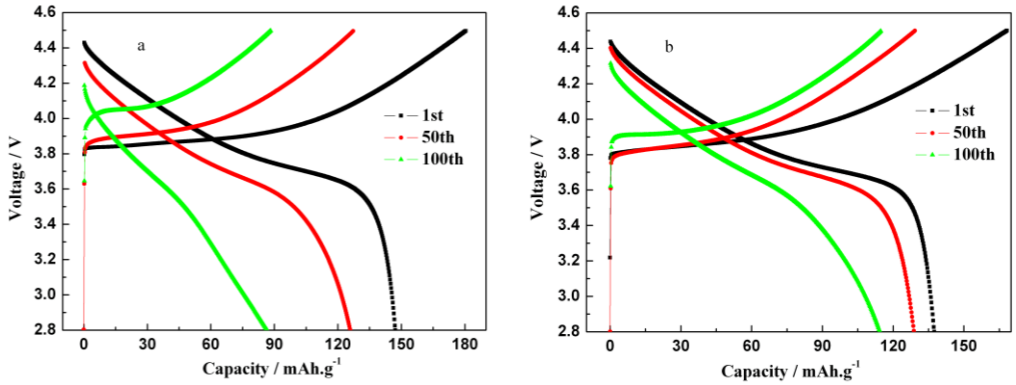

Fig. 2.6. Charge-discharge curves of (a) pristine $LiNi_{1/3}Co_{1/3}Mn_{1/3}O_2$; and (b) 3 wt% V_2O_5-coated $LiNi_{1/3}Co_{1/3}Mn_{1/3}O_2$ at 2 C and at 1^{st} (black), 50^{th} (red) and 100^{th} (green).

In order to detailed study the changes of charge-discharge processes with cycles, Fig.2.6 shows the charge and discharge curves of pristine and V_2O_5-coated materials at different cycles. During the charge processes, the plateaus of the two samples appeared at about 3.8 V and slowly increased to 4.5 V. For the pristine sample, the plateaus became higher as cycling and reached to about 4.05 V at the 100^{th} cycle. But for the coated samples, the changes was smaller and the plateaus were 3.91 V at the 100^{th} cycle. For the discharge processes of the pristine sample, the plateaus became more and more vague with cycling. In contrast, the changes of the plateau for the coated samples were minor. The increase of the separations between charge plateau and discharge plateau originated from the increase of overpotential which was caused by the side-reactions between the electrode and electrolyte. The V_2O_5 coating layer suppressed side-reactions at the interface of electrode/electrolyte and so the coated samples showed smaller changes of the charge-discharge plateaus than the pristine sample.

2.3.3 Electrochemical analysis

Cyclic voltammetry (CV) is an effective analysis technique for studying the oxidation/reduction processes in electrode reaction. It should be pointed out that the redox potentials of ions do depend on the metal-metal interactions within the layers [21]. Therefore, for layered cathode materials, the changes of the metal circumstance which caused by the increase of cation mixing can be reflected by cyclic voltamgrams. In our research, CV were conducted to investigate the oxidation/reduction properties on before and after cycled cells. As shown in Fig.2.7a, the pristine sample showed a well refined redox peaks at 3.887 and 3.689 V, while the coated samples showed peaks at 3.866 V and 3.697 V, which can be assigned to the Ni^{2+}/Ni^{4+} couple [19]. It suggests that the coated V_2O_5 layers do not take participate in the redox reaction in the voltage range of 2.8-4.5 V. It should also be noted that the separation of cathodic and anodic peaks of coated sample are smaller than that of the pristine samples, which suggested that the polarization of the electrode was decreased due to the improved surface conductivity by surface coating. To further understanding the changes of redox properties of the materials, the CV response of the cells cycled 100 times have also been conducted as shown in Fig.2.7b. The cathodic peaks of the 3 wt% V_2O_5 coated samples shifted to a higher voltage side by 0.1 V and the anodic peaks get shifted to a lower voltage side by 0.05-0.07 V. The shift of the peaks originated from either the side reactions between the electrodes and electrolytes or polarization on the surface of the electrodes. The pristine samples, however, underwent a more manifest changes during the redox processes. The cathodic peak shifted to 4.117 V while the anodic peaks became indistinct. This means that the pristine electrode underwent an intense surface and structure changes by side reactions during charge-discharge cycles. This behavior implies that the V_2O_5 surface layer relieved the side-reactions between the electrode and electrolyte on cycling by preventing directly interactions between electrode and electrolyte.

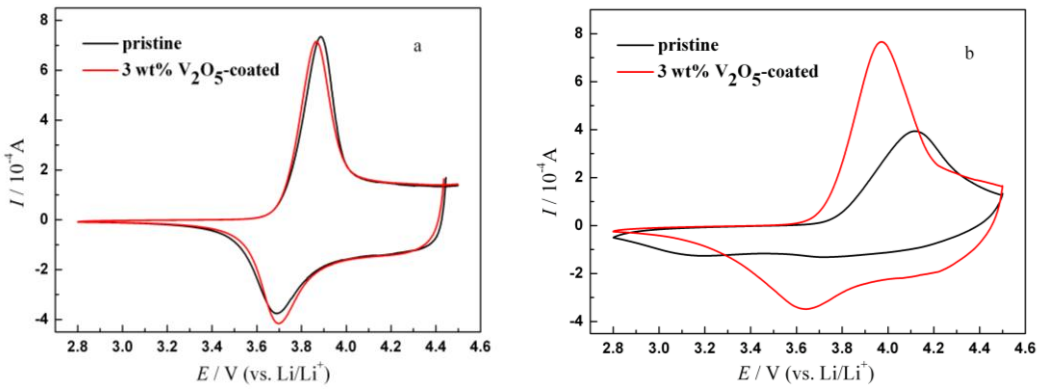

Fig. 2.7. Cyclic voltammograms (scan rate of 0.2 mV/s between 2.8 and 4.5 V) of pristine and 3 wt% V_2O_5-coated samples (a) on fresh cells; (b) on cells after 100 cycles of galvanostatic charge-discharge.

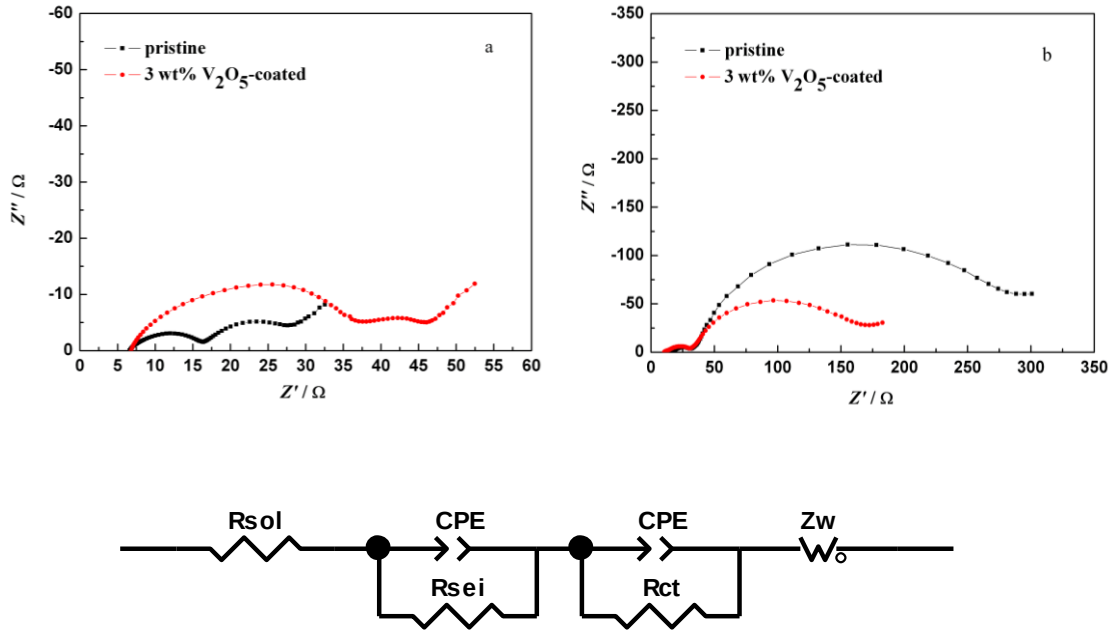

Fig. 2.8. EIS Nyquist plots of pristine and 3 wt% V_2O_5-coated materials with cycling, (a) at the 2nd cycle; (b) at the 100th cycle; (c) Voigt-type of equivalent circuit.

In order to further study how the coating layer suppressing the side-reactions between the electrode and electrolyte, the electrochemical impedance spectroscopy (EIS) measurements were carried out after the 2nd and 100th charge-discharge cycles. For each measurement, the cells were first galvanostatically cycled to the desired cycle numbers (between 4.5 V and 2.8 V at the current of 300 mA/g), followed by

charging them to 4.5 V at a small current of 15 mA/g, discharged to 3.8 V at the same current, and then allowed the cell to relax to its open circuit potential for 3 h. Fig.2.8a and Fig.2.8b show the Nyquist plots of both of the samples. The impedance spectra were fitted by the equivalent circuit model as shown in Fig.2.8c. The R_{sol} represents electrolyte resistance, R_{sei} represents the impedance of the natural and artificial solid electrolyte interface and the impedance of electrons through the active materials. This part corresponds to the first semicircle from the high to medium frequency region in the Nyquist plots. The R_{ct} represents the charge transfer resistance which corresponding to the second semicircles in the low-frequency region. And the last parts in the lowest frequency region are due to the diffusion of lithium ions in the solid electrodes, as introduced by Warburg [6]. The fitting results are depicted in Table 2.3. At the second cycle, the R_{sei} value of the 3 wt% V_2O_5-coated material is 27.55 Ω, however, for the pristine samples, the R_{sei} value is only 6.92 Ω. Because at the initial state of the battery, the amorphous V_2O_5 layer produced a resistance for the transfer of Li^+ ions and electrons in the electrode and electrolyte interface layer. Upon cycling, the R_{sei} value of pristine samples increased rapidly. The side reactions made the surface of electrodes become rough, and the transfer of charge and electrons at this region became more and more difficult. Both of the two samples showed small charge transfer resistance at the second cycles. So it (R_{ct}) played a minor role at the initial stage of the cycles. But the R_{ct} values of the pristine electrode increased faster than the V_2O_5-coated materials upon cycling. The R_{ct} value of the pristine material was 12.04 Ω at the second cycle, rapidly increased to 267.1 Ω at the 100^{th} cycles. However, for 3 wt% V_2O_5-coated sample, the R_{ct} values was 16.31 Ω at the second cycle and slowly increased to 141.6 Ω at the 100^{th} cycle. The abrupt increase in charge-transfer resistance of the $Li[Ni_{1/3}Co_{1/3}Mn_{1/3}]O_2$ has been reported by others, and considered as the main reasons for the capacity fading [22]. From the EIS data, we can conclude that the V_2O_5-coating layer can stable the interface of electrode/electrolyte and slow down the increase of charge transfer resistance. And also it in turns limits the increase of the total cell resistance and suppress the capacity fading of the V_2O_5-coat $Li[Ni_{1/3}Co_{1/3}Mn_{1/3}]O_2$.

Table 2.3 Fitting results of the AC impedance parameters

Samples	R_{sol} (Ω) At the 2nd	R_{sol} (Ω) At the 100th	R_{sei} (Ω) At the 2nd	R_{sei} (Ω) At the 100th	R_{ct} (Ω) At the 2nd	R_{ct} (Ω) At the 100th
pristine	4.32	14.99	6.92	21.47	12.04	267.1
3 wt%-coated	6.53	10.69	27.55	23.64	16.31	141.6

2.4 Conclusions

V_2O_5 has been uniformly coated on the surface of layered $Li[Ni_{1/3}Co_{1/3}Mn_{1/3}]O_2$, and the surface coating layer have been confirmed by multiple techniques.According to the electrochemical performance investigations, the one with 3 wt% V_2O_5-coated sample showed the best performance in terms of cycle and rate capacities. After 100 cycles, discharge capacities retention have been improved from 59.2% to 83.2% by V_2O_5-coating. As evidenced by CV and EIS, the V_2O_5-coating layer suppressed the side-reactions between the electrode and electrolyte and the increase of charge-transfer resistance upon cycling. Unfortunately, a dissolution of V from the charged V_2O_5-coated samples have been detected when stored the electrode at high charged state for a long time. This result inspired us to look for other suitable coating layer material to enhanced the electrochemical properties of $LiNi_{1/3}Co_{1/3}Mn_{1/3}O_2$.

2.5 References

[1] H. Q. Li and H. S. Zhou: "Enhancing the performances of Li-ion batteries by carbon-coating: present and future", *Chem. Commun.* Vol. 48 pp. 1201-1217, 2012

[2] X. Z. Liu, H. Q. Li, E. Yoo, M. Ishida and H. S. Zhou: "Fabrication of $FePO_4$ layer coated $LiNi_{1/3}Co_{1/3}Mn_{1/3}O_2$: Towards high-performance cathode materials for lithium ion batteries", *Electrochim. Acta*, Vol. 83, pp. 253-258, 2012

[3] S. T. Myung, K.Amine and Y. K. Sun: "Surface modification of cathode materials from nano- to microscale for rechargeable lithium-ion batteries", *J. Mater. Chem.*, Vol. 20, pp. 7074-7095, 2010

[4] S. K. Hu, G. H. Cheng, M. Y. Cheng, B. J.Hwang and R. Santhanam: "Cycle life improvement of ZrO_2-coated spherical $LiNi_{1/3}Co_{1/3}Mn_{1/3}O_2$ cathode material for lithium ion batteries", *J. Power Source*, Vol. 188, pp. 564-589, 2009

[5] M. Wang, F. Wu, Y. F. Su and S. Chen: "Modification of $LiNi_{1/3}Co_{1/3}Mn_{1/3}O_2$ cathode material by CeO_2-coating", *Science China Series E*, Vol. 52, pp. 2737-2741, 2009

[6] L. A. Riley, S. Van Ana, A. S. Cavanagh, Y. Yan, S. M. George, P. Liu, A. C. Dillon and S. H. Lee: "Electrochemical effects of ALD surface modification on combustion synthesized $LiNi_{1/3}Co_{1/3}Mn_{1/3}O_2$ as a layered-cathode material", *J. Power Source*, Vol. 196, pp.3317-3324, 2011

[7] S. H. Yun, K. S. Park and Y. J. Park: "The electrochemical property of ZrFx-coated $LiNi_{1/3}Co_{1/3}Mn_{1/3}O_2$ cathode material", *J. Power Source*, Vol. 195 pp. 6108-6115, 2010

[8] K. S. Lee, S. T. Myung, D. W. Kim and Y. K. Sun: "AlF_3-coated $LiCoO_2$ and $LiNi_{1/3}Co_{1/3}Mn_{1/3}O_2$ blend composite cathode for lithium ion batteries", *J. Power Source*, Vol. 196, pp. 6974-6977, 2011

[9] Y. K. Sun, S. W. Cho, S. W. Lee, C. S. Yoon and K. Amine: "AlF_3-coating to improve high voltage cycling performance of $LiNi_{1/3}Co_{1/3}Mn_{1/3}O_2$ cathode materials for lithium secondary batteries", *J. Electrochem. Soc.*, Vol. 154, pp. A168-A172, 2007

[10] H. S. Kim, Y. Kim, S. Kim and S. W. Martin: "Enhanced electrochemical

properties of $LiNi_{1/3}Co_{1/3}Mn_{1/3}O_2$ cathode material by coating with $LiAlO_2$ nanoparticles", *J. Power Source*, Vol. 161, pp. 623-627, 2006

[11] P. Zhang, L. Zhang, X. Ren, Q. Yuan, J. Liu and Q. Zhang: "Preparation and electrochemical properties of $LiNi_{1/3}Co_{1/3}Mn_{1/3}O_2$-PPy composites cathode materials for lithium-ion battery", *Synthetic Metal*, Vol. 161, pp. 1092-1097, 2011

[12] C. V. Rao, A. L. M Raddy, Y. Ishikawa and P. M. Ajayan: "$LiNi_{1/3}Co_{1/3}Mn_{1/3}O_2$-Graphene Composite as a Promising Cathode for Lithium-Ion Batteries", *ACS Applied Mater Interface*, Vol. 3, pp. 2966-2972, 2011

[13] K. S. Park, A. Benayad, M. S. Park, A. Yamada and S. G. Doo: "Tailoring the electrochemical properties of composite electrodes by introducing surface redox-active oxide film: VO_x-impregnated $LiFePO_4$ electrode", *Chem. Commun.*, Vol. 46, pp. 2572-2574, 2010

[14] K. S. Park, A. Benayad, M. S. Park, W. Choi and D. Im: "Suppression of O_2 evolution from oxide cathode for lithium-ion batteries: VO_x-impregnated $0.5Li_2MnO_3$-$0.5LiNi_{0.4}Co_{0.2}Mn_{0.4}O_2$ cathode", *Chem. Commun.*, Vol. 46, pp. 4190-4192, 2010

[15] J.W. Lee, S. M. Park and H. J. Kim: "Enhanced cycleability of $LiCoO_2$ coated with vanadium oxides", *J. Power Source*, Vol. 188, pp. 583-587, 2009

[16] J. Livage, "Sol-gel chemistry and electrochemical properties of vanadium oxide gels", *Solid State Ionics*, Vol. 86-88, pp. 935-942, 1996

[17] J.Cho: "VO_x-coated $LiMn_2O_4$ nanorod clusters for lithium battery cathode materials", *J. Mater. Chem.*, Vol. 18, pp. 2257-2261, 2008

[18] J. Wang, X. Yao, X. Zhou and Z. Liu: "Synthesis and electrochemical properties of layered lithium transition metal oxides", *J. Mater. Chem.*, Vol. 21, pp. 2544-2549, 2011

[19] K. M. Shaju, G. V. Subba and B. V. R. Chowdari: "Performance of layered $LiNi_{1/3}Co_{1/3}Mn_{1/3}O_2$ as cathode for Li-ion batteries", *Electrochim. Acta*, Vol. 48, pp. 145-151, 2002

[20] Y. Koyama, N. Yabuuchi, I. Tanaka, H. Adachi and T. Ohzuku: "Solid-state chemistry, and electrochemistry of $LiNi_{1/3}Co_{1/3}Mn_{1/3}O_2$ for advanced lithium-ion

batteries - I. First-principles calculation on the crystal and electronic structures", *J. Electrochem. Soc.*, Vol. 154, pp. A1545-A1551, 2004

[21] J. Reed and G. Ceder: "Charge, potential, and phase stability of layered $Li(Ni_{0.5}Mn_{0.5})O_2$", *Electrochem. Solid State Letter*, Vol. 5, pp. A145-A148, 2002

[22] J. Li, L. Wang, Q. Zhang and X. He: "Electrochemical performance of SrF_2-coated $LiNi_{1/3}Co_{1/3}Mn_{1/3}O_2$ cathode materials for Li-ion batteries", *J. Power Source*, Vol. 190, pp. 149-153, 2009

Chapter 3. PEDOT modified $LiNi_{1/3}Co_{1/3}Mn_{1/3}O_2$ with enhanced electrochemical performance for lithium ion batteries

3.1 Introduction

Despite the great progress for $LiNi_{1/3}Co_{1/3}Mn_{1/3}O_2$ by surface coating have been achieved, increasing of rate capability and cycle life still remain as necessary developments before it is more widely feasible applications [1-5]. In chapter 2, we studied the electronic and ionic double conductive material V_2O_5 as coating layer to improve its electrochemical performance of $LiNi_{1/3}Co_{1/3}Mn_{1/3}O_2$. The dissolution of V at a high cutoff voltage prohibited it acted as a more positive role in coating layer materials. Inspired by this work, herein, no metal dissolution but conductive coating layer material, organic conductive polymer Poly-3,4-ethylenedioxythiophene (PEDOT), come into our sight.

Previously reports demonstrated that conductive polymers, when used as a coating layer, showed positive effects on the performances $Li_{1.2}Mn_{0.54}Co_{0.13}Mn_{0.13}O_2$ [6], $LiFePO_4$ [7] and $LiNi_{0.5}Mn_{1.5}O_4$ [8] etc. Poly-3,4-ethylenedioxythiophene (PEDOT), as a good electric conductor, has attracted the attention of battery researchers until recently. For example, Schougaard et al. fabricated poly(3,4-ethylenedioxythiophene) PEDOT/$LiFePO_4$ composites by a soft chemical approach to enhance the rate capacity [9]. PEDOT/$LiCoO_2$ composite has also been synthesized by electrochemical deposition [10]. *In situ* polymerization method was developed more recently by using Fe^{3+} as oxidant during preparation of PEDOT coated FeF_3 [11]. However, the effective coating of PEDOT on layered $LiNiCoMnO_2$ series cathode has not been investigated so far. For $LiNiCoMnO_2$ series cathode, the utilization of an external oxidant during in situ polymerization of the conductive coating layer would result in residue of the ion impurity in the final products. Thus, a facile and effective strategy to fabricate PEDOT modified $LiNiCoMnO_2$ series cathode should be developed toward superior rate and cycle performance.

In this chapter, we report the fabrication of PEDOT modified $LiNi_{1/3}Co_{1/3}Mn_{1/3}O_2$ by a facile method. To avoid the introduction of foreign ions in the products, commercial PEDOT solution was used as coating material. Evidence of the surface coating was obtained by TEM and IR. Rate and cycle performance were conducted to investigate the PEDOT effects on the electrochemical performance of $LiNi_{1/3}Co_{1/3}Mn_{1/3}O_2$. CV on cycled cells were performed to demonstrate the improvements of electrochemical properties after PEDOT modification.

3.2 Experimental and Characterization

3.2.1 Preparation of PEDOT coated $LiNi_{1/3}Co_{1/3}Mn_{1/3}O_2$

$LiNi_{1/3}Co_{1/3}Mn_{1/3}O_2$ was prepared according to the reference [12]. 0.5g of pristine $LiNi_{1/3}Co_{1/3}Mn_{1/3}O_2$ and target amount of PEDOT aqueous solution were mixed and grounded in an agate mortar for more than 30 min, then the mixture were dried at 80 ℃ in vacuum for one night. The final product was obtained by annealing at different temperature in air. To explore the optimum coating conditions, the coating amount were changed from 1 wt% to 4 wt% and the annealing temperature varied from 200 ℃ to 400 ℃. For convenience, the samples were marked as X wt%-T in which X represents the coating amount and T represents the annealing temperature.

3.2.2 Characterization

XRD (Bruker D8 with Cu *Kα* radiation, λ= 0.1546nm) was used to characterize the structure of the pristine and coated samples. The coating layer and surface morphology before and after modification were examined by TEM on a JEOL 3100F instrument. The PEDOT layer was examined by Fourier transform infrared (FTIR) measurements on a JASCO instrument of FT/IR-6200 from 4000 to 400 cm^{-1}. Raman spectroscopy was conducted on a Micro Raman spectrophotometer (Ventuno21, JASCO).

3.2.3 Fabrication of batteries and electrochemical test

Electrochemical performance of all the samples were conducted using coin-type cells (CR2032) consisting of a cathode, a Celgard separator and a Li metal with 1 M $LiPF_6$ in EC/DEC (1:1 vol%) as the electrolyte. All the cells were assembled in an Ar-filled glove box. The cathode electrode was fabricated from a mixture of active material:acetylene black:polytetra-fluoroethylene (PTFE) 80:15:5 (mass%) impressed on an aluminum mesh current collector. The galvanostatic charge-discharge tests were conducted on a Hokuto Denko in a potential range of 2.8-4.5V (vs. Li/Li^+) at a certain current density. CV was examined by coin cells on a Solartron Instrument Model 1287 with different scan rates. Thermal stability was examined by differential scanning calorimetry (DSC) on EXSTAR 7000 X-DSC in a temperature range of 30-320 ℃ at a heating rate of 10 ℃/min. Before DSC measurements, the cells were first charging to 4.3 V at a current of 15 mA/g and then charge at 4.3 V for another 3 hours. After that, the cells were disassembled in an Ar filled glove box, the charged samples were collected and sealed in Al-pan for DSC measurements.

3.3 Results and Discussion

3.3.1 Confirmation of surface coating layer

XRD patterns of the pristine $LiNi_{1/3}Co_{1/3}Mn_{1/3}O_2$ and 2 wt%-300 PEDOT coated samples are showed in Fig.3.1. All the patterns of pristine $LiNi_{1/3}Co_{1/3}Mn_{1/3}O_2$, can be well indexed to the space group *R-3m*. The splitting of the peaks (108), (110) and (006), (102) is an indication of a well ordered α-$NaFeO_2$ structure, the ratios of I_{003}/I_{104} is above 1.2, which indicates the desirable cation mixing [13,14]. For the coated sample, all the diffraction peaks can also be well accordance with the pristine sample, showing negligible structure changes by surface coating. No impurities or secondary phase were observed from XRD patterns. The lower and thinner organic coating layer can not be detected by XRD. In addition, the relatively low heat treatment temperature seemed not allow for the formation of new phase or structure.

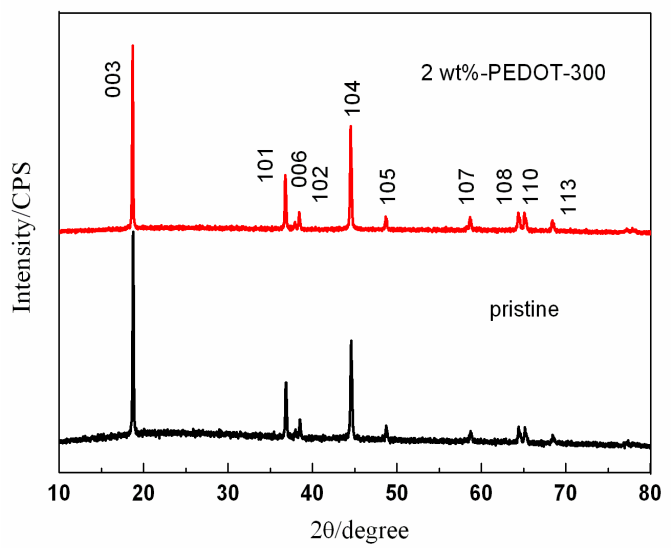

Fig. 3.1. XRD patterns of pristine $LiNi_{1/3}Co_{1/3}Mn_{1/3}O_2$ (Black line) and 2 wt% PEDOT-300 (Red line).

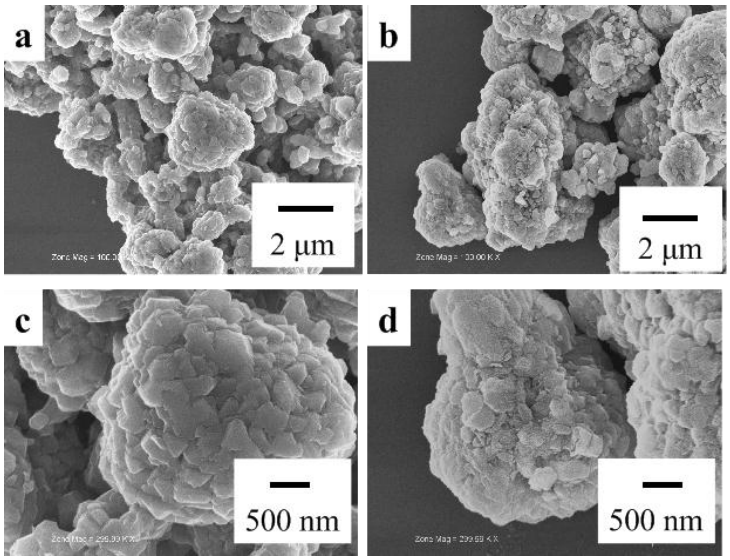

Fig. 3.2. SEM images of pristine $LiNi_{1/3}Co_{1/3}Mn_{1/3}O_2$ (a, c) and 2 wt% PEDOT-300 ℃ (b, d).

SEM images of pristine and 2 wt%-300 coated samples in Fig. 3.2 show the surface morphology and particle size changes after surface modification. Both of the samples exhibit secondary spherical structures with a diameter varied from 1 μm to 5 μm. The primary particle size is in the range of 200-400 nm. There are no obvious changes in particle size after surface coating. The edge and surface is clean and smooth for the

pristine as shown in Fig.3.2c. In contrast, it becomes rough and ambiguous after coating as shown in Fig.3.2d.

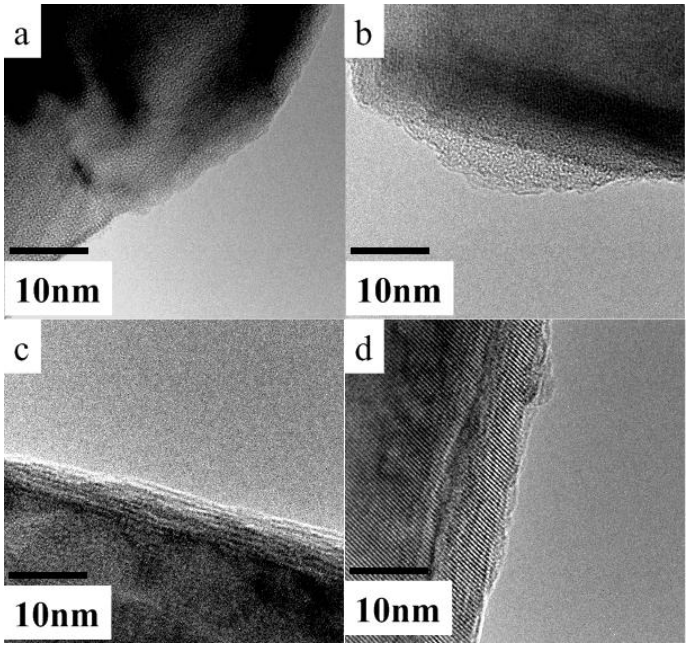

Fig. 3.3. TEM images of (a) pristine $LiNi_{1/3}Co_{1/3}Mn_{1/3}O_2$ powder, (b) 4 wt% PEDOT-300 ℃, (c) 2 wt% PEDOT without heat treated (d) 2 wt% PEDOT-300 ℃.

In order to observe the detailed existence of PEDOT on the surface, TEM were conducted on different samples. Fig.3.3a displays the image of as prepared pristine $LiNi_{1/3}Co_{1/3}Mn_{1/3}O_2$ with a clear and clean surface. For 4 wt% PEDOT coated sample, a coarser surface with a coating layer about 10 nm can be seen clearly in Fig.3.3b, while only a 4 nm coating layer can be observed for the 2 wt% coated sample as shown in Fig.3.3c. With the decreasing of coating amount, the surface layer became thinner. Heat treatment can decompose part of the organic component. Thus, after annealing the 2 wt% PEDOT coated sample at 300 ℃ for 5 h, a thinner layer can be obtained as observed in Fig.3.3d, there is only a very thin amorphous layer on the particle surface. From these results, we can find that a heat treating even at 300 ℃ can decompose part of the amorphous coating layer.

The existence of PEDOT on the particle surface can be further confirmed by

comparison of the IR spectrum of pristine $LiNi_{1/3}Co_{1/3}Mn_{1/3}O_2$ and coated sample. As shown in Fig.3.4a, pristine $LiNi_{1/3}Co_{1/3}Mn_{1/3}O_2$ exhibits two well separated band at 590 and 540 cm^{-1} which come from the M-O vibration [15]. No significant blue-shift or red-shift can be observed after surface coating in this region, indicating no strong interaction between PEDOT and $LiNi_{1/3}Co_{1/3}Mn_{1/3}O_2$, or no distortion of the intrinsic lattice structure of $LiNi_{1/3}Co_{1/3}Mn_{1/3}O_2$. The presence of PEDOT is confirmed by the C=C ring and C-O-R vibration at about 1180 cm^{-1} and the C-S vibration at 939 cm^{-1} [9]. These results demonstrate that the PEDOT has coated on the surface. Raman spectra were also employed to obtain more information about the surface structure as shown in Fig.3.4b. Raman bands centered at about 590 cm^{-1} can be assigned to the M-O symmetrical stretching vibration which attribute Raman modes of A_{1g} of the layered $LiNi_{1/3}Co_{1/3}Mn_{1/3}O_2$ [16-18]. No Raman bands from PEDOT is recorded due to the low weight content of the coating layer. Raman bands of the heat treated samples exhibit a 4 cm^{-1} blue shift compared to the samples without heat treatment. The reason might be that the heat treatment leads to more closely interact between the surface coating layer and the core material so that the M-O vibration at the surface layer was influenced. It is also evidenced the heat treatment made the coating layer contact with the core $LiNi_{1/3}Co_{1/3}Mn_{1/3}O_2$ more closely.

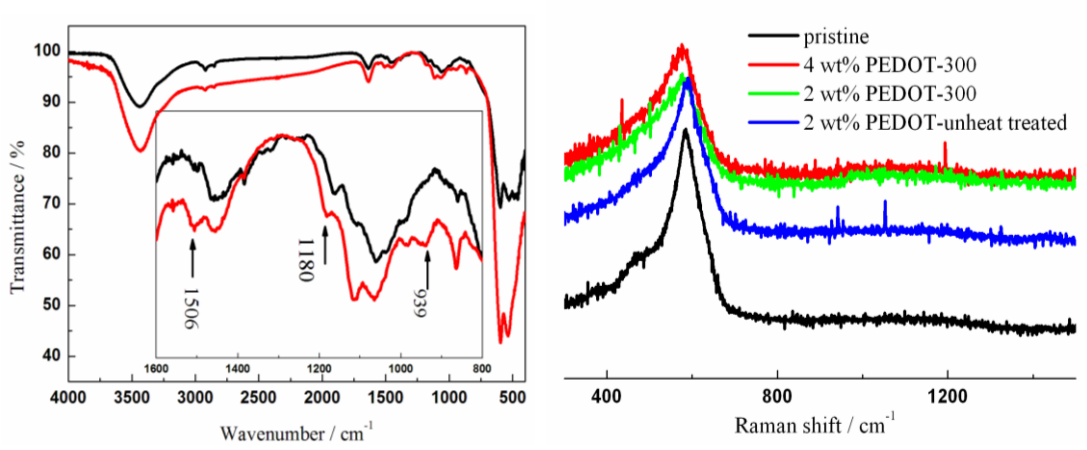

Fig. 3.4. (a: left) FTIR of pristine $LiNi_{1/3}Co_{1/3}Mn_{1/3}O_2$ (Black) and PEDOT-coated sample (Red); (b: right) Raman spectrum of pristine and PEDOT coated samples.

3.3.2 Electrochemical performance

Coin cells using metallic Li as the counter electrode were assembled and galvanostatic charge/discharge test is employed to evaluate the cycle and rate performances after surface modification by PEDOT. The charge-discharge cycle performance was conducted in the voltage range of 2.8-4.5 V at a current of 150 mA/g. As shown in Fig.3.5a, the pristine material suffered a serious capacity fading upon cycling with a discharge capacity of 116.6 mAh/g at the 80th cycle. While for the PEDOT coated samples, the discharge capacities of 1 wt%-300, 2 wt%-300 and 4 wt%-300 are 125.6, 133.7 and 132.2 mAh/g at the 80th cycle, respectively. This result clearly demonstrated that the PEDOT coating layer can improve the cycle performance of $LiNi_{1/3}Co_{1/3}Mn_{1/3}O_2$, and also make us believe that an appropriate thickness of coating layer is very important to the coating effects.

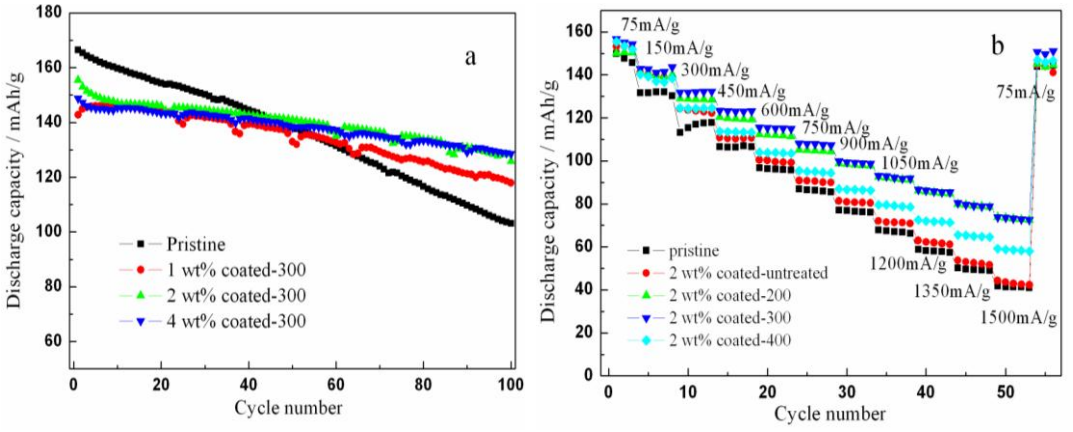

Fig. 3.5. (a) Cycle performance of pristine $LiNi_{1/3}Co_{1/3}Mn_{1/3}O_2$ and PEDOT coated samples with different coating amount in the voltage range of 4.5 and 2.8 V vs. Li^+/Li; (b) rate performance of pristine and 2 wt% PEDOT coated samples with different annealed temperature.

Rate capability of cathode is an important feature for the cathode in widely application especially as power source for automobile. Actually, this work is originally inspired with the expectation that the conductive polymer can improve the surface conductivity to enhance the rate capacity. Thus, the rate capacities were

examined as shown in Fig.3.5b. In order to get the optimum coating condition, the influence of heat treatment temperature was studied on 2 wt% PEDOT coated samples have been studied. All the rate tests were conducted in the potential range of 2.8-4.5V (vs. Li^+/Li) with varied current densities from 75 mA/g to 1500 mA/g. The rate performance of 2 wt% coated samples without any heat treatment is only slightly improved in comparison with the pristine $LiNi_{1/3}Co_{1/3}Mn_{1/3}O_2$. After annealing, there is an obvious improvement of the discharge capacity especially at high current densities. For example, at the same charge-discharge current of 1500 mA/g, the coated samples with no heat treatment, 200℃ heat treatment, 300℃ heat treatment, 400℃ heat treatment delivered a discharge capacity of 44.3, 73.8, 73.9, and 59.2 mAh/g, respectively. In contrast, the pristine sample only showed a discharge capacity of 41.8 mAh/g at the charge-discharge current of 1500 mA/g. It is obviously the different heating temperature played an important role on the PEDOT coating effects. This may because the heat treatment not only results in some changes of the surface morphology as has been confirmed by TEM, but also an effect on the vibrational of M-O at the interface of coating layer and the core material as evidenced by Raman spectrum. The two changes together promote the electron and ion transfer between the electrode and electrolyte. Thus, the enhancement of electrochemical performance by surface coating can be interpreted from two aspects. One is the coating layer with heat treatment obviously alleviate the surface polarization by facilitating the electron transfer at the interface of electrode and electrolyte. The other is the coating layer separates the active material from directly contraction with the electrolyte, which can impeded the side-reactions at the interface. It is understandable that the charged electrodes with their metal ions at high valence states are easy to react with the electrolyte and lead to the capacity fading.

3.3.3 Electrochemical analysis

In order to better understand the effects of the improvement of electrochemical performance, the galvanostatic intermittent titration technique (GITT) measurements on fresh and cycled cells were conducted to investigate the polarization effects before

and after cycled charge/discharge processes. Before the GITT measurements, the cells were firstly gavanostatic charge/discharged for a certain number of cycles. GITT measurements were performed by charging/discharging the aged cells at a constant current (20 mA/g) for an interval of 1 hour followed by an open circuit stand for 3 hours to allow the cell voltage to relax to its quasi-equilibrium state. As shown in Fig.3.6a and 3.6b, there are no obvious differences between the pristine and the coated sample for the fresh cells. However, after 100 charge/discharge cycles, the differences in charge potential for the pristine and coated sample became more obviously. The increase of charge potentials upon cycling is mainly caused by the aggravation of surface polarization. There is an obviously increase of charge potentials for both of the pristine and coated samples. If define the difference of charge potentials between the fresh cells and cycled cells as ΔE, it is clear that ΔE for the pristine is larger than that of the coated sample. The PEDOT coating layer suppresses the deterioration of the surface polarization at a certain degree. It is a general consensus that mass transport in the electrolyte and the solid phase of the electrodes, contact problems between the solid phases and slow electrochemical reactions account for the polarization of the batteries [19]. That is to say, the PEDOT coating layer suppressed the surface polarization by facilitating the mass transfer at the interface of electrode and electrolyte. As the increasing of charge/discharge current, there is an increasing of charge potential and a decreasing of discharge potential which implies a decreasing energy efficiency. This should be mainly attributed to the polarization of the batteries. The average charge potential of pristine sample was 4.32 V when the charge-discharge current at 1500 mA/g, while, the corresponding value for the 2 wt%-300 PEDOT coated sample was 4.21 V as shown in Fig.3.6c. Apparently, the PEDOT coating layer suppressed the increase of charge potential especially at a high charge-discharge current. Since the polarization effects depends on the C-rate, the average charge/discharge potentials with different charge discharge currents is shown in Fig.3.6d. The average charge (discharge) potentials increase (decrease) obviously with the increasing of C-rates. The PEDOT coated sample showed a suppressed effects on the changes of average potentials along with

the changes of C-rate. This is primarily because the PEDOT coating layer prevent the surface polarization by promoting the mass transfer at the interface of electrode and electrolyte. The surface coating by PEDOT not only improve the charge/discharge capacities, but also enhance the energy efficiency.

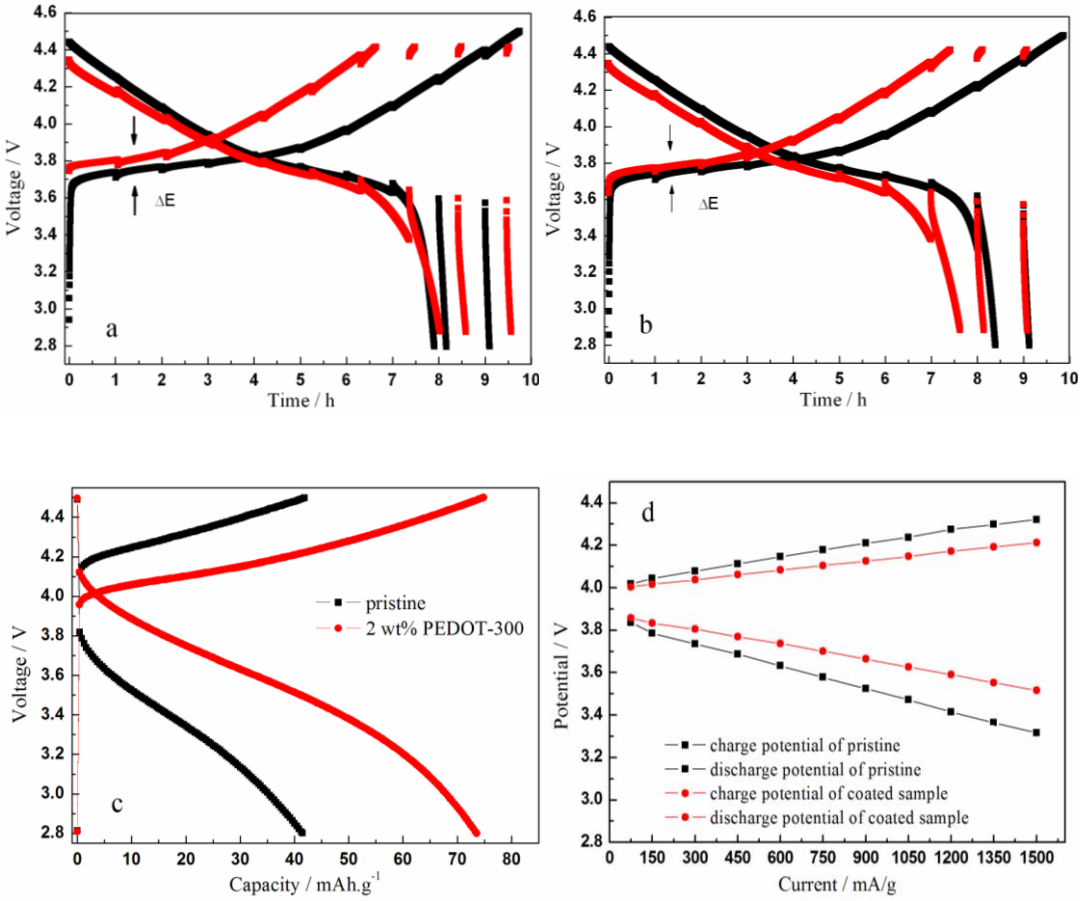

Fig. 3.6. GITT of pristine $LiNi_{1/3}Co_{1/3}Mn_{1/3}O_2$ (a) and 2 wt% PEDOT-300 coated sample (b) on fresh (black line) and cycled cells (red line); charge-discharge profiles at 1500 mA/g (c) and average potential with different charge-discharge current (d).

Cyclic voltammertry (CV) is a useful tool to study the electrochemical performances and electrode kinetics of oxide materials. CV at different scan rates was performed to evaluate the PEDOT coating effects. CV measurements were conducted at the voltage range of 2.0-4.6V (vs. Li^+/Li) with varied scan rates from 0.1 to 0.5 mV/s on both of the fresh and cycled cells of pristine and 2 wt%-300 PEDOT coated

samples.

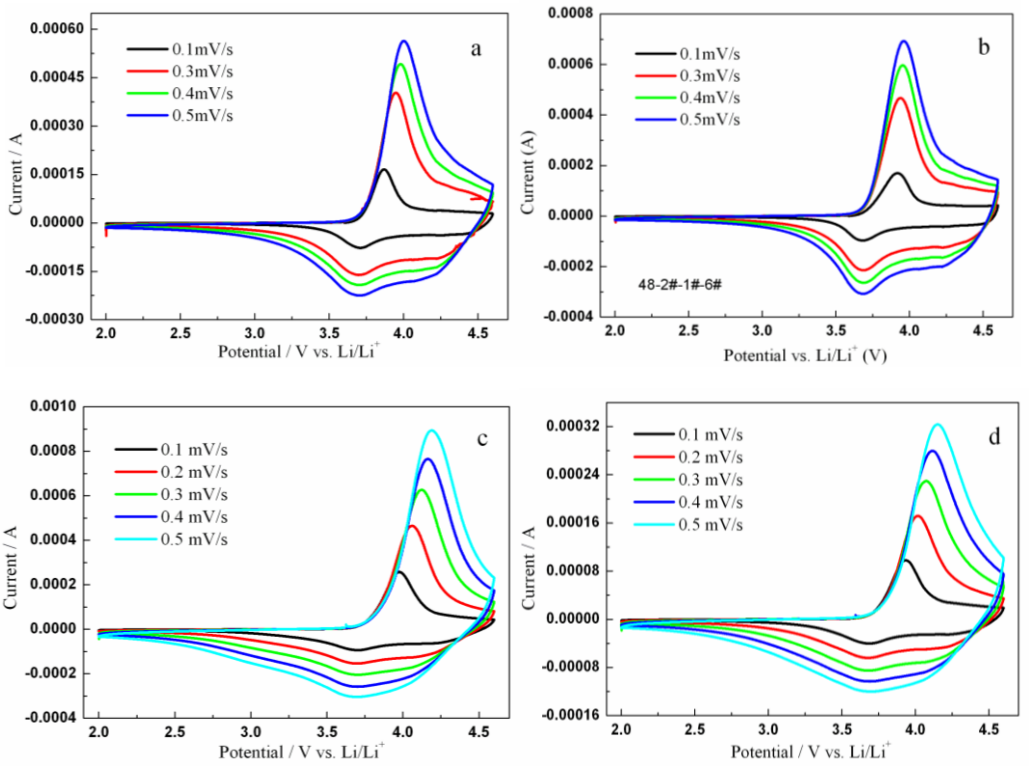

Fig. 3.7. CV curves of pristine and 2 wt% PEDOT-coate-300 ℃ sample before and after charge-discharge cycles at a series of sweep rates, (a) pristine-fresh; (b) coated-fresh; (c) pristine-cycled; (d) coated-cycled.

As shown in Fig.3.7, at a sweep rate of 0.1 mV/s, a couple of well refined peaks at 3.98/3.70 V for the pristine sample and 3.94/3.69 V for the coated samples were recorded. These peaks originated from the redox of Ni^{2+}/Ni^{4+}couple [20]. After charge/discharge cycles, as shown in Fig.3.7c and 7d, there is an obvious shift of both of the cathodic and anodic peaks. The cathodic peaks shifted to a higher potential while the anodic peaks shifted to a lower potential. After the charge/discharge cycles, the surface polarization become more seriously due to the side-reactions between the electrode and electrolyte. At high sweep rates, there are also some changes should be noted. Firstly, the current density and redox peaks area increase for all of the four samples, since the peak area divided by the sweep rate which present the capacity. Secondly, there are a increase cathodic peak potentials which may result from the polarization of the batteries. In contrast, there were almost no changes for the anodic

peak potentials of all the samples. The unasymmetric changes of the charge and discharge processes make us aware of that the polarization of batteries showed a greater impact on the charge processes than the discharge processes.

For the comparison of the changes of cathodic peak potentials, plots of cathodic peak potentials versus sweep rates were shown in Fig. 3.8. The peak potentials of the pristine samples is remarkably larger than the coated samples, especially at higher sweep rates. The potential difference means that polarization effects become more manifest at higher sweep rate. The battery polarization is mainly caused by the mass transfer barriers at the interface of electrode and electrolyte. The shift level of the coated samples decreases compared with the pristine one on both of the fresh and cycled cells, which demonstrates the alleviation of polarization due to the promotion of mass transfer properties with the help of PEDOT coating layer.

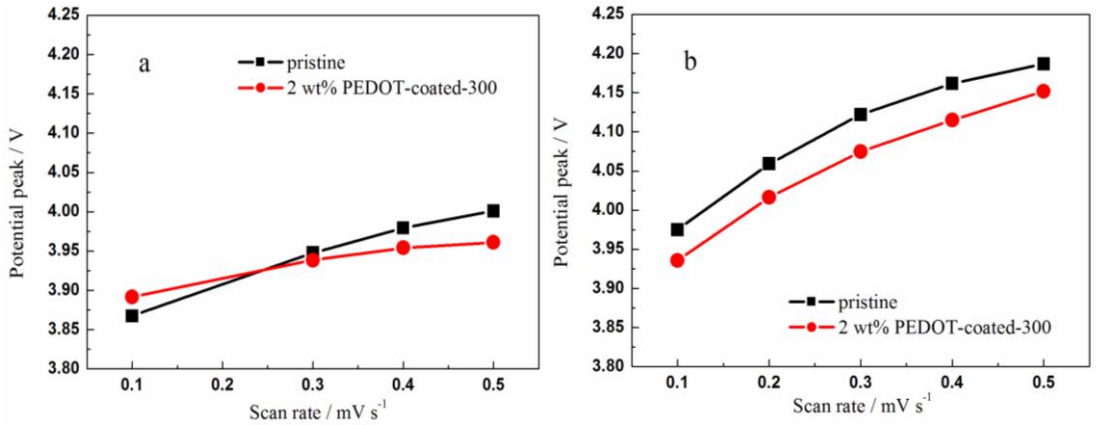

Fig. 3.8. Changes of peak potentials as function of scan rate (a) on fresh cells; (b) on charge-discharged cells.

3.3.4 Thermal Stability

Thermal stability of cathode materials plays an important role in judging their practical application in lithium ion batteries. A DSC study was conducted after charging the cathodes to 4.3 V to evaluate the effects of PEDOT coating on the thermal stability of $LiNi_{1/3}Co_{1/3}Mn_{1/3}O_2$. Fig. 3.9 shows the DSC profiles of the

pristine and 2 wt%-300 PEDOT coated samples. The pristine $LiNi_{1/3}Co_{1/3}Mn_{1/3}O_2$ showed an exothermic peak at 283.1 ℃ with an exothermic heat generation of 129.0 J/g. While the exothermic peak of coated samples shifted to 284.6 ℃ with an exothermic heat generation of 69.3 J/g. The thermal decomposition temperature showed a minor increase, but the exothermic heat generation decrease obviously. The improved thermal stability of the coated sample rooted in the PEDOT coating layer, which prevents the oxidized cathode electrode from directly contact with the electrolyte, thus, reducing the exothermic reaction.

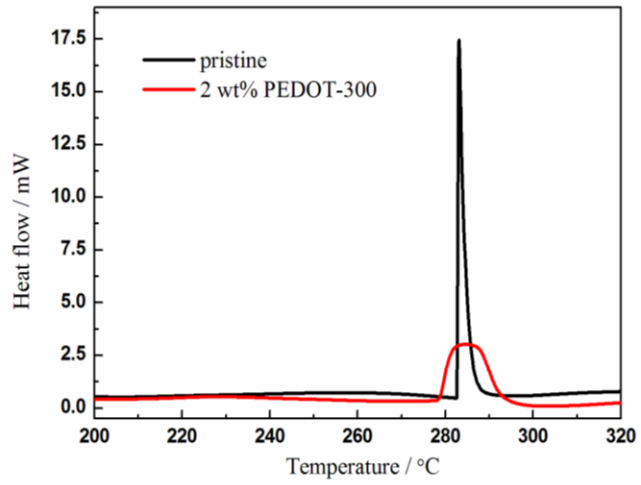

Fig. 3.9. DSC profiles of pristine and 2 wt% PEDOT-300 electrodes charged to 4.3V.

3.4 Conclusions

The effect of PEDOT coating on electrochemical performances of $LiNi_{1/3}Co_{1/3}Mn_{1/3}O_2$ cathode was investigated and the optimum coating condition is with coating amount of 2 wt% and heat treated at 300 ℃. The rate capacity have been significant improved from 41.8 mA/g to 73.9 mAh/g at a charge-discharge current of 1500 mA/g. The energy efficiency has also been improved obviously. Compared the GITT curves and varied sweep rate of CV before and after charge-discharge cycles, the PEDOT coating layer obviously suppressed the battery polarization, especially at a high charge/discharge current. The PEDOT coating layer was found to improve the

thermal stability by reducing the exothermic heat generation. The main reason for the improved performance of PEDOT-coated $LiNi_{1/3}Co_{1/3}Mn_{1/3}O_2$ could be attributed to the conductive polymer layer promote the mass transfer at the interface of electrode and electrolyte which alleviate the surface polarization. This study demonstrated that surface coating with PEDOT is a facile but effective way to enhance the rate capabilities of $LiNi_{1/3}Co_{1/3}Mn_{1/3}O_2$ for lithium ion battery.

3.5 References

[1] Z. H. Chen, Y. Qin, K. Amine and Y. K. Sun:"Role of surface coating on cathode materials for lithium-ion batteries", *J. Mater. Chem.*, Vol. 20, pp. 7606-7612, 2010

[2] T. Ohzuku and Y. Makimura:"Layered lithium insertion material of $LiCo_{1/3}Ni_{1/3}Mn_{1/3}O_2$ for lithium-ion batteries", *Chem. Lett.*, pp. 642-643, 2001

[3] D. Aurbach, K. Gamolsky, B. Markovsky, G. Salitra, Y. Gofer, U. Heider, R. Oesten and M. Schmidt:"The study of surface phenomena related to electrochemical lithium intercalation into Li_xMO_y host materials (M = Ni, Mn)", *J. Electrochem. Soc.*, Vol. 147, pp. 1322-1331, 2000

[4] H. Li and H. Zhou:"Enhancing the performances of Li-ion batteries by carbon-coating: present and future", *Chem. Commun.*, Vol. 48, pp. 1201-1217, 2012

[5] M. Gu, I. Belharouak, J. Zheng, H. Wu, J. Xiao, A. Genc, K. Amine, S. Thevuthasan, D. R. Baer, J. Zhang, N. D. Browning, J. Liu and C. Wang:"Formation of the Spinel Phase in the Layered Composite Cathode Used in Li-Ion Batteries", *ACS Nano*, Vol. 7, pp. 760-767, 2013

[6] C. Wu, X. Fang, X. Guo, Y. Mao, J. Ma, C. Zhao, Z. Wang and L. Chen:"Surface modification of $Li_{1.2}Mn_{0.54}Co_{0.13}Ni_{0.13}O_2$ with conducting polypyrrole", *J. Power Source*, Vol. 231, pp. 44-49, 2013

[7] H. Y. Hui and J. B. Goodenough:"High-Rate $LiFePO_4$ Lithium Rechargeable Battery Promoted by Electrochemically Active Polymers", *Chem. Mater.*, Vol. 20, pp. 7237-7241, 2008

[8] J. H. Cho, J. H. Park, M. H. Lee, H. K. Song and S. Y. Lee:"A polymer electrolyte-skinned active material strategy toward high-voltage lithium ion batteries: a polyimide-coated $LiNi_{0.5}Mn_{1.5}O_4$ spinel cathode material case", *Energy Environ. Sci.*, Vol. 5, pp. 7124-7131, 2012

[9] D. Lepage, C. Michot, G. Liang, M. Gauthier and S. B. Schougaard:"A Soft Chemistry Approach to Coating of $LiFePO_4$ with a Conducting Polymer", *Angew. Chem. Int. Ed.*, Vol. 50, pp. 6884-6887, 2011

[10] L. J. Her, J. L. Hong and C. C. Chang:"Preparation and electrochemical

characterizations of poly(3,4-dioxyethylenethiophene)/$LiCoO_2$ composite cathode in lithium-ion battery", *J. Power Source*, Vol. 157, pp. 457-463, 2006

[11] D. Ma, Z. Y. Cao, H. G. Wang, X. L. Huang, L. M. Wang and X. B. Zhang:"Three-dimensionally ordered macroporous FeF_3 and its in situ homogenous polymerization coating for high energy and power density lithium ion batteries", *Energy Environ. Sci.*, Vol. 5, pp. 8538-8542, 2012

[12] J. Wang, X.Yao, X. Zhou and Z. Liu:"Synthesis and electrochemical properties of layered lithium transition metal oxides", *J. Mater. Chem.*, Vol. 21, pp. 2544-2549, 2011

[13] K. M. Shaju, G. V. Subba Rao and B. V. R. Chowdari:"Performance of layered $LiCo_{1/3}Ni_{1/3}Mn_{1/3}O_2$ as cathode for Li-ion batteries", *Electrochim. Acta*, Vol. 48, pp. 145-151, 2002

[14] X. Liu, H. Li, E. Yoo, M. Ishida and H. Zhou:"Fabrication of $FePO_4$ layer coated $LiCo_{1/3}Ni_{1/3}Mn_{1/3}O_2$: Towards high-performance cathode materials for lithium ion batteries", *Electrochim. Acta*, Vol. 83 , pp. 253-258, 2002

[15] Z. Wang, Y. Sun, L. Chen and X. Huang:"Electrochemical characterization of positive electrode material $LiCo_{1/3}Ni_{1/3}Mn_{1/3}O_2$ and compatibility with electrolyte for lithium-ion batteries", *J. Electrochem. Soc.*, Vol. 151, pp. A914-A921, 2004

[16] L. A. Riley, S. V. Atta, A. S. Cavanagh, Y. Yan, S. M. George, P. Liu, A. C. Dillon and S. H. Lee:"Electrochemical effects of ALD surface modification on combustion synthesized $LiCo_{1/3}Ni_{1/3}Mn_{1/3}O_2$ as a layered-cathode material", *J. Power Source*, Vol. 196, pp. 3317-3324, 2011

[17] C. Julien, M. A. Camacho-Lopez, T. Mohan, S. Chitra, P. Kalyani and S. Gopukumar:"Combustion synthesis and characterization of substituted lithium cobalt oxides in lithium batteries", *Solid State Ionics*, Vol. 135, pp. 241-248, 2000

[18] C. Julien:"Local cationic environment in lithium nickel-cobalt oxides used as cathode materials for lithium batteries", *Solid State Ionics*, Vol. 136-137, pp. 887-896, 2000

[19] A. Nyman, T. G. Zavalis, R. Elger, M. Behm and G. Lindbergh:"Analysis of the Polarization in a Li-Ion Battery Cell by Numerical Simulations", *J. Electrochem. Soc.*,

Vol. 157, pp. A1236-A1246, 2010

[20] X. Z. Liu, P. He, H. Q. Li, M. Ishida and H. S. Zhou:"Improvement of electrochemical properties of $LiCo_{1/3}Ni_{1/3}Mn_{1/3}O_2$ by coating with V_2O_5 layer", *J. Alloys Comp.*, Vol. 552, pp. 76-82, 2013

Chapter 4. Fabrication of $FePO_4$ layer coated $LiNi_{1/3}Co_{1/3}Mn_{1/3}O_2$: Towards high-performance cathode materials for lithium ion batteries

4.1 Introduction

Research and development new coating layer material to enhance the electrochemical performance of $Li[Ni_{1/3}Co_{1/3}Mn_{1/3}]O_2$ still challenge the materials scientists [1-3]. In the last chapter, we investigated PEDOT as coating layer to modify the surface of $Li[Ni_{1/3}Co_{1/3}Mn_{1/3}]O_2$ and an improved rate performance have been obtained. However, the cycle performance are still remain to be further improved for its possible decomposition with a long-term cycles at high cutoff voltage. Based on the results from two former chapters, acceptable coating materials for layered cathode should have additional features of no ion dissolution and high stability at high cutoff voltage.

Recent research progresses indicate that phosphate has become a popular coating material for its high stability. The strong covalency of the PO_4 polyanion with metal ions and the strong P=O bond can stabilize the interface of the electrode and electrolyte and then enhance the resistance of chemical attack [4]. The interest for $FePO_4$ coating layer is related to its high stability and abundant resource. It has been coated on the surface of $LiMn_2O_4$ [5], $Li_xNi_{0.9}Co_{0.1}O_2$ [6] and $LiCoO_2$ [7], respectively, and obtained enhanced cycle performance especially at elevated temperature. To our knowledge, $FePO_4$ has not been coated on $LiNi_{1/3}Co_{1/3}Mn_{1/3}O_2$.

In this chapter, we report the effect of $FePO_4$ coating on the electrochemical properties and thermal stability of $LiNi_{1/3}Co_{1/3}Mn_{1/3}O_2$. The synthesis process was conducted in an aqueous solution by co-precipitation method followed by a heat treatment in air. X-ray diffraction (XRD) and Transmission Electron Microscope (TEM) have been conducted to confirm the structure and surface morphology. The cycle and rate performance of $LiNi_{1/3}Co_{1/3}Mn_{1/3}O_2$ have been improved by $FePO_4$ coating. Cyclic Voltammetry (CV) and Electrochemical Impedance Spectroscopy

(EIS) were used to investigate the mechanism of the improvement in the electrochemical properties of the $FePO_4$-coated $LiNi_{1/3}Co_{1/3}Mn_{1/3}O_2$ material.

4.2 Experimental and Characterization

4.2.1 Preparation of $FePO_4$ coated $LiNi_{1/3}Co_{1/3}Mn_{1/3}O_2$

$LiNi_{1/3}Co_{1/3}Mn_{1/3}O_2$ powder was synthesized by co-precipitation method using carbonate as precipitant [8]. Coating process was conducted in aqueous suspension by coprecipitation. Firstly, $LiNi_{1/3}Co_{1/3}Mn_{1/3}O_2$ (2 g) was dispersed in 20 ml deionized water. After that, aqueous solution of $FeCl_3$ (with certain amount) was added to the slurry with vigorous stirring for 30 min. Then, stoichiometric amount of $NH_4H_2PO_4$ was added with stirring for 4 h. The slurry was dried at 80 ℃ for one night. Finally, the obtained powder was annealed in air at different temperature. The coating amount were changed from 1 wt% to 5 wt% and heat treat temperature from 300 to 600 ℃. For convenience, the samples are marked with X wt%- T ℃ in which X represent the coating amount and T represent the annealed temperature.

4.2.2 Characterization

XRD (Bruker D8 with Cu K_γ radiation, λ=0.15406 nm) was employed to analyze the structure of the pristine and coated samples. The surface morphology before and after surface coating were examined by TEM on a JEOL 3100F instrument with a voltage of 300 KV. The uniformity of the surface coating layer was confirmed by scanning electron microscopy (SEM, JSM-6700F) equipped with energy-dispersive X-ray spectrometry (EDS).

4.2.3 Fabrication of batteries and electrochemical test

The electrochemical performance of all the samples were conducted by coin cells (CR 2032) consisting of a cathode, metallic lithium anode, polypropylene separator and an electrolyte of 1M $LiPF_6$ in EC/DMC (1:2 vol.%). The cathode was fabricated

from a 80:15:5 (mass%) mixture of active material:acetylene black:polytetra-fluoroethylene (PTFE). The above mixture were mixed and grounded in an agate mortar and then pressed onto an aluminum mesh which served as a current collector and then dried at 80 ℃ for 12 h at vacuum. The cells were assembled in an Ar-filled glove box and subjected to galvanostatic cycles using a Hokuto Denko in a potential range of 2.8-4.5 V (vs. Li^+/Li) at certain current densities. The specific capacity and current density are based on the mass of synthesized cathode materials (for the coated materials, the coating layer was included). Cyclic Voltammetry (CV) were done with coin cells on a Solartron Instrument Model 1287 with a scan rate of 0.2 mV/s using lithium metal as both counter and reference electrodes. The electrochemical impedance spectroscopy (EIS) were also done with coin cells on a Solartron Instrument Model 1287 electrochemical interface and a 1255 B frequency response analyzer controlled by Z-plot. The measurements were performed in the frequency range 0.5 MHz to 0.01 Hz with an ac signal amplitude of 5 mV. Data analysis was done using the software Zview 2.70 (Scribner Associates Inc., USA). The thermal stabilities of pristine and coated sample were examined by differential scanning calorimetry measurement (Pyris 1), where the cell first charge to 4.5 V by a current of 15 mA g^{-1} and charge at this voltage for 5 h. The cells were disassembled in an Ar filled glove box to collect the charged cathode. Approximately 4 mg of the samples were hermetically sealed in a high-presure DSC Al pan. The measurement was conducted in a temperature range of 25-350 ℃ at a heating rate of 10 ℃ min^{-1} under a nitrogen atmosphere.

4.3 Results and Discussion

4.3.1 Confirmation of surface coating layer

Fig.4.1 shows the XRD patterns of pristine and $FePO_4$ coated powders (1, 2, 3, 4, 5 wt%). For the patterns of pristine, all the peaks can be indexed to the hexagonal α-$NaFeO_2$ structure with $R\bar{3}m$ space group. The splitting of the [(108),(110)] and [(006),(102)] indicate that the materials have a well ordered structure. The intensity

ratio of $I_{(003)}/I_{(004)}$ has been reported to be strongly correlated to undesirable cation mixing. The layered cathode materials with a ratio of $I_{(003)}/I_{(004)}$ >1.2 is an indication of desirable cation mixing and will show good electrochemical performance[9-10]. For the patterns of the coated samples, no impurities and secondary phases have been observed. In order to confirm the contents of coating layer, the $FePO_4$ coating layer was synthesized using the same route without adding of layered $LiNi_{1/3}Co_{1/3}Mn_{1/3}O_2$. The XRD patterns (Fig.4.1b) show that it can indexed to JCPDS card 01-071-3497 as compound $FePO_4$ with hexagonal structure. However, there are no corresponding peaks can be detected in the XRD patterns of coated samples. It is considered that such a lower amount of $FePO_4$ in coated samples can not be detected due to the accuracy limited of X-ray diffraction.

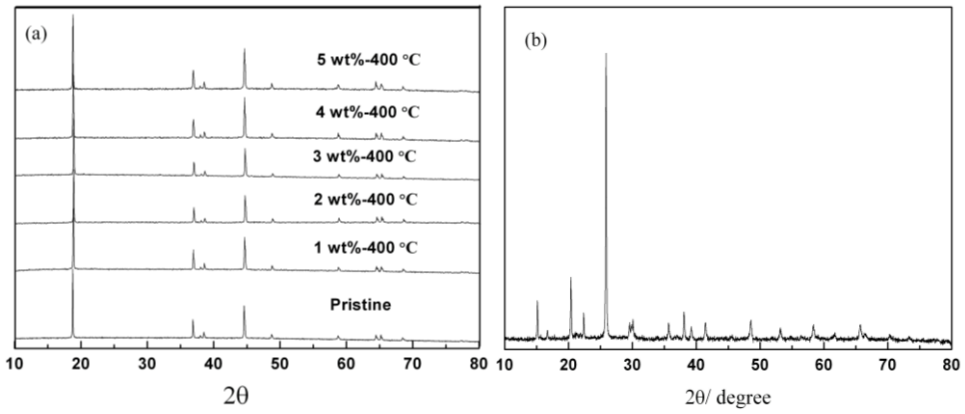

Fig. 4.1. XRD patterns of pristine and $FePO_4$-coated $LiNi_{1/3}Co_{1/3}Mn_{1/3}O_2$ powder (a) and $FePO_4$ (b).

Fig.4.2. shows the TEM images of pristine and 2 wt%-400 ℃ coated samples to confirm the surface morphology. The pristine sample shows a very smooth edges and there are no other layers on the surface in Fig.4.2a. However, as shown in Fig.4.2b, we find that the surface of coated sample was homogeneously covered by a $FePO_4$ layer with a thickness about 20-30 nm. The distribution of $FePO_4$ coating layer on the surface of $LiNi_{1/3}Co_{1/3}Mn_{1/3}O_2$ was measured by EDS mapping. As shown in Fig.4.3, the bright spots correspond to the presence of each element and the spot intensity is an indicator of the concentration of element. Based on the mapping, Fe in the sample is

homogeneously distributed in the composite, indicating uniform distribution of $FePO_4$ on the surface of $LiNi_{1/3}Co_{1/3}Mn_{1/3}O_2$.

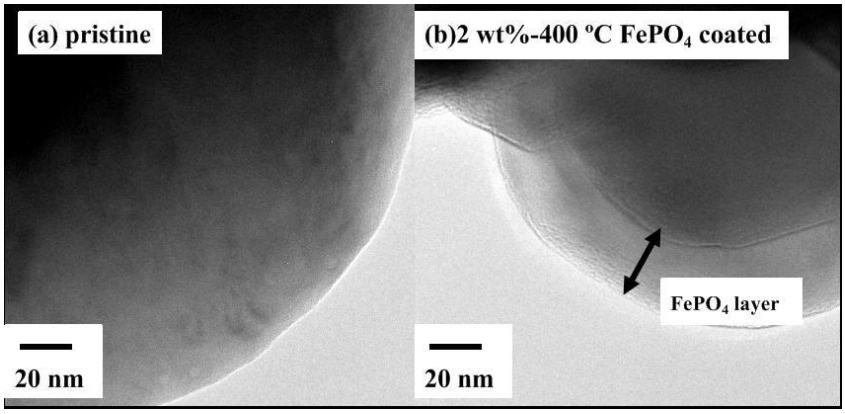

Fig. 4.2. TEM images of (a) pristine and (b) 2 wt%-400 ℃ $FePO_4$-coated sample.

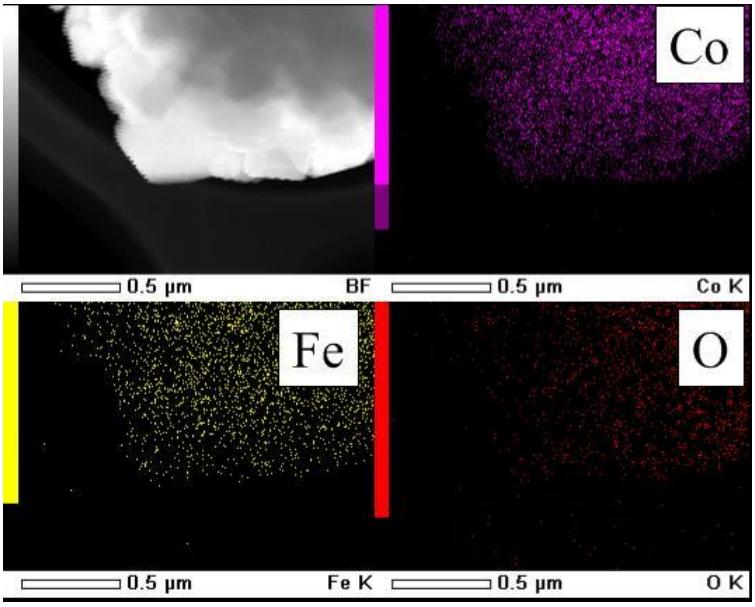

Fig. 4.3. EDS mapping patterns of 2 wt%-400 ℃ $FePO_4$-coated sample.

4.3.2 Electrochemical performance and analysis

The cycle performance and rate capability of pristine and coated $LiNi_{1/3}Co_{1/3}Mn_{1/3}O_2$ were tested to investigate the effect of $FePO_4$ coating. The cycle performances of coated samples with different $FePO_4$ contents and heat treated

temperature are shown in Fig.4.4. These charge-discharge was conducted at a current of 150 mA g^{-1} in the voltage range of 2.8-4.5V. As shown in Fig. 4.4a, with 1 wt%, 2 wt%, 3 wt%, 4 wt% and 5 wt% coating, the discharge capacities are 138.4, 143.5, 132.1, 101.3 and 61.8 mAh g^{-1} at the 100th cycle, respectively. Meanwhile, the discharge capacities is about 103.2 mA h g^{-1} at the 100th cycles for the pristine sample. It is indicated that cycle performance has been improved by $FePO_4$ coating with a coating amount of 1 wt% to 3 wt%. However, the discharge capacity decreased obviously when the coating amount increase to 4 wt% and 5 wt%. Therefore, this result indicates that only an appropriate amount of $FePO_4$ coating layer can facilitate the diffusion of Li ions. With a thicker layer, the excess insulating $FePO_4$ may inhibit the intercalation-deintercalation of Li cations and lead to a worse electrochemical performance [5]. The optimal coating amount is 2 wt% according the capacity retention.

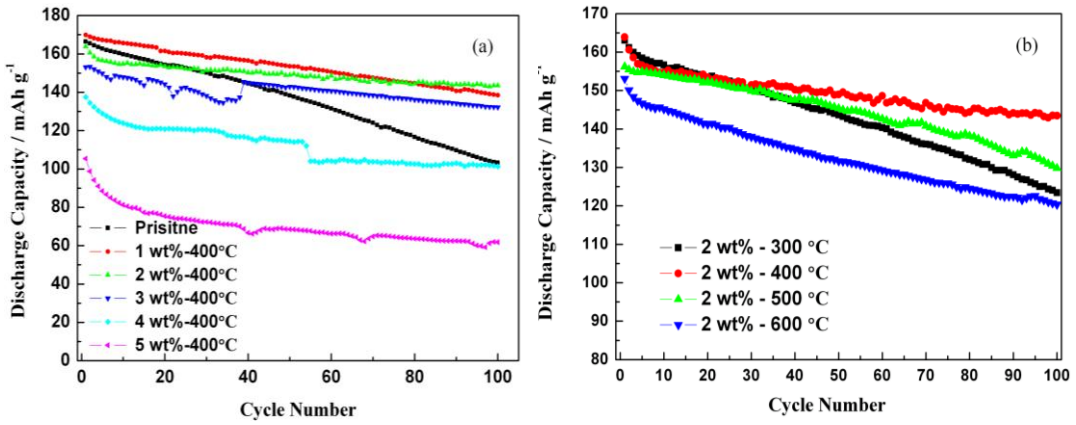

Fig. 4.4. (a) Cycling performance of pristine and $FePO_4$-coated $LiNi_{1/3}Co_{1/3}Mn_{1/3}O_2$ in the voltage range of 2.8-4.5 V at a current of 150 mA g^{-1}; (b) Cycle performance of 2 wt% $FePO_4$-coated $LiNi_{1/3}Co_{1/3}Mn_{1/3}O_2$ with different sintered temperature.

The effects of heat treated temperature on cycle performance were also investigated as shown in Fig.4.4b. At 100th cycle, the discharge capacity are 123.42 mAh g^{-1} (2 wt%-300 ℃), 143.45 (2 wt%-400 ℃), 129.82 (2 wt%-500 ℃), and 120.35 (2 wt%-600 ℃), respectively. Obviously, the sample which was heat treated at 400 ℃

showed the larger discharge capacity among all the measured samples. Although, the reasons why the sample sintered at 400 ℃ exhibited the best cycle performance is unclear, we considered that with low heat treated temperature, the contact between the coating layer and the cathode material is not very closely, so that the coating layer may peel off from the cathode surface during charge-discharge cycles. However, with higher heat treated temperature, the Fe^{3+} ions in the coating layer may diffusion into the cathode and affect the crystal lattice thus lead to bad Li ion transport between the electrode and electrolyte. Thus, an appropriate heat treat temperature would largely affect the electrochemical performance. Based on the above data, we conclude that the 2 wt%-400 ℃ sample showed the optimum $FePO_4$ coating condition.

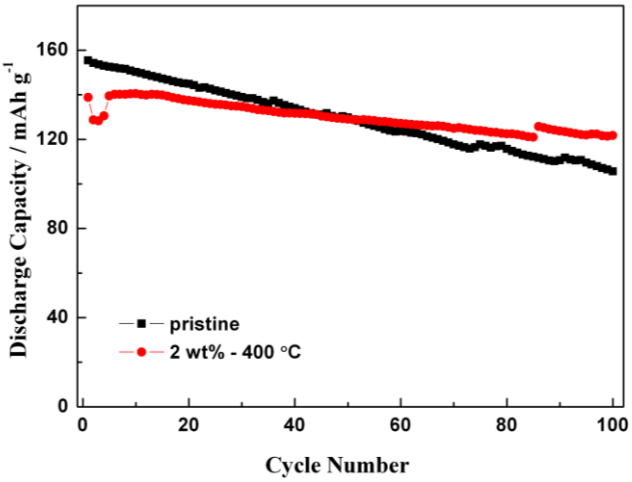

Fig. 4.5. Cycling performance of pristine and 2 wt% $FePO_4$-coated in the voltage range of 3.4-4.5 V at a current of 150 mA g^{-1}.

Table 4.1. Discharge capacities of pristine and 2 wt% -400 ℃ $FePO_4$-coated $LiNi_{1/3}Co_{1/3}Mn_{1/3}O_2$ electrodes at certain cycles with different cutoff voltages (4.5-2.8 V) / (3.4-2.8 V).

	1^{st} (mAh/g)	50^{th} (mAh/g)	100^{th} (mAh/g)
Pristine	166.4/155.5	138.3/129.8	103.2/105.7
Coated	163.9/138.9	149.0/129.1	143.4/121.7

The cycle performance were tested in a voltage range of 2.8-4.5 V, however, the reaction $FePO_4 + Li^+ + e \leftrightarrow LiFePO_4$ occurs at about 3.45 V [11]. So it is necessary to

confirm whether the increase of discharge capacity of coated sample due to the react between the $FePO_4$ coating layer and Li^+. The cycle performance of pristine and 2 wt%-400 ℃ coated sample were tested at the voltage range of 4.5-3.4 V (Fig.4.5). Even at such a high cut-off voltage, the 2 wt%-400 ℃ coated sample still showed an improved cycle performance than that of the pristine. Thus, the $FePO_4$ coating layer showed little discharge contribution in the above experiments. Table 1 summarized the discharge capacity of pristine and 2 wt%-400 ℃ for the 1st, 50th and 100th cycles with different cut-off voltage. It demonstrates that the capacity fading can be significantly prevented by surface $FePO_4$ coating. And the improvement of capacity retention are not originated in the discharge capacity contribution by $FePO_4$ coating layer.

We have tested CV to further confirm whether there were some redox reactions in $FePO_4$ coating layer with different coating amounts and heat treated temperature as shown in Fig.4.6. For the pristine, 2 wt%-400 ℃ and 5 wt%-400 ℃ coated samples, only a couple of peaks which can be attributed to the redox reactions of Ni^{2+}/Ni^{4+} [12]. Only with increasing the coating amount and heat treated temperature, a 10 wt.% and heat treated at 700 ℃, a couple of redox peaks appeared at 2.55 V / 2.84 V, which can be assigned to the redox of Fe^{2+}/Fe^{3+} (Fig.4.6d and 4.6e). Thus, we can conclude that the coated samples which with a coating layer less than 5 wt% and heat treated temperature at 400 ℃ showed no Fe^{2+}/Fe^{3+} redox reactions and thus, no charge/discharge capacity contributions from the $FePO_4$ coating layer.

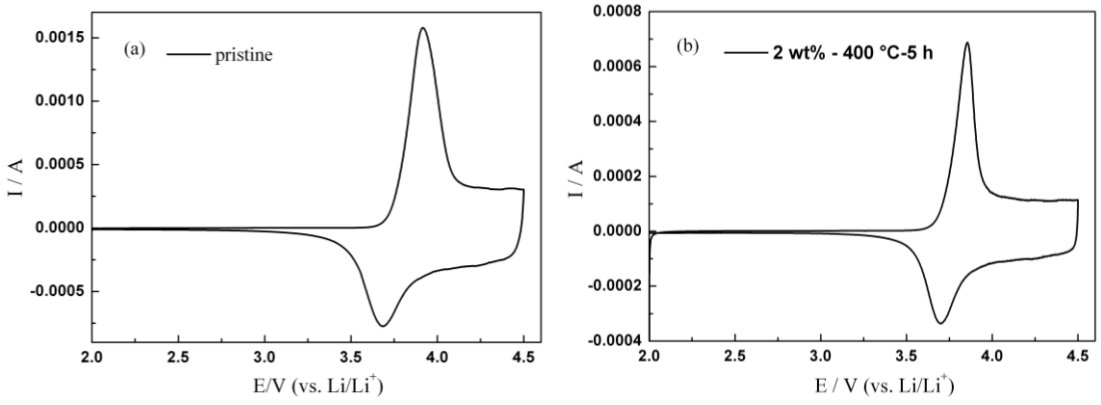

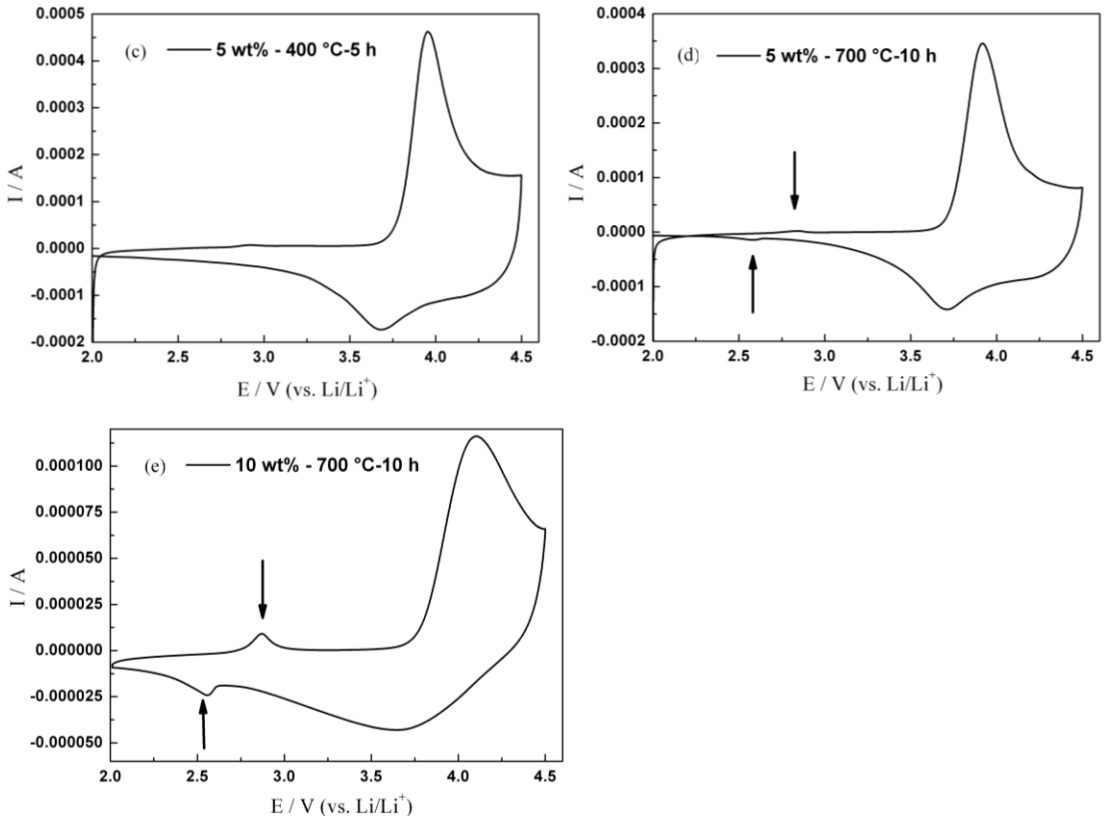

Fig. 4.6. Cyclic voltammograms of pristine and $FePO_4$-coated samples (with different synthesis conditions), at scan rate of 0.2 mV/s between 2.0 and 4.5 V.

Fig. 4.7a and 4.7b show the charge and discharge curves of pristine and 2 wt% -400 ℃ $FePO_4$ coated samples with different cycles at a constant current of 150 mA g^{-1} (about 1 C rate) in the potential range of 2.8-4.5 V versus Li/Li^+. The first charge/discharge curves of both samples show a typical potential plateaus of layered compound at about 3.9 V region, originating from the Ni^{2+}/Ni^{4+} redox couples [13]. The first discharge capacities are 166 mAh g^{-1} and 164 mAh g^{-1} for pristine and the 2 wt%-400 ℃ coated sample, respectively. At the 50^{th} cycles, the discharge capacity of 2 wt%-400 ℃ coated sample is 149.0 mAh g^{-1}, however, the discharge capacity of pristine is only 138.3 mAh g^{-1}. Furthermore, the discharge capacities of coated samples is 143.5 mAh g^{-1}, much higher than the pristine of 103.2 mAh g^{-1} at the 100^{th} cycles. Meanwhile, there is also an increase of charge plateaus and a decline of discharge plateaus with the increase of cycles. This phenomenon is considered as originating from the increase of electrode polarization which caused by the

side-reactions between the electrode and electrolyte. For the pristine sample, the charge plateau increase to above 4.0 V at the 100th cycle. For the coated samples, the charge plateau is still lower than 3.9 V at the 100th cycle. The changes of behaviors for discharge curves is more obvious than the charge curves. At the 100th cycles, the discharge plateau of pristine is diminished, meanwhile, there is only a small changes for the coated samples.

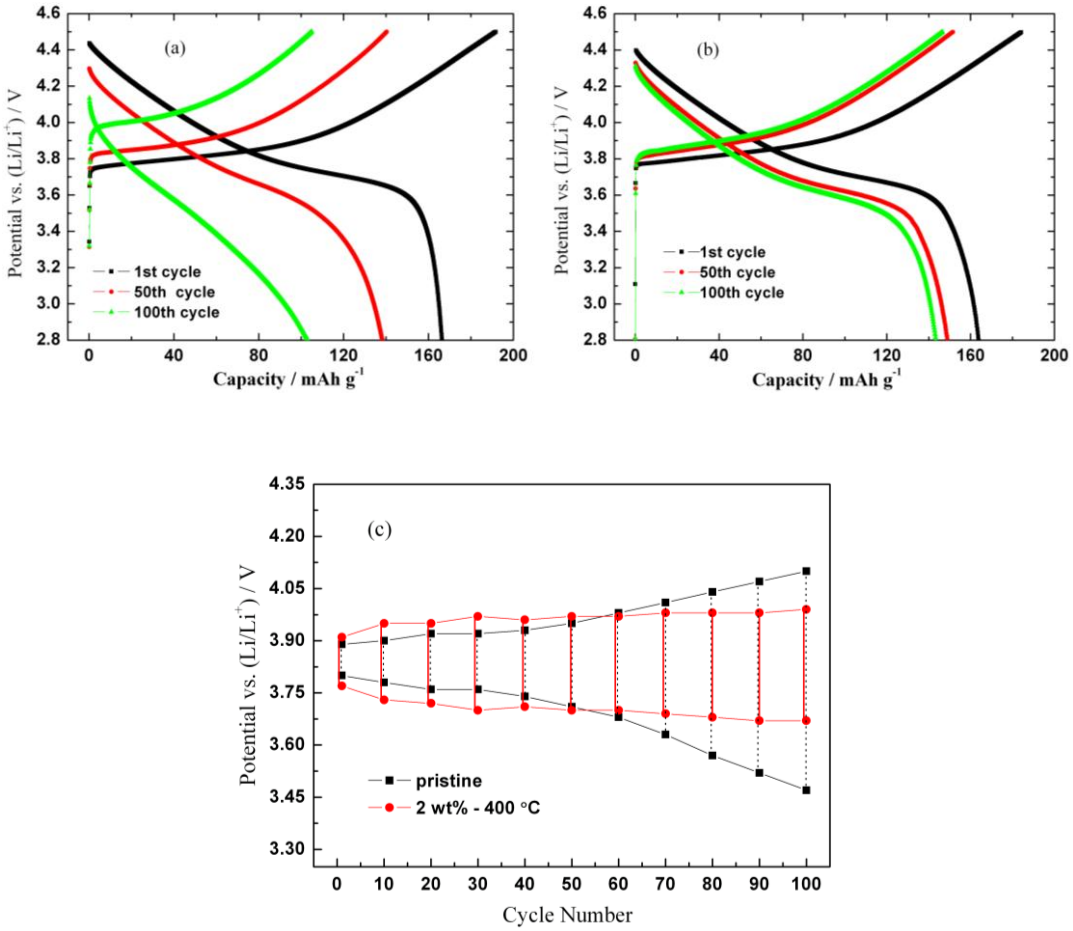

Fig. 4.7. The charge-discharge curves of (a) pristine; (b) 2 wt% -400 ℃ $FePO_4$-coated $LiNi_{1/3}Co_{1/3}Mn_{1/3}O_2$ in the voltage range of 2.8-4.5 V at a current of 150 mA g^{-1} and (c) changes of voltage at half charge/discharge capacity with different cycles.

The changes of voltage at the state half of charge/discharge were also tracked as shown in Fig.4.7c. Until the first 50 cycles, there is little changes of the charge or discharge potentials for the pristine sample. As the charge-discharge cycle continues, there is an obvious increase of charge potential and a decrease of discharge potential.

However, for the 2 wt%-400 ℃ $FePO_4$ coated samples, the changes of potential is relatively small. The departure of charge potential and discharge potential is an direct evidence that the decrease of charge/discharge efficiency. The surface coating not only suppress the capacity fading, but also prohibited the voltage decay.

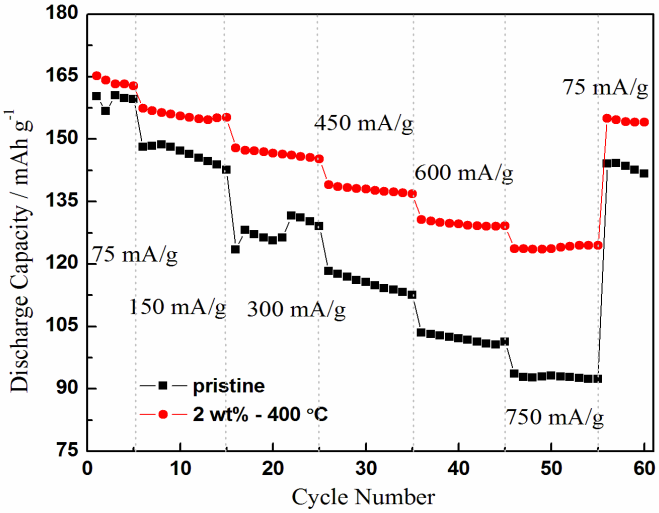

Fig. 4.8. Rate capabilities of pristine and 2 wt% $FePO_4$-coated $LiNi_{1/3}Co_{1/3}Mn_{1/3}O_2$ in the voltage range of 2.8-4.5 V.

Rate capability is also an important feature in judging their use in practical lithium ion batteries. The $FePO_4$-coating layer may improve the C-rate performance of the coated samples because of the phosphate coating layer can facilitate the charge transfer between the electrode and electrolyte [14]. Fig.4.8 shows the discharge capacities gradually decrease with increasing the charge-discharge currents. Meanwhile, it is clearly observed that the 2 wt%-400 ℃ coated sample has better rate capability than the pristine sample, especially at high rates. This result make us believe that the $FePO_4$ coating layer on $LiNi_{1/3}Co_{1/3}Mn_{1/3}O_2$ can functions as an promoter for Li transport to the host structure as a result of the reduced interfacial resistance between the electrode and electrolyte. This is also been certified by the following impedance experiments.

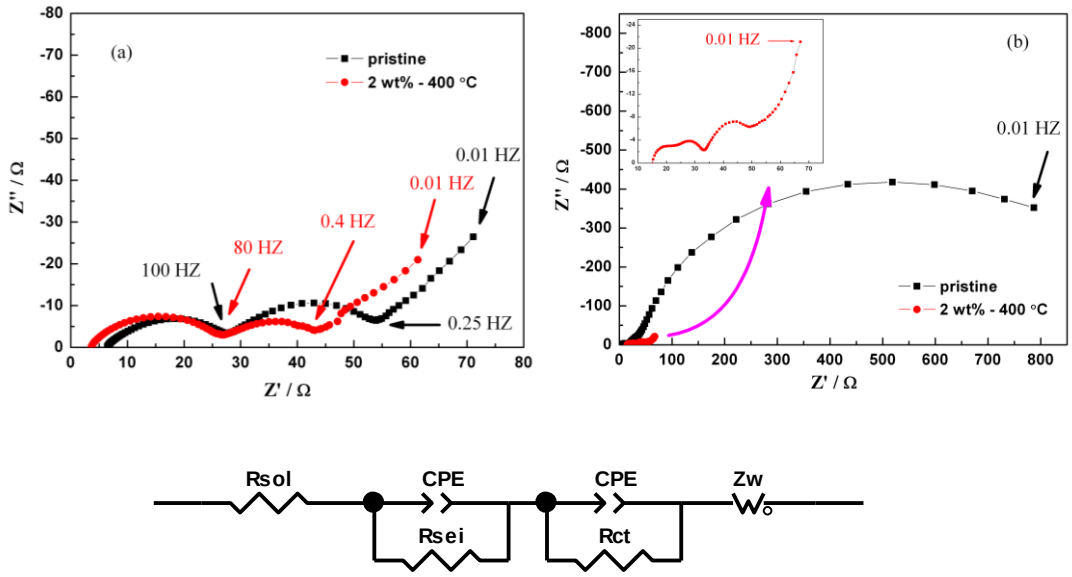

Fig. 4.9. EIS Nyquist plots of pristine and 2wt% $FePO_4$-coated $LiNi_{1/3}Co_{1/3}Mn_{1/3}O_2$ with cycling, (a) at the 1st cycles; (b) at the 100th cycles discharge to 2.8 V; (c) Voigt-type of equivalent circuit.

EIS test was carried out to further understand the $FePO_4$ coating effect on charge-discharge process. EIS plots of the pristine and 2 wt%- 400 ℃ sample at 4.5 V, after the 1st and 100th cycle, are shown in Fig.4.9a and Fig.4.9b, respectively. Before each measurement, the cells were first galvanostatically charge-discharge to the desired cycles (at a current of 150 mA g^{-1} with a voltage range of 4.5-2.8 V), followed by charging the cells to 4.5 V at a current of 15 mA g^{-1} and then charged for 3 h at this voltage. The Nyquist plots were fitted to the model in Fig.4.9c. Generally, an Nyquist plots include three parts, a semicircle in the high frequency range which correspond to the R_{sei} (the impedance of the natural and artificial solid electrolyte interface and the impedance of electrons through the active materials) in the model, a semicircle in the medium-to-low frequency range which correspond to the R_{ct} (charge-discharge resistance at the interface of electrode and electrolyte) and a sloping line at low frequency which correspond to Z_w (diffusion of lithium ion in the solid electrode). The fitting results are listed in Table 2. At the 1st cycle, the R_{ct} of 2 wt%-400 ℃ is a little smaller than the R_{ct} of the pristine. It is because the $FePO_4$ coating layer can facilitate

the Li ion transport and reduce the charge transfer resistance. This is also why the coated sample showed an improved rate capacity.The R_{ct} of pristine sample increase to about 40 times larger at the 100th cycles than that at the 1st cycle. However, the R_{ct} of 2 wt%-400 ℃ is only two times of the initial value. This EIS results clearly indicate that the $FePO_4$ coating layer can significantly suppress increase of R_{ct} with cycling. The increase of R_{ct} of $LiNi_{1/3}Co_{1/3}Mn_{1/3}O_2$ is mainly caused by side-reactions between the electrode and electrolyte [15].

4.3.3 Thermal stability

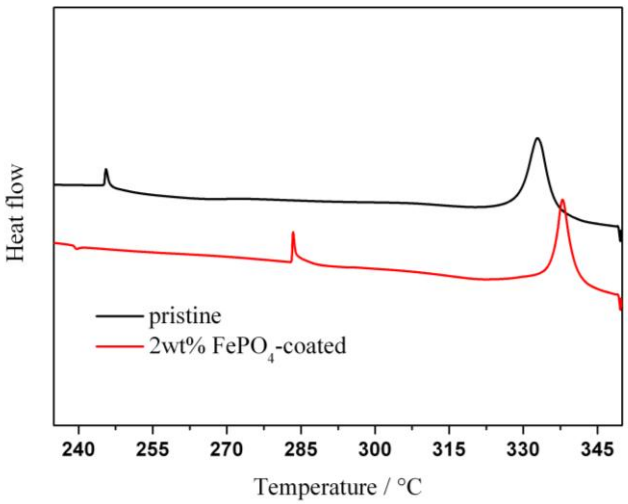

Fig. 4.10. DSC profiles of pristine and 2 wt% $FePO_4$-coated $LiNi_{1/3}Co_{1/3}Mn_{1/3}O_2$ electrode charged to 4.5 V.

Fig.4.10 shows the DSC profiles of pristine and 2 wt%-400 ℃ electrodes at charged state of 4.5 V. The small peaks at 245 and 283 ℃ for the pristine and the 2 wt% - 400 ℃ samples were attributed to the absorption of gas on the surface of the electrode materials. The pristine $Li_{1-x}Ni_{1/3}Co_{1/3}Mn_{1/3}O_2$ showed an exothermic peak at 332.9 ℃ with an exothermic heat generation of 66.2 J g^{-1}. While the $FePO_4$ coated samples showed an exothermic peak at 337.9 ℃ with an exothermic heat generation of 49.6 J g^{-1}. The enhanced thermal stability of the $FePO_4$ coated sample should be attributed to the stabilization of cathode surface by $FePO_4$ coating. As reported by other phosphate coated samples, the strong P=O bond and the strong covalency

between the PO_4 polyanions and Fe^{3+} can stabilize the cathode surface and thus strengthen the thermal stability of the materials [16].

4.4 Conclusion

In this paper, $LiNi_{1/3}Co_{1/3}Mn_{1/3}O_2$ is successfully coated with different amounts of $FePO_4$ by a co-precipitation method followed with heat treatment at different temperature. Among all the coated samples, the one with 2 wt% $FePO_4$ and treated at 400 ℃ showed the best performance in terms of cycle and rate capacities. The effect of $FePO_4$ coating layer are as follows: (1) prevent from the side-reaction at the interface of electrode and electrolyte and thus suppressing the increase of charge transfer resistance upon charge-discharge cycles; (2) stabilize the cathode surface by the strong P=O bond and the strong covalency between the PO_4 polyanions and Fe^{3+} and thus improve the thermal stability of the materials.

4.5 References

[1] J. B. Goodenough: "Cathode material: A personal perspective", *J. Power Source.*, Vol. 174, pp. 996-1000, 2007

[2] H. Q. Li and H. S. Zhou: "Enhancing the performances of Li-ion batteries by carbon-coating: present and future", *Chem. Commun.*, Vol. 48, pp. 1201-1217, 2012

[3] S. T. Myung, K. Amine and Y. K. Sun: "Surface modification of cathode materials from nano- to microscale for rechargeable lithium-ion batteries", *J. Mater. Chem.*, Vol. 20, pp. 7074-7095, 2010

[4] J. Cho, Y. W. Kim, B. Kim, J. G. Lee and B. Park: "A breakthrough in the safety of lithium secondary batteries by coating the cathode material with $AlPO_4$ nanoparticles", *Angew. Chem. Int. Ed.*, Vol. 42 , pp. 1618-1621, 2003

[5] C. B. Qing, Y. Bai, J. M. Yang and W. F. Zhang: "Enhanced cycling stability of $LiMn_2O_4$ cathode by amorphous $FePO_4$ coating", *Electrochim. Acta.*, Vol. 56, pp. 6612-6618, 2011

[6] H. Lee, Y. Kim, Y. Hong, Y. Kim, M. G. Kim, N. S. Shin and J. Cho: "Structural characterization of the surface-modified $Li_xNi_{0.9}Co_{0.1}O_2$ cathode materials by MPO_4 coating (M = Al, Ce, SrH, and Fe) for Li-ion cells", *J. Electrochem. Soc.*, Vol. 153, pp. A781-A786, 2006

[7] G. Li, Z. Yang and W. Yang: "Effect of $FePO_4$ coating on electrochemical and safety performance of $LiCoO_2$ as cathode material for Li-ion batteries", *J. Power Source.*, Vol. 183, pp. 741-748, 2008

[8] J. Wang, X. Y. Yao, X. F. Zhou and Z. P. Liu: "Synthesis and electrochemical properties of layered lithium transition metal oxides", *J. Mater. Chem.*, Vol. 21, pp. 2544-2549, 2011

[9] T. Ohzuku, A. Ueda and M. Nagayama:"Electrochemistry and Structural Chemistry of $LiNiO_2$ (R3m) for 4 Volt Secondary Lithium Cells", J. Electrochem. Soc., Vol. 140, pp. 1862-1870, 1993

[10] H. Sclar, D. Kovacheva, E. Zhecheva, R. Stoyanova, R. Lavi, G. Kimmel, J. Grinblat, O. Girshevitz, F. Amalraj, O. Haik, E. Zinigrad, B. Markovsky and D.

Aurbach:"On the Performance of $LiNi_{1/3}Mn_{1/3}Co_{1/3}O_2$ Nanoparticles as a Cathode Material for Lithium-Ion Batteries", *J. Electrochem. Soc.*, Vol. 156, pp. A938-A948, 2009

[11] Y. H. Huang and J. B. Goodenough: "High-Rate $LiFePO_4$ Lithium Rechargeable Battery Promoted by Electrochemically Active Polymers", *Chem. Mater*., Vol. 20, pp. 7237–7241, 2008

[12] Y. Koyama, N. Yabuuchi, I. Tanaka, H. Adachi and T. Ohzuku :"Solid-State Chemistry and Electrochemistry of $LiCo_{1/3}Ni_{1/3}Mn_{1/3}O_2$ for Advanced Lithium-Ion Batteries", *J. Electrochem. Soc.*, Vol. 151, pp. A1545-A1551, 2004

[13] Y. Koyama, N. Yabuuchi, I.; Tanaka, H. Adachi, T. Ohzuku: "Solid-state chemistry, and electrochemistry of $LiCo_{1/3}Ni_{1/3}Mn_{1/3}O_2$ for advanced lithium-ion batteries - I. First-principles calculation on the crystal and electronic structures", *J. Electrochem. Soc.*, Vol. 151, pp. A1545-A1551, 2004

[14] D. Lee, B. Scrosati, Y. K. Sun:"$Ni_3(PO_4)_2$-coated $Li[Ni_{0.8}Co_{0.15}Al_{0.05}]O_2$ lithium battery electrode with improved cycling performance at 55 ℃", *J. Power Source.*, Vol. 196, pp. 7742-7746, 2011

[15] Y. Y. Huang, J. T. Chen, J. F. Ni, H. H. Zhou, X. X. Zhang: "A modified ZrO_2-coating process to improve electrochemical performance of $LiCo_{1/3}Ni_{1/3}Mn_{1/3}O_2$", *J. Power Source.*, Vol. 188, pp. 538-545, 2009

[16] K. T. Lee, S. Jesong and J. Cho:"Roles of Surface Chemistry on Safety and Electrochemistry in Lithium Ion Batteries", *Accounts of Chem. Res.*, Vol. 46, pp. 1161-1170, 2013

Chapter 5. Study on the capacity fading mechanism of pristine and $FePO_4$ coated $LiNi_{1/3}Co_{1/3}Mn_{1/3}O_2$ by Electrochemical and Magnetical techniques

5.1 Introduction

Many researchers have endeavored to improve the electrochemical performances of cathode by surface coating because they are found critically dependent on the surface chemistry [1]. In order to get a successful coating, several standards should be complied for selecting the coating layer materials, such as: a low reactivity with electrolyte especially at the charged state, good thermal stability, electronic conductivity and well Li^+ ion conductivity [1-3]. Besides tremendous works about the surface coating of $LiNi_{1/3}Co_{1/3}Mn_{1/3}O_2$, we also investigated different coating layers such as V_2O_5, PEDOT and $FePO_4$ from the view of stability and conductivity to improve the electrochemical performance of $LiNi_{1/3}Co_{1/3}Mn_{1/3}O_2$ [4-6]. However, the in-depth understanding of the role of coating layers during the charge/discharge processes is still inadequate. The mechanism should be further examined in order to design and tailor new coated materials with better electrochemical properties. Among all the three kinds of coating materials, $FePO_4$ coated samples showed the most stable capacity retention as shown in Fig. 5.1. Thus, pristine and $FePO_4$ coated sample were taken to study the mechanism of performance improvement.

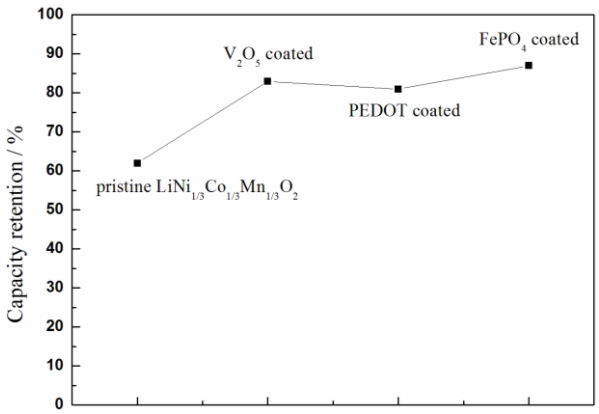

Fig. 5.1. Comparison of the 100th cycle capacity retention by different coating materials.

Galvanostatic intermittent titration technique (GITT) method is popularly used to determine the open circuit voltage (OCV) and lithium ion diffusion coefficient in cathode materials, which can reflect the lithium ion dynamics and also the changes upon charge/discharge cycles. Cyclic voltammetry (CV) measurement at varied scan rates can be used to explore the electrode kinetic behaviors according to the increased separation of cathodic and anodic peak potentials and currents. Electrochemical impedance spectroscopy (EIS) can effectively reflect the changes of internal resistance during charge/discharge process and also the changes with increasing of cycles [7]. Combining all of the above electrochemical analysis techniques, we may get clear picture on the dynamic changes of Li ion kinetics with increasing charge/discharge cycles and the improvements by surface coating.

Magnetic susceptibility measurements are very sensitive to the local structure and can elegantly characterize the cation mixing of the layered cathode. A. Mauger et al. associated the cation mixing in layered cathode with magnetic properties, and found that the Ni^{2+} ion in substitution to Li^{+} on the (3b) lattice site, Ni^{2+} (3b) generates a Ni^{2+}(3b)-Mn^{4+}(3a) ferromagnetic interaction. The strengthened ferromagnetic interactions lead to an increase of magnetic ordering temperature which can be deduced from the magnetic measurements [8-10]. The samples with lower cation mixing ratio tend to show better battery performances. Reviewing the relevant literatures, it is noted that most of the published papers are committed to the cation mixing of as-synthesized materials rather than cycled samples. It is lack of reports on the cation mixing evolutions with cycled samples, not to mention the evolutions of coated samples.

With an aim to better understanding the factors influencing the electrochemical performances by surface coating, in this chapter, a compositive investigations on the cycled samples of both pristine and coated $LiNi_{1/3}Co_{1/3}Mn_{1/3}O_2$ samples were carried out by combining galvanostatic intermittant titration technique (GITT), cyclic voltammetry (CV), electrochemical impedance spectroscopy (EIS) and magnetic techniques.

5.2 Experiment

5.2.1 Material preparation and electrochemical techniques

Pristine $LiNi_{1/3}Co_{1/3}Mn_{1/3}O_2$ and 2 wt% $FePO_4$ coated $LiNi_{1/3}Co_{1/3}Mn_{1/3}O_2$ were prepared by co-precipitation method as chapter 4. All of the battery assemble and electrochemical performance test were done as shown in chapter 4.

The galvanostatic charge/discharge tests were first conducted for desired cycles before taking the GITT, CV and EIS measurements. The tests were performed on Hokuto Denko with a potential range between 2.8-4.5V. GITT, CV and EIS were conducted on Solartron instrument Model 1287 electrochemical interface. For GITT measurements, the cells were firstly charged at a constant current flux of 20 mA/g for 1 hour and followed by an open circuit stand of the cell for 3 hours between 2.8-4.5 V. CV measurements were conducted in the voltage range of 2.8-4.5 V at different scan rates. EIS were done on Solartron 1255B frequency response analyzer in a frequency range of 0.5 MHz to 0.05 Hz with AC of 5 mV. Data analysis was conducted using the Zview 2.70 software (Scribner Associates Inc., USA).

5.2.2 Magnetical techniques

Magnetic susceptibility measurements were performed with SQUID magnetometer (Quantum Design MPMS XL) in the temperature range of 4-300 K with an applied field of 1000 Oe. To prepare the sample for test, disassemble the cells after 100 charge/discharge cycles, and then collect the electrode materials from the current collector, wash it by blank EC/DEC solution and ethanol, respectively, and then dried at 100 ℃ over night in vacuum. For non-cycled cells, the fresh electrode materials as synthesized were used for measurements. The powder samples were placed into small plastic capsule, settled in a holder and finally inserted into the helium cryostat of the SQUID apparatus. The temperature dependence of the susceptibility data were recorded in a zero-field cooling (ZFC) mode. The samples were cooled to 4 K under 0 Oe field and then a magnetic field 1000 Oe is applied, the magnetization were

measured upon heating.

5.3 Results and Discussion

5.3.1 Charge-discharge performance

The 2 wt%-400 ℃ $FePO_4$ coated sample was chosen since it showed the best electrochemical performances among the coated samples with various coating amounts and different heat treated temperatures as shown in chapter 4. All coated samples showed a well ordered hexagonal α-$NaFeO_2$ structure with *R3m* space group, as confirmed by the XRD patterns. The $FePO_4$ coating layer was confirmed by SEM, TEM and EDS, it uniformly distributed on the surface of $LiNi_{1/3}Co_{1/3}Mn_{1/3}O_2$. These characterization data have been given in chapter 4.

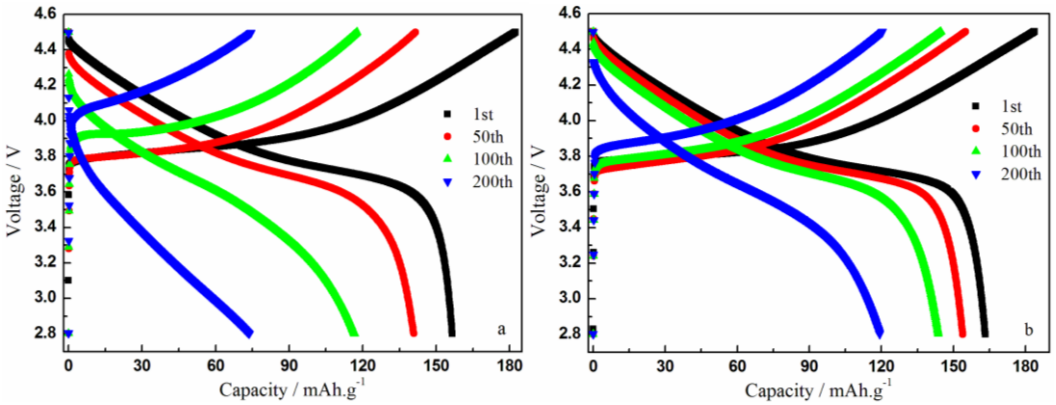

Fig. 5.2. Charge/discharge profiles at different cycles of (a) pristine and (b) 2 wt% coated sample in the cutoff voltage of 2.8-4.5 V at a current of 150 mA/g.

The cells were first charge-discharge to the desired cycles at a current of 150 mA/g in a cutoff voltage range of 2.8-4.5 V *vs.* Li/Li^+. Fig. 5.2 shows the charge/discharge profiles at the 1^{st}, 50^{th}, 100^{th}, 200^{th} cycles of pristine $LiNi_{1/3}Co_{1/3}Mn_{1/3}O_2$ (Fig. 5.2a) and $FePO_4$ coated $LiNi_{1/3}Co_{1/3}Mn_{1/3}O_2$ (Fig. 5.2b). The initial charge/discharge profiles shows a typical potential plateaus at 3.9 V region, mainly originating from the Ni^{2+}/Ni^{4+} redox couples as our previous report. With the increase of cycles, there is a capacity fading accompanied by a voltage decay. It is clearly shows that the $FePO_4$

coated samples display an enhanced capacity and better voltage retention. In order to fully understand the performance degradation and the roles of surface coating, further studies on Li ion dynamics especially the evolutions upon cycles are needed. Detailed study of CV, EIS and GITT on different cycled cells combined with the magnetic properties of fresh and 100 cycled samples are presented in the following sections.

5.3.2 Electrochemical analysis on different cycled cells

5.3.2.1 Investigate the evolution of activation energy

As we know, the interfacial charge transfer at the interface of electrode and electrolyte is the rate determine step in the whole Li ion transfer process. Moreover, the activation energy of that process can be calculated by the temperature dependence charge-transfer resistance (R_{ct}). The plots of log(T/R_{ct}) against 1000/T showed linear relationship obeying the Arrhenius equation [11].

$$\ln\frac{T}{Rct} = \ln A - \frac{Ea}{R}\frac{1}{T}$$

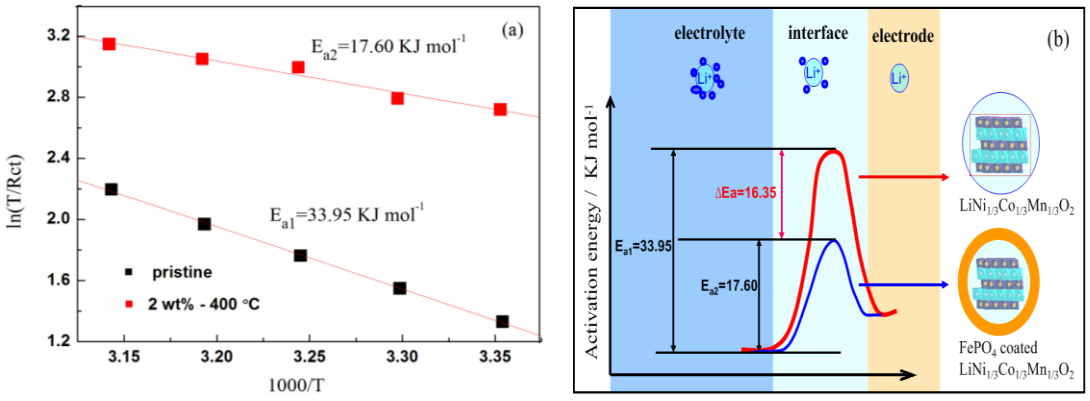

Fig. 5.3. (a)Temperature dependency for interfacial charge-transfer resistance of pristine and 2 wt%-400 ℃ sample; (b) Image figure of improvement of activation energy by $FePO_4$ coating.

Here E_a is the activation energy, T is absolute temperature, R_{ct} is the charge transfer resistance, R is gas constant, A is the pre-exponential factor. According to this

equation, the E_a can be calculated from the slope of plots. R_{ct} are the fitting results from temperature dependent EIS plots as expressed in chapter 4. Thus, the temperature dependence charge-transfer resistance (R_{ct}) were summarized. As shown in Fig. 5.3a, E_{a2} of 2 wt%-400 ℃ sample is 17.60 kJ mol^{-1}, which is lower than E_{a1} (33.95 kJ mol^{-1}) of the pristine sample. As illustrated in Fig. 5.3b, the $FePO_4$ coating layer decreased the activation energy of the charge transfer process, somewhat acting as a `catalyst`, which speed up the charge transfer processes at the interface of electrode and electrolyte.

5.3.2.2 CV studies on different cycled samples

CV is a facile technique for evaluation of the electrochemical performance and electrode kinetics of cathode materials. Fig. 5.4 shows the CV curves of pristine and coated samples after 50 cycles (5.4a and 5.4d), 100 cycles (5.4b and 5.4e) and 200 cycles (5.4c and 5.4f). From CV curves of pristine $LiNi_{1/3}Co_{1/3}Mn_{1/3}O_2$ electrode after 50 cycles in Fig. 5.4a, a pair of well-defined redox peaks was observed with the oxidation peak at 3.86 V and reduction peak at 3.71 V when using a sweep rate of 0.1 mV/s. The peaks can assigned to the redox of Ni^{2+}/Ni^{4+} couples in layered cathode materials [4]. With the increase of sweep rates, the oxidation peaks shift to higher potentials and the reduction peaks shift to lower potentials. It means the lithium extraction at higher potentials and lithium insertions at lower potentials when at higher sweep rates. The increased potential gaps indicate more irreversible behaviors, that is to say the decrease of coulombic efficiency at higher sweep rates. With the increase of charge/discharge cycles, it is noted: first, the oxidation peaks gradually shift to higher potentials with the increased cycles, which indicate the extraction of Li ions from the cathode becomes more difficult as the increasing of cycles; second, the reduction peaks grow widen and more difficult to define especially for the 200 cycled cell of the pristine samples (as shown in Fig. 5.4c), this is mainly caused by the polarization and accumulation of by-products from side-reactions at the interface of electrode and electrolyte, another reason might be the changes of the coordination of

Ni ions since the shape and positions of CV peaks highly depended on the coordination configuration of active metal ions [4]. The CV observation is in good agreement with the charge/discharge profiles, such as increased charge plateaus, decreased discharge plateaus and gradually diminished discharge plateaus along increased cycle number; finally, a new reduction peaks at about 3.0 V appeared for the pristine sample, it is the characteristic peak of Mn with a spinel structure. This new peak implies a structure evolution occurred as some spinel structure appeared in local area along with the increase of charge/discharge cycles [12].

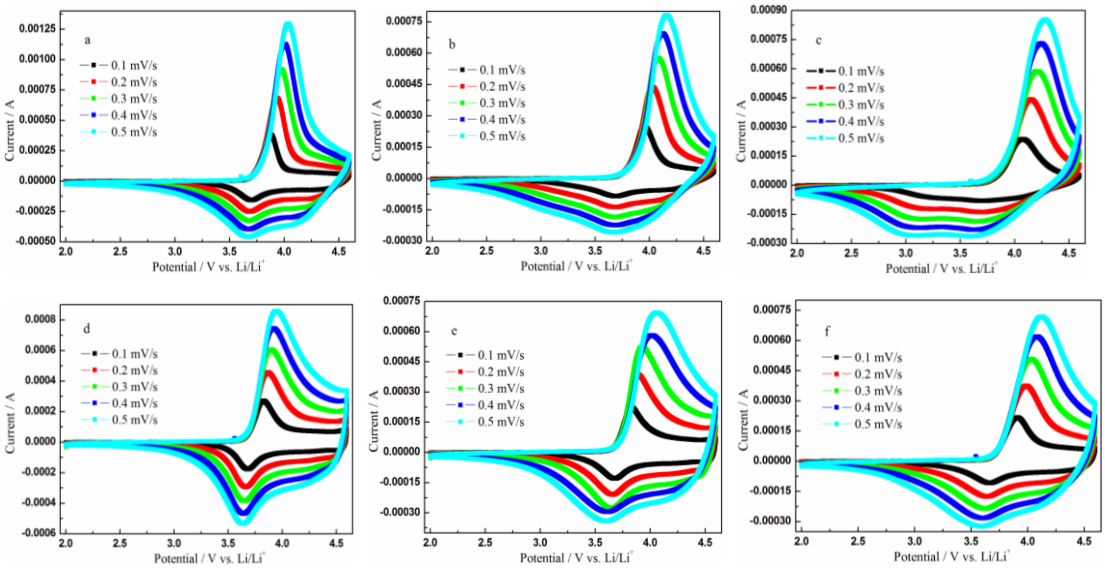

Fig. 5.4. CV curves of pristine after 50, 100 and 200 cycles samples (a-c) and and $FePO_4$ coated sample (d-f)

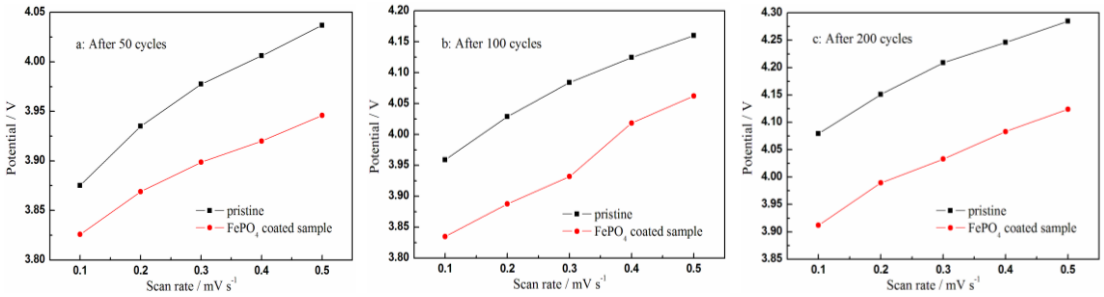

Fig. 5.5. Cathodic peak potentials vs. scan rates on 50, 100 and 200 cycled samples.

From the observation of CV curves, the $FePO_4$-coated samples show obviously improvements in comparison with the pristine sample. Firstly, the peak shifts of the

coated samples are smaller than the pristine one at the same cycle, which can be seen more clearly in Fig. 5.5. Although the oxidation peaks of the coated sample shifted to higher potential along the increase of cycle number, its peak potentials are always lower than those of pristine samples at the same cycle of charge/discharge. For example, the peaks of 200 cycled coated samples are even lower than those of the 100 cycled pristine samples. This indicates the extraction of lithium ion suffered less resistance than the pristine samples with the increase of charge/discharge cycles. Secondly, the coated samples show better maintenance of its reduction peak during the cycle testes. Well-defined reduction peaks can be observed for the 50 cycled coated samples, after 200 cycles of charge/discharge as shown in Fig. 5.5c, the reduction peaks of coated sample become broader but can still be defined. While for the pristine samples, their reduction peaks are already difficult to define only after 100 cycles of charge/discharge, as shown in Fig. 5.5b. These results indicate that the coated samples perform a better structure stability during the charge/discharge cycles. In fact, the side-reactions between electrode and electrolyte would gradually accumulate with the increase of cycle number, leading to a structure evolution mainly as Ni coordination changes and appearance of spinel phases. A coating layer can modify the interface of electrode/electrolyte well and slow down the side reactions at the interface. So the $FePO_4$ coated samples demonstrate suppressed structure evolution at prolonged cycles of charge/discharge.

5.3.2.2 EIS studies on different cycled samples

Internal resistance, which can significantly impact the Li ion kinetics of oxide cathodes, is another important factor related to the capacity fading of lithium ion batteries [13]. EIS is a reliable technique to identify the Li ion kinetics and internal resistance in cathode [14]. To gain further understanding on the evolutions of electrochemical properties the coated and pristine samples after 50, 100 and 200 charge/discharge cycles were analyzed by EIS at different state of charge, respectively. All of the cells were subjected to galvanostatic charge/discharges for

desired cycles before EIS measurement. During the EIS tests, the cycled cells were charged at 20mA/g for one hour and followed relaxed to its open circuit potential (OCP) for 3 hours. Then the EIS measurement was performed in the frequency range of 0.5 MHz to 0.1 Hz with an ac signal of 5 mV. This procedure was repeated in the voltage range of 2.8-4.5 V. The Li ion intercalation and de-intercalation during charge and discharge process are normally modeled as a multi-step processes. The Nyquist plots showed two typical semi-circles in Fig. 5.6 for certain cycled pristine $LiNi_{1/3}Co_{1/3}Mn_{1/3}O_2$ and $FePO_4$ coated samples during the charge processes. For clarity, only three plots of initial state, half charged state and fully charged state samples were selected. Generally, the EIS profile can be expressed by several parts, which in sequence from the high frequency end are: (I) the ohmic resistance of the electrolyte (R_{sol}), (II) the resistance at the electrode/electrolyte interface and electron pass through the active material, this part can be represented by resistive/capacitive combination because of the electric double layer ($R_f \parallel CPE_f$), (III) the charge transfer resistance and double layer capacitance ($R_{ct} \parallel CPE_{ct}$), (IV) the impedance to the Li ion diffusion in the solid state electrode (Zw), as introduced by Warburg [15]. In our experiment, some of the Nyquist plots of the cell samples showed no Warburg diffusion because of the frequency limitation. The equivalent circuits which model the elementary reactions was adopted as shown inner the corresponding figures. The capacitance $CPE \propto A/l$, where A is the geometric surface area and l is the thickness of the surface film. It is known that the side-reactions with prolonged cycles of pristine $LiNi_{1/3}Co_{1/3}Mn_{1/3}O_2$ lead to the accumulation of by-products on the electrode surface and thus the surface area thickness l would increase. This can be reflected by the decrease of CPE part in the corresponding equivalent circuits. For the impedance plots of the 200 cycled pristine samples, the low frequency semicircle is absent and only half of the second semi-circuit is observed. So the corresponding circuit elements were excluded from the equivalent circuit (inner the Fig. 5.6b). All of the experimental data are fitted using the equivalent circuit and quantitative analysis of the resistance changes is conducted.

As shown in Fig. 5.6a, during the charge process, the first semi-circle changed very

little even charged the cell to 4.5 V, which indicates the Li ion concentration in the cathode material has relatively small effects on the surface film resistance. By carefully examining the data in Fig. 5.6b-5.6d, all of the other cycled cells show similar trends except of the 50 cycled coated samples. The increase of charge transfer resistance is far greater than that the surface film resistance especially for more times cycled cells. The surface $FePO_4$ coating layer suppressed the increase of charge-transfer resistance and thus the 50 cycled coated samples showed a comparable surface film resistance and charge transfer resistance. As charging (accompanied by the decreasing of Li ion concentration in the cathode material), the resistance first decreased, then maintained as a constant state and finally increased back to a large value at the end of charge. The observed change trends are similar to the previous reports of $LiNi_{1/3}Co_{1/3}Mn_{1/3}O_2$ and other layered cathode material such as $LiCoO_2$ [7]. The physical processes can be described as: (I) a large resistance appeared at the initial of delithiation, (II) along with the delithiation process, the increased lithium vacancy promote the charge transfer and the resistance decreases, a constant value is obtained at a potential range in consistent with the charge plateau, (III) the resistance increases again at the end of charge due to the increase of interlayer repulsive force at higher delithiation state.

To quantitatively clarify the evolution of R_{ct} with prolonged cycles, the fitting results are shown in Fig. 5.7. With delithiation, the R_{ct} first decreases, then reaches a constant and finally increases again. This trend is similar with the changes of semi-circles in Nyquist polts. These observations confirm that R_{ct} plays an important role in the total resistance of the cells. The R_{ct} reaches a constant at the potential which is in constant with the charge plateau of the corresponding charge process. There is only a small difference of R_{ct} between the 50 cycled cells of pristine and coated samples. With the increase of charge/discharge cycles, rapid increase of R_{ct} is observed for the pristine samples, and the value of R_{ct} reaches a constant appears at a much higher potential range. For the coated samples, a relatively smaller increase of R_{ct} can be clearly observed, and the potential ranges corresponding to a constant, R_{ct} changes little with the increased cycles. The R_{ct} values for the coated samples after

200 cycles are even smaller than that of 100 cycled pristine samples. These observations can be well correlated with the changes of the charge plateaus at the corresponding cycles as shown in Fig. 5.2. The increase of R_{ct} caused kinetics barriers and performance degradation with prolonged cycles. The improvements of electrochemical performances for $FePO_4$ coated sample can be mainly attributed to the slow increase of R_{ct} values.

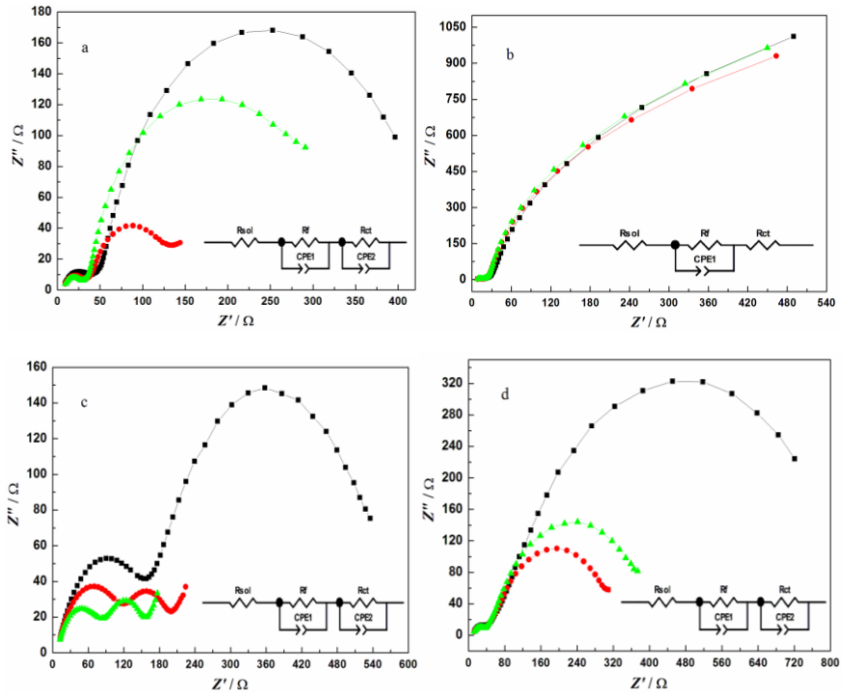

Fig. 5.6. Nyquist plots at different charge states (black: initial state, red: half charged state, green: fully charged state) on different cycled cells a: pristine after 50 cycles, b: pristine after 200 cycles, c: coated sample after 50 cycles, d: coated sample after 200 cycles.

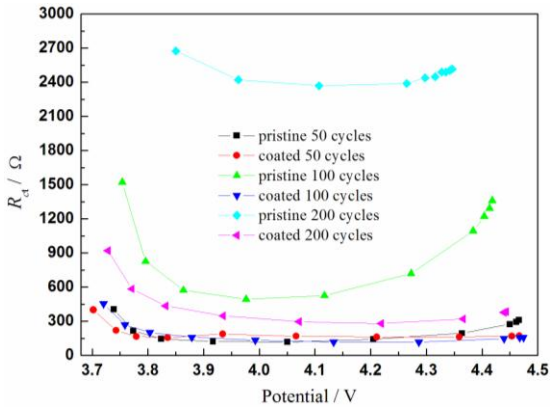

Fig. 5.7. R_{ct} values as function of cell voltage obtained by fitting the impedance data with the equivalent circuits.

5.3.2.3 GITT studies on different cycled samples

Fig. 5.8a and 5.8b show the open circuit voltage (OCV) curves of the pristine $LiNi_{1/3}Co_{1/3}Mn_{1/3}O_2$ and $FePO_4$ coated samples after 50, 100 and 200 cycles. The certain cycled cells were first charged at a current of 20 mA/g for 1 h and followed by an open circuit operation for 3 h to allow the cells relaxing to its equilibrium state. In respect to the charge/discharge profiles, similar but more detailed information can be obtained. There is an obvious increase of charge plateaus and decrease of discharge plateaus for the pristine samples at increased cycles. Also the capacity fading can be confirmed by the OCV in Fig. 5.8a.While, the OCV of coated samples exhibit a limited change of the charge plateau and discharge plateau with the increased cycles. It demonstrated that the surface coating can effectively suppress the capacity and voltage fading by suppressing the deterioration of surface polarization. This is coincidence with the charge/discharge profiles analysis.

GITT is established as a powerful technique with high accuracy to determine the Li ion diffusion coefficient D_{Li} to host materials of varying compositions [14,16,17]. The apparent diffusion coefficient obtained from the GITT is usually used to demonstrate the phase separation and cation ordering in layered cathode materials [16]. To further clarify the kinetics evolution, especially the changes of ionic transport properties at prolonged cycles, the apparent D_{Li} was calculated according to the GITT of the pristine and coated samples. The previous study of other researchers on Li ion diffusion coefficients usually involved the battery behaviors in the first several charge/discharge cycles. Few reports have focused on the ionic transport evolution with prolonged cycles. In this section, we not only studied the Li ion diffusion coefficient D_{Li} as a function of cycle number, but also compared the change trends between the pristine and coated samples as the increased cycles.

In GITT, the lithiation and deliathiation of the cathode material at a thermodynamic equilibrium state is obtained by applying a constant current density (I_0) for a limited time period τ and following a long period of open circuit to reach the equilibrium state. The whole GITT process is finished by several titration circles. In

this study, the cells were subjected to 50, 100 and 200 charge/discharge cycles at 150 mA/g in the voltage range of 2.8-4.5 V prior to the GITT measurement. The cells were charged at a constant current flux of 20 mA/g for an interval τ of 1 h, followed by an open circuit stand for 3 h to allow the cell voltage to a steady state value, *Es*. The sequence was repeated in the voltage range of 2.8-4.5 V. The D_{Li} in the cathode materials can be calculated according to the Fick's second law of diffusion. It is found that the single titration of varied cell voltage *vs.* $t^{1/2}$ (time) showed a straight line behavior. Combined with a series of assumptions and simplifications, the equation can be written as: [7,16]

$$D_{Li} = \frac{4}{\pi}\left(\frac{m_B V_m}{M_B A}\right)^2\left(\frac{\Delta E_s}{\Delta E_\tau}\right)^2 \qquad (\tau << L^2 / D_{Li})$$

where m_B is the active mass, V_m is the molar volume of the compound, M_B is the molecular weight, A is the total contact area between the electrode and electrolyte, and L is the thickness of electrode. The ΔE_s and ΔE_τ are the change in the equilibrium state potentials and the total transient change in cell voltage during respective single titration as shown in Fig. 5.8c. The V_m value deduced from the crystallographic data are 20.1 and 20.3 cm^3/mol for the fresh materials of pristine and coated sample, respectively. We assumed the V_m remains unchanged with the change of Li contents and prolonged cycles. The geometric surface area of the electrode, a round pest with a diameter of 8 mm, is taken as the total contact area A between the electrode and electrolyte. There should be a change of contact area with different cycles because of the deposition of by-products on the electrode surface, however, it is difficult to be precisely determined. Therefore, we consider contact area A as a constant in our calculation.

The empirical D_{Li} calculated from the GITT curves (charge process) as a function of cell voltage for different cycled pristine and $FePO_4$ coated samples are plotted in Fig. 5.8d. In the previous report on the D_{Li} values of pristine $LiNi_{1/3}Co_{1/3}Mn_{1/3}O_2$, a minimum in the plot of D_{Li} vs. voltage was observed, which was regarded as the phase transition or some order-disorder transition during cycling. The minimum of D_{Li} usually appeared at the voltage of 3.7 V [7]. However, there is no minimum D_{Li} in the

results of our cycled samples. This might because the first point we got is at a potential of 3.75 V, which is higher than the equilibrium potential of minimum D_{Li}. A D_{Li} value of $1.80*10^{-10}$ cm^2/s at 3.77 V is obtained based on our experiment, which is in the same order of magnitudes to the previously reported results of $LiNi_{1/3}Co_{1/3}Mn_{1/3}O_2$ [7].

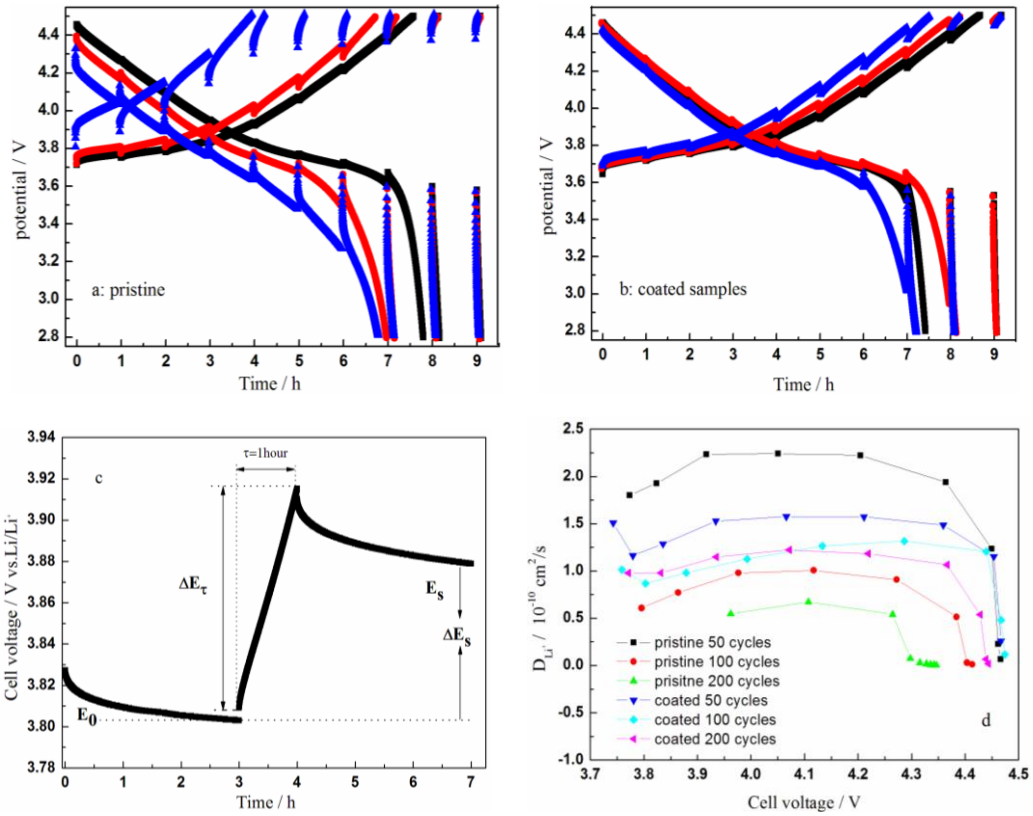

Fig. 5.8. OCV (open circuit voltage) at different cycled cells for (a) pristine, (b) coated samples; (c) applied current flux and the resulting voltage profile for a single titration; (d) The calculated D_{Li} from the GITT data for the different cycled samples.

With the removal of lithium ions, The D_{Li} undergoes a slight increase and then remain stable till the voltage to 4.4 V. The D_{Li} decreases abruptly as further delithiation above 4.4 V, which results from that the deep delithiation leading to strengthened attractive force of lithium ions from the oxidized transition metal layer. For long cycled samples, the D_{Li} values of pristine samples decrease more rapidly than those of coated samples at the corresponding lithium concentration of cathode. It is noted that the 50 cycled samples show an exception: the D_{Li} values of pristine is a

little bigger than that of the coated samples. The reason is not yet clear at present. The D_{Li} values of coated samples show a slight decrease compared with those of pristine sample. As we know, the D_{Li} can directly reflect the lithium ion diffusion status inside the active materials, it is probably that a structure rearrangement and local structure changes occurred with the increasing of charge/discharge cycles. Obviously, the surface coating by $FePO_4$ in this study suppressed this tendency. For $LiNi_{1/3}Co_{1/3}Mn_{1/3}O_2$, the most possible structure rearrangement might arise from the disorder of Li and Ni since the diameter of Li^+(0.76 Å) is very similar to that of Ni^{2+}(0.69 Å). In case of large Li/Ni ion exchange, serious distortion force caused by the ion exchange would lead to irreversible crystal structure transformation, which is definitely detrimental to the cycle life and rate performance. It is highly needed to study whether there is a disorder of Li/Ni with the prolonged cycles.

5.3.3 Magnetic analysis

For the layered cathode materials, the charge capacity is highly dependent on the cation order, especially the Li/Ni order. A sample with high ordered structure usually delivers a well reversible charge/discharge capacities and structure stability [18]. Our recent research on $LiNi_{0.42}Mn_{0.42}Co_{0.16}O_2$ showed that sample with a high cation mixing ratio of Li/Ni exhibit an obvious anisotropic stress, smaller inter-slab space of unit cell, and negative effects on capacity, cycle and rate performance [19]. However, to our knowledge, it is lack of direct evidence to show the Li/Ni mixing ratio evolution upon the prolonged charge/discharge cycles. Magnetic technique is an intelligent technique to characterize the cation mixing ratio of layered $Li(NiCoMn)O_2$ and has been recently used to study the cationic order of fresh cathode materials synthesized at different temperatures [20]. Herein, we did the magnetic studies on both fresh synthesized and 100 cycled $LiNi_{1/3}Co_{1/3}Mn_{1/3}O_2$ samples to see the Li/Ni mixing ratio evolution with prolonged cycles, and made carefully comparison of the magnetic properties between cycled pristine and cycled coated samples.

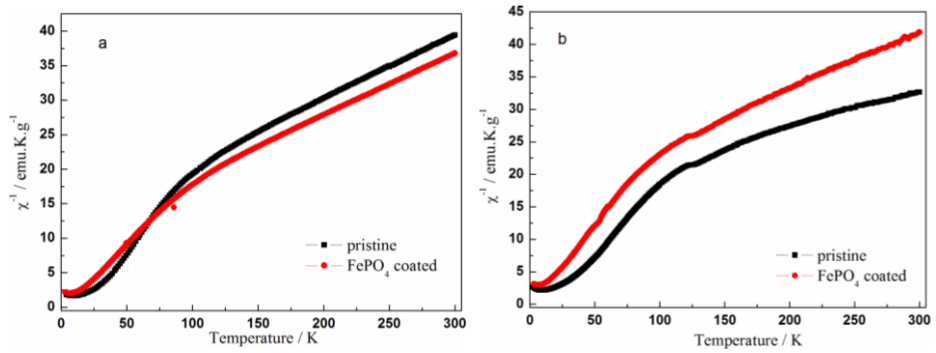

Fig. 5.9. Temperature dependence of inverse magnetic susceptibility of the fresh (a) and cycled samples (b). The Curie-Weiss ($\chi_m^{-1}(T)=(T-\Theta_p)/C_p$) fit was applied to these data above the temperature of 150K to calculate the Weiss constants.

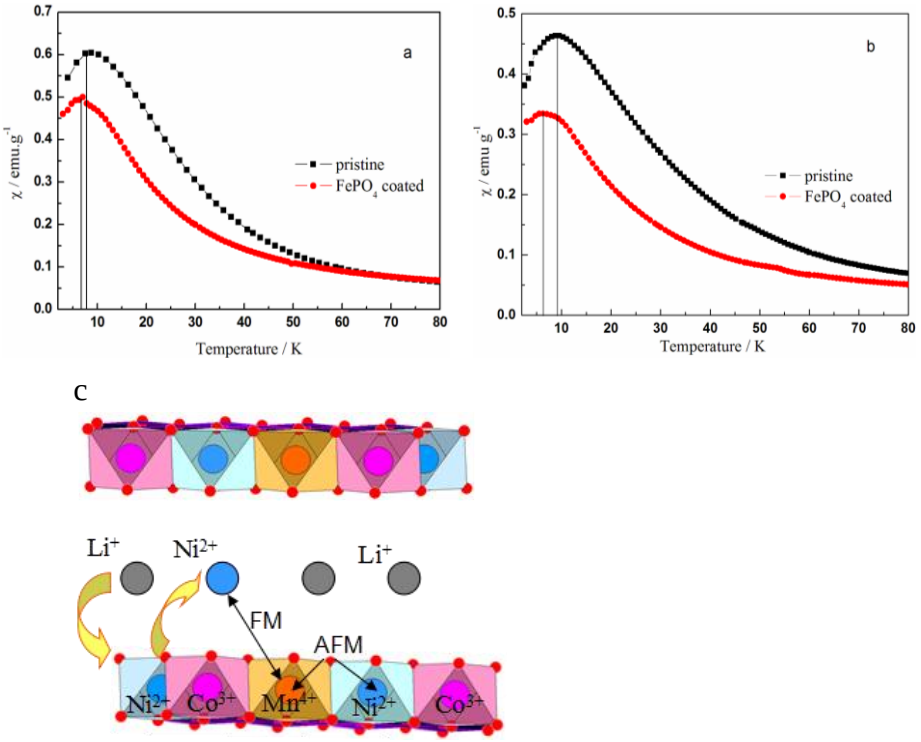

Fig. 5.10. Magnetic susceptibility fresh (a) and cycled (b), schematic of magnetic interactions between Mn^{4+} and Ni^{2+} in different layers (c).

The temperature dependence of the reciprocal magnetic susceptibility of fresh and cycled samples is shown in Fig 5.9a and 5.9b. As described in other's research, at high temperatures range, the layered $Li(NiMnCo)O_2$ series compounds are Curie-Weiss paramagnets [20]. As the temperature down, strengthened interlayer and

intralayer magnetic interactions lead to a deviation from the Curie-Weiss law. In this research, above 130 K, the linear variations of χ_m^{-1} with T were fitted by Curie-Weiss law: $\chi_m^{-1} = (T - \Theta_p)/C_p$, where Θ_p is the Weiss temperature and C_p is the Curie constant. The values of fitting parameters Θ_p are listed in Table 5.1.

Table 5.1. Weiss constants of fresh and cycled samples by fitting the data of Fig. 5.9 with Curie-Weiss equation $\chi_m^{-1}(T) = (T - \Theta_p)/C_p$

130K	NCM333	2Fe	NCM333	2Fe
Θ	-120.9177	-108.4407	-239.6840	-168.7403
Cp	10.6315	11.0840	16.2311	11.1371

The negative value of Θ_p reveals an intrinsic dominate antiferromagnetic interactions. Among the possible magnetic interactions, Mn^{4+}-O-Mn^{4+}, Ni^{2+}-O-Ni^{2+} and Mn^{4+}-O-Ni^{2+} via 90° bonding angles, as shown in Fig. 5.10c, are antiferromagnetic interactions, and the other two are ferromagnetic interactions according to the Kanamori-Goodenough rules [21]. In the studied materials, the large negative Θ_p value indicates that the antiferromagnetic interactions held the dominate positions. From the probability point of view, Mn^{4+}-O-Ni^{2+} accounts for half of the intralayer magnetic interactions if the metal ions are uniformly-distributed in $LiNi_{1/3}Co_{1/3}Mn_{1/3}O_2$ compound. The introduce of non-magnetic Co^{3+} would dilute the magnetic interactions, which has been confirmed by previous research [22]. For the fresh synthesized material, there was no significant difference in Θ_p values between the pristine and coated samples. However, after charge/discharge cycles, the Θ_p of the coated samples was -178.64 K, larger than that of cycled pristine sample (-239.68 K). The surface coating suppressed the decrease of Θ_p value upon charge/discharge cycles. As we know, the increase of Li/Ni disorder directly increases the nonmagnetic Li^+ percentage in the transition metal layer, which would reinforce the antiferromagnetic interactions. After charge/discharge cycles, both the Θ_p values of pristine and coated samples decreased, which originated from the increase of Li/Ni disorder. In this case, the coated sample showed depressed effects on the Li migration

from the lithium layer to the transition metal layer. That is to say, the surface coating can alleviate the interlayer Li^+ migrations during charge/discharge cycles.

The ZFC susceptibilities of the pristine and coated samples show a cusp at lower temperatures, which is a typical spin-glass transition. In layered $Li(NiCoMn)O_2$, the non-magnetic Co^{3+} and trace of Li^+ in transition metal layers can dilute the magnetic interactions and therefore, the formation of large size magnetic clusters are disturbed and a spin-glass behavior is observed as reported in $LiNi_{0.4}Mn_{0.4}Co_{0.1}O_2$ and $LiNi_{0.45}Mn_{0.45}Co_{0.1}O_2$ previously [20,22]. In $LiNi_{1/3}Co_{1/3}Mn_{1/3}O_2$, the increase of non-magnetic Co^{3+} further decreases the magnetic clusters and the blocking temperature. As shown in Fig. 5.10a, the blocking temperatures for pristine and coated $LiNi_{1/3}Co_{1/3}Mn_{1/3}O_2$ are about 7.5 K and 7.0 K, respectively. There was no obvious change of the blocking temperature by $FePO_4$ coating since the total amount of $FePO_4$ is only 2 wt% and the magnetic Fe^{3+} ions is less than 0.7 wt% in the final coated material. For the cycled samples shown in Fig. 5.10b, the cusp appeared at a higher temperature of 9 K for the pristine samples. In contrast, there was no obvious change for the blocking temperature of the coated samples before and after charge/discharge cycles. One of the main reasons for the increase of blocking temperatures of cycled pristine sample can be attributed to the enhanced ferromagnetic interactions. For an ideal atoms arrangement, all of the transition metal cations locate in the transition metal layers and there are only magnetic interactions of Mn^{4+}-O-Ni^{2+}, Mn^{4+}-O-Mn^{4+} and Ni^{2+}-O-Ni^{2+} via 90 ° bonds inside transition metal layers as shown in Fig. 5.10c. The possible migration of Ni^{2+} to the lithium layers can markedly change the M^{n+}-O-M^{n+} bond angles from 90 ° to 180 °. As presented in the last part, the Mn^{4+}-O-Ni^{2+} interactions account for half of the magnetic interactions, which means they govern the overall magnetic behaviors. The magnetic interactions in Mn^{4+}-O-Ni^{2+} are antiferromagnetic via 90 ° bonds but would transfer to ferromagnetic when the bond angles chang to 180 ° according to the Kanamori-Goodenough rules [21]. So, the enhanced ferromagnetic interactions of the cycled pristine samples are from the increase of Mn^{4+}-O-Ni^{2+} ferromagnetic interactions via 180 ° due to the migration of Ni^{2+} to the lithium layer. The unchanged blocking temperature of the

coated sample after cycles demonstrated that there is only few Ni^{2+} migrated to the lithium layer upon charge/discharge cycles, which indicates the Li/Ni disorder upon charge/discharge cycles can be suppressed by surface coating of $FePO_4$ layer.

5.4 Conclusions

Capacity fading mechanism of $LiNi_{1/3}Co_{1/3}Mn_{1/3}O_2$ and performance improvement by surface coating of $FePO_4$, have been investigated. Results in this chapter help us build a clear picture of the performance degradation process with prolonged cycles for the layered cathode $LiNi_{1/3}Co_{1/3}Mn_{1/3}O_2$ as: (1) more and more serious surface polarizations, (2) gradually increase of charge transfer resistance R_{ct}, (3) decrease of Li ion diffusion coefficient, (4) increase of Li/Ni disorder. The surface coating layer directly severed as a protective layer in the interface of electrode/electrolyte, showed positive effects in prohibiting these four tendencies. It is usually considered that the coating layer can suppress the interface polarization and help to decrease the charge transfer resistance R_{ct} caused by side-reactions at the interface. In our research, the coated samples also showed enhanced Li ion diffusion coefficients and increase of Li/Ni disorder arrangement with prolonged cycles, however, it is obvious the surface coating layer can not directly take effects on the inner structure. The provided information made us believe that the deterioration of electrode surface lead to Li/Ni disorder with prolonged cycles. It is a gradually processes from interface to internal atom arrangement, which the deterioration of surface polarization and increase of R_{ct} lead to the decrease of Li ion diffusion coefficients and increase of Li/Ni disorder. Results shown in this study can help researchers understand the capacity fading of $LiNi_{1/3}Co_{1/3}Mn_{1/3}O_2$ and effects of surface coating layer, and to further design of proper coating layer for layered cathode materials for Li ion batteries.

5.5 References

[1] K. T. Lee, S. Jeong, and J. Cho: "Roles of Surface Chemistry on safety and Electrochemistry in Lithium Ion Batteries", *Accounts of Chem. Res.*, Vol. 46(5), pp. 1161-1170, 2013

[2] S. T. Myung, K.Amine and Y. K. Sun: "Surface modification of cathode materials from nano- to microscale for rechargeable lithium-ion batteries", *J. Mater. Chem.*, Vol. 20, pp. 7074-7095, 2010

[3] Z. H. Chen, Y. Qin, K. Amine and Y. K. Sun: "Role of surface coating on cathode materials for lithium-ion batteries", *J. Mater. Chem.*, Vol. 20, pp. 7606-7612, 2010

[4] X. Z. Liu, P, He, H. Q. Li, M. Ishida, and H. S. Zhou: "Improvement of electrochemical properties of $LiNi_{1/3}Co_{1/3}Mn_{1/3}O_2$ by coating with V_2O_5 layer", *J. Alloys. Com.*, Vol. 552, pp. 76-82, 2013

[5] X. Z. Liu, H. Q. Li, D. Li, M. Ishida, and H. S. Zhou: "PEDOT modified $LiNi_{1/3}Co_{1/3}Mn_{1/3}O_2$ with enhanced electrochemical performance for lithium ion batteries", *J. Power Source*, Vol. 243, pp. 374-380, 2013

[6] X. Z. Liu, H. Q. Li, E. J. Yoo, M. Ishida, and H. S. Zhou: "Fabrication of $FePO_4$ layer coated $LiNi_{1/3}Co_{1/3}Mn_{1/3}O_2$: Towards high-performance cathode materials for lithium ion batteries", *Electrochimica Acta*, Vol. 83, pp. 253-258, 2012

[7] K. M. Shaju, G. V. Subba Rao, and B. V. R. Chowdari: "Influence of Li-ion kinetics in the cathodic performance of layered $LiNi_{1/3}Co_{1/3}Mn_{1/3}O_2$", *J. Electrochem. Soc.*, Vol. 151 (9), pp. A1324-A1332, 2004

[8] X. Y. Zhang, W. J. Jiang, A. Mauger, Q. Lu, F. Gendron, and C. M. Julien: "Minimization of the cation mixing in $Li_{1+x}(NMC)_{1-x}O_2$ as cathode material", *J. Power Source*, Vol. 195, pp. 1292-1301, 2010

[9] A. M. A. Hashem, A. E. Abdel-Ghany, A. E. Eid, J. Trottier, K. Zaghib, A. Mauger, and C. M. Julien: "Study of the surface modification of $LiNi_{1/3}Co_{1/3}Mn_{1/3}O_2$ cathode material for lithium ion battery", *J. Power Source*, Vol. 196, pp. 8632-8637, 2011

[10] X. Y. Zhang, A. Mauger, Q. Lu, H. Groult, L. Perrigaud, F. Gendron, and C. M. Julien: "Synthesis and characterization of $LiNi_{1/3}Co_{1/3}Mn_{1/3}O_2$ by wet-chemical

method", *Electrochimica Acta*, Vol. 55, pp. 6440-6449, 2010

[11] Y. Mizuno, M. Okubo, D. Asakura, T. Saito, E. Hosono, Y. Saito, K. Ohishi, T. Kudo and H. S. Zhou: "Impedance spectroscopic study on interfacial ion transfers in cyanide-bridged coordination polymer electrode with organic electrolyte", *Electrochim. Acta.*, Vol. 63, pp. 139-145, 2012

[12] Y. Cho, P. Oh, and J. Cho: "A New Type of Protective Surface Layer for High-Capacity Ni-Based Cathode Materials: Nanoscaled Surface Pillaring Layer", *Nano letter*, Vol. 13, pp. 1145-1152, 2013

[13] X. F. Bie, F. Du, Y. H. Wang, K. Zhu, H. Ehrenberg, K. Nikolowski, C.Z. Wang, G. Chen and Y. J. Wei: "Relationships between the crystal/interfacial properties and electrochemical performance of $LiNi_{1/3}Co_{1/3}Mn_{1/3}O_2$ in the voltage window of 2.5-4.6 V", *Electrochimica Acta*, Vol. 97, pp. 357-363, 2013

[14] K. M. Shaju, G. V. S. Rao and B. V. R. Chowdari: "Li ion kinetic studies on spinel cathodes, $Li(M_{1/6}Mn_{11/6})O_4$ (M = Mn, Co, CoAl) by GITT and EIS", *J. Mater. Chem.*, Vol. 13, pp. 106-113, 2003

[15] L. A. Riley, A. V. Atta, A. S. Cavanagh, Y. Yan, S. M. George, P. Liu, A. C. Dillon and S. H. Lee: "Electrochemical effects of ALD surface modification on combustion synthesized $LiNi_{1/3}Co_{1/3}Mn_{1/3}O_2$ as a layered-cathode material", *J. Power Source*, Vol. 196, pp. 3317-3324, 2011

[16] W. Weppner, and R. A. Huggins: "Determination of Kinetic-Parameters of Mixed-Conducting Electrodes and Application to System Li3Sb", *J. Electrochem. Soc.*, Vol. 124 (10), pp. 1569-1578, 1977

[17] J. S. Hong, and J. R. Selman: "Relationship between calorimetric and structural characteristics of lithium-ion cells II. Determination of Li transport properties", *J. Electrochem. Soc.*, Vol. 147 (9), pp. 3190-3194, 2000

[18] A. A. Ghany, K. Zaghib, F. Gendron, A. Mauger and C. M. Julien: "Structural,magnetic and electrochemical properties of $LiNi_{0.5}Mn_{0.5}O_2$ as positive electrode for Li-ion batteries", *Electrochimica Acta*, Vol. 52, pp. 4092-4100, 2007

[19] H. J. Yu, Y. M. Qian, M. Otani, D. M. Tang, S. H. Guo, Y. B. Zhu and H. S. Zhou: "Studies of the Lithium/Nickel Ions Exchange in the Layered

$LiNi_{0.42}Mn_{0.42}Co_{0.16}O_2$ Cathode Material for Lithium Ion Batteries: Experimental and First-Principles Calculations", *Energy Envir. Sci.*, DOI: 10.1039/C3EE42398K, 2013

[20] J. Xiao, N. A. Chernova and M. S. Whittingham: "Layered Mixed Transition Metal Oxide Cathodes with Reduced Cobalt Content for Lithium Ion Batteries", *Chem.Mater.*, Vol. 20, pp. 7454-7464, 2008

[21] J.B.Goodenough, : "*Magnetism and the Chemical bond*", Wiely, New York, 1963.

[22] N. A. Chernova, M. Ma, J. Xiao, M. S. Whittingham, J. Breger and C. P. Grey: "Layered $Li_xNi_yMn_yCo_{1-2y}O_2$ cathodes for lithium ion batteries: Understanding local structure via magnetic properties", *Chem. Mater.*, Vol. 19, pp. 4682-4693, 2007

Chapter 6 Conclusions

The main goal of this PhD work was to investigate the electrochemical performance improvement of layered cathode $LiNi_{1/3}Co_{1/3}Mn_{1/3}O_2$ by surface coating, and study the mechanism of performance improvement. Three typical materials V_2O_5, PEDOT and $FePO_4$ have been investigated as coating layer, coating conditions such as coating amount and sintered temperature can profoundly affect the coating effects. Furthermore, we have endeavoured to provide an insight into understanding performance degradation of $LiNi_{1/3}Co_{1/3}Mn_{1/3}O_2$ and how to choose and synthesize a proper surface coating layer for $LiNi_{1/3}Co_{1/3}Mn_{1/3}O_2$. It is appropriate to draw the conclusions as following:

In chapter 2, we studied V_2O_5 as coating layer to enhance the electrochemical performance of $LiNi_{1/3}Co_{1/3}Mn_{1/3}O_2$. Materials characterizations such as SEM, TEM, and EDS confirmed V_2O_5 has been uniformly coated on the surface of $LiNi_{1/3}Co_{1/3}Mn_{1/3}O_2$, but the layered structure experienced no changes by surface coating. The XPS results demonstrated that the over 90% V in the coating layer maintained the valence of +5. The optimal coating amount is 3wt% in terms of the cycle and rate capability. The discharge capacities retention have been improved from 59.2% to 83.2% by 3wt% V_2O_5-coating (at a charge/discharge current of 300 mA/g). The improved performance was attributed to the suppression of side-reactions between the electrode and electrolyte and the increase of charge-transfer resistance by V_2O_5 coating layer. However, the dissolution of V from the charged V_2O_5-coated samples limited its long time storage at the charged state.

In chapter 3, organic polymer PEDOT have been investigated as coating layer. The optimized coating conditions is with a coating amount of 2wt% and heat treated at 300 ℃. The PEDOT coating layer was confirmed by SEM, TEM and IR. The rate capacity have been significant improved from 41.8 mA/g to 73.9 mAh/g at a charge-discharge current of 1500 mA/g. The main reason for the improved performance of PEDOT-coated $LiNi_{1/3}Co_{1/3}Mn_{1/3}O_2$ could be attributed to the conductive polymer layer promote the mass transfer at the interface of electrode and

electrolyte which alleviate the surface polarization.

In chapter 4, polyanions compound $FePO_4$ was studied as coating layer. The optimized coating amount is 2 wt% and post heat treated at 400 ℃. The uniformly surface coating of $FePO_4$ can be confirmed by TEM and EDS. The capacity stability have been significantly strengthened and the capacity retention is 87.7% after 100 cycles compared with 62.0% of the pristine material (at a current of 150 mA/g). This capacity retention is better than other two coating materials. The special advantages of $FePO_4$ coating layer owing to that the strong P=O bond and covalency between the PO_4 polyanions and Fe^{3+} which obviously improved the surface stability.

In chapter 5, we further discussed the capacity fading mechanism of $LiNi_{1/3}Co_{1/3}Mn_{1/3}O_2$ and performance improvement by surface coating of $FePO_4$. A clearly picture of performance degradation of $LiNi_{1/3}Co_{1/3}Mn_{1/3}O_2$ with prolonged cycles was built as: (1) more and more serious surface polarizations, (2) gradually increase of charge transfer resistance R_{ct}, (3) decrease of Li ion diffusion coefficient, (4) increase of Li/Ni disorder. The $FePO_4$ coating layer at the electrode surface showed positive effects in prohibiting these four tendencies. It does not only suppress the interface polarization and decrease the charge transfer resistance R_{ct} caused by side-reactions at the interface, but also enhanced the Li ion diffusion coefficients and increase of Li/Ni disorder arrangement with prolonged cycles. The provided information made us believe that the performance degradation of layered cathode is gradually changed from the surface to the internal structure.

In general, fundamental results and data shown in this study can help researchers further understand the capacity fading of $LiNi_{1/3}Co_{1/3}Mn_{1/3}O_2$ and effects of surface coating layer, and to further design of proper coating layer for layered cathode materials for Li ion batteries. For layered cathode materials, the stability of coating layer should be taken precedence of all others.

Appendix

1. Comprehensive understanding the advantages and disadvantages of the three kinds of coating materials.

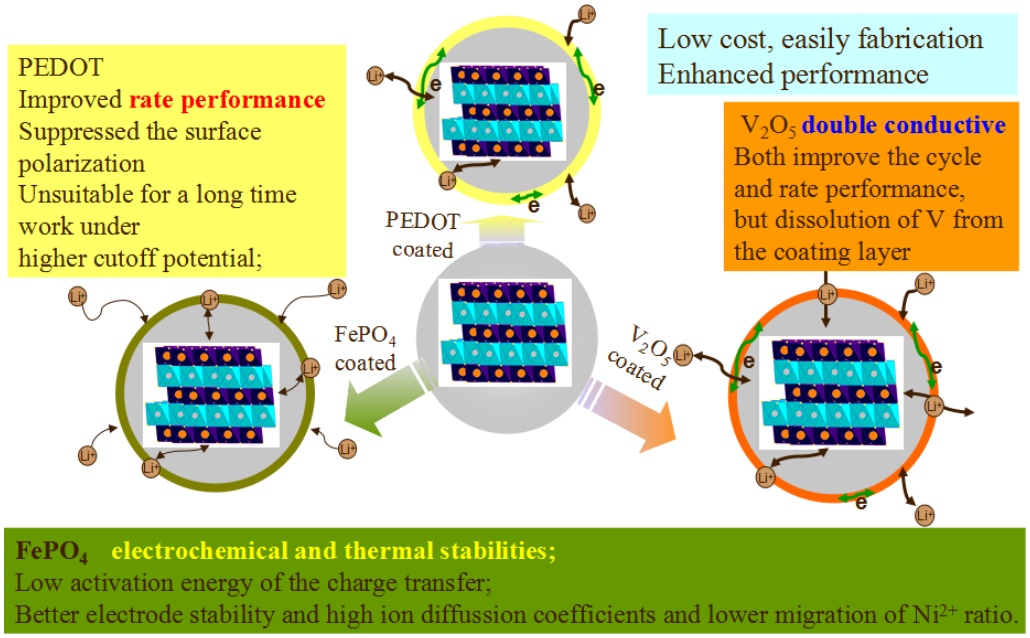

2. Schematic of performance degradation mechanism for pristine $LiNi_{1/3}Co_{1/3}Mn_{1/3}O_2$. The gradually evolution was from the surface to the internal structure.

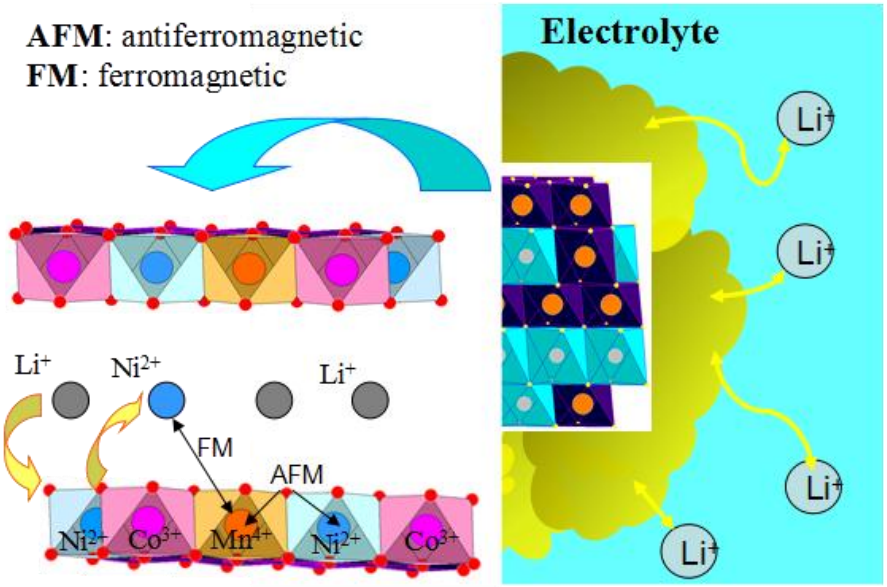

List of Research Results

JOURNAL PAPER

First-author

[1] Xizheng Liu, Huiqiao Li, Eunjoo Yoo, Masayoshi Ishida, Haoshen Zhou, "Fabrication of $FePO_4$ layer coated $LiNi_{1/3}Co_{1/3}Mn_{1/3}O_2$: Towards high-performance cathode materials for lithium ion batteries" *Electrochimica Acta*, Vol. 83, pp. 253-258, Nov. 2012

[2] Xizheng Liu, Ping He, Huiqiao Li, Masayoshi Ishida, Haoshen Zhou, "Improvement of electrochemical properties of $LiNi_{1/3}Co_{1/3}Mn_{1/3}O_2$ by coating with V_2O_5 layer" *Journal of Alloys and Compounds*, Vol. 552, pp. 76-82, Mar. 2013,

[3] Xizheng Liu, Huiqiao Li, De Li, Masayoshi Ishida, Haoshen Zhou, "PEDOT modified $LiNi_{1/3}Co_{1/3}Mn_{1/3}O_2$ with enhanced electrochemical performance for lithium ion batteries" *Journal of Power Sources*, Vol. 243, pp. 374-380, Dec. 2013

Co-authored

[1] Yu Zhao, Xizheng Liu, Huiqiao Li, Tianyou Zhai and Haoshen Zhou, "Hierarchical micro/nano porous silicon Li-ion battery anodes" *Chem. Commun.*, Vol. 48, pp. 5079-5081, 2012

[2] Huiqiao Li, Xizheng Liu, Tianyou Zhai, De Li and Haoshen Zhou, "Li_3VO_4: A Promising Insertion Anode Material for Lithium-Ion Batteries" *Adv. Energy Mater.*, Vol. 3, pp. 428–432, 2013

[3] De Li, Tao Zhang, Xizheng Liu, Ping He, Ruwen Peng, Mu Wang, Min Han, Haoshen Zhou, "A hybrid phase-transition model of olivine $LiFePO_4$ for the charge and discharge processes" *J Power Sources*, Vol. 233, pp. 299-303, 2013

[4] Yuchao Wang, Fengyan Li, Lin Xu, Ning Jiang and Xizheng Liu, "Multidimensional crystal frameworks based on heteropoly blue building block of $[SiW_{10}MoV_2O_{40}]^{6-}$: synthesis, structures and magnetic properties" *Dalton Trans.*, Vol. 42, pp. 5839-5847, 2013

[5] Yuchao Wang, Lin Xu, Ning, Jiang, Lili Zhao, Fengyan Li, Xizheng Liu, "Multidimensional frameworks constructed from Keggin-type heteropoly blue of

molybdenum–tungsten cluster" *Cryst Eng Comm.*, Vol. 13, pp. 410-413, 2011

[6] Bo Bi, Lin Xu, Bingbing Xu, Xizheng Liu, "Heteropoly blue-intercalated layered double hydroxides for cationic dye removal from aqueous media" *Applied Clay Sci.*, Vol. 54, pp. 242-247, 2011

PRESENTATIONS:

[1] 劉　喜正, 石田　政義, 周　豪慎, "Improvement of Electrochemical properties of $LiNi_{1/3}Co_{1/3}Mn_{1/3}O_2$ by coating with $FePO_4$ layer", つくば, 2013 年, 03 月, A-1(oral)

[2] Xizheng Liu, Masayoshi Ishida, Haoshen Zhou, "Improvement of high rate properties of $LiNi_{1/3}Co_{1/3}Mn_{1/3}O_2$ by coating with V_2O_5 layer", 電気化学第 79 回大会, 浜松, 2012 年, 03 月, 29 日-31 日, 1D10 (oral)

[3] Xizheng Liu, Eunjoo Yoo, Masayoshi Ishida, Haoshen Zhou, "$FePO_4$ coated $LiNi_{1/3}Co_{1/3}Mn_{1/3}O_2$ cathode enhanced electrochemical properties for lithium ion batteries" 16th International Meeting on Lithium Batteries, ICC Jeju, Korea, June 17-22, 2012, P2-243, (poster)

[4] 劉　喜正, 李　会巧, 劉　銀珠, 石田　政義, 周　豪慎, "$LiNi_{1/3}Co_{1/3}Mn_{1/3}O_2$への$FePO_4$被覆による電池特性" 第53回電池討論会, 福岡, 2012 年, 11 月, 14 日-16 日, 1B16 (oral)

[5] 劉　喜正, 石田　政義, 周　豪慎, "リチウムイオン電池用三元系正極の表面被覆による電気化学特性"　第 8 回新エネルギーシンポジウム, つくば,2013 年, 03 月, B-1 (oral)

[6] 劉　喜正, 李　徳, 石田　政義, 周　豪慎, "導電性ポリマーによって表面改質された $LiNi_{1/3}Co_{1/3}Mn_{1/3}O_2$ の電池特性" 電気化学第 80 回大会, 仙台, 2013 年, 03 月, 29 日-31 日, 1A17 (oral)

[7] Xizheng Liu, Ping He, Huiqiao Li, Masayoshi Ishida and Haoshen Zhou, "Electrochemical properties of V_2O_5 coated $LiNi_{1/3}Co_{1/3}Mn_{1/3}O_2$ as cathode material for lithium ion battery" The 19th international conference on solid state ionics, Kyoto Japan, June 2-7, 2013, Mon-D-030(poster)

Acknowledgements

It is the end of my student life, it is just the beginning.....

At this special moment, I would like to say thanks to those kindly people who have give me so much help on my way.

First of all, I would like to say great thanks to my supervisors, Prof. Masayoshi Ishida (University of Tsukuba) and Prof. Haoshen Zhou (AIST), for providing me an opportunity to pursue Ph.D. at University of Tsukuba, conduct my Ph.D. research at AIST. Without Prof. Ishida's fruitful supervision and solicitous care, I cannot integration and adapt to the study and daily life so smoothly in Japan. The breaking though ideas and valuable guidance from Prof. Zhou throughout my Ph.D. work, are essential to make this dissertation possible. The flexible work environment, his kind and encouraging words, always kept my spirits high and allowed me go and do the research, no matter the results were good or bad. During this three years and a half, I learned more in wandering the cross disciplines between materials science and electric systems.

I also would like to thank my vice-supervisors Prof. Nishioka, Assistant Prof. Hanada, and Assistant Prof. Nakayama for their helpful discussions and knowledgeable inputs. From them, I know that the ability of expression is equally important as the research results. I learned how to tell a 'story'.

I want to thank the Japanese Government for the financial support (Monbusho Scholarship) during the doctoral course.

I would like to thank Dr. Tianyou Zhai and Dr. Xi Wang for their kindly help on TEM measurements and useful discussions.

I wish to express my thanks to all of my group members (all members and OB) in Energy Conversion Lab (Ishida Ken at University of Tsukuba). Thank to Dr. M. Ishikawa, Dr. Z. Zhou, Dr. C. Hwang, Dr. Y. Saito, Mr. S. Guo, Miss L. Duan, Ms. N. Thu Thi Hoai, Mr. K. Abe, Mr. S. Kitagawa, Mr. F. Yosua et al. The time spent with them while working in lab, in trips and in every parties were very fun, and will be my beautiful memories forever. They let me closer to the real Japan and Japanese student

life.

Special gratitude goes to all the group members in Energy Interface Technology Group at AIST whose support in various capacities ensured the completion of my Ph.D. research. I am grateful to Dr. Huiqiao Li and Dr. P. He for their kindly help. They taught me how to fabricate a battery, how to revise the paper from I was know nothing about lithium ion battery. Thank to Dr. E. Yoo, for her kindly help about how to give a presentation in Japanese. Thank to Dr. M. Okubo, one year group study lead by him, let me get a solid knowledge foundation of electrochemistry. Thank to Dr. E. Hosono, Dr. H. Kitaura, Mr. J. Okagaki for their kindly help in daily research.

I also would like to express my appreciation to Dr. Haijun Yu, Dr. De Li, and Dr. Yu Zhao. It is my fortunate to join in group and take the research with you together for more than three years. Discussions, trips and parties, especially the togetherness during the violent earthquake in 3.11 2011..... All by all, is and will be in my memory. Thank to Dr. Y. Wang, Dr. T. Zhang, Dr. Z. Song, Dr. F. Li, Dr. Y. Wang, Dr. N. Li, Dr. K. Liao et al, for their kindly help in my daily research and life.

I would also like to thank all of my friends in Preparatory School for Chinese Students to Japan (Mr. L. Liu, Mr. R. Tao, Dr. H. Zhu, Mr. M. Luan, Mr. L. Wang, Mr. F. Yan, Mr. T. Ma et al) and University of Tsukuba (Mr. J. Zhang, Ms. Y. Zhao, Miss Z. Luo, Mr. L. Zhang, Miss J. Li) who give me so much fun during this three and half years in Japan. With you, I no longer feel lonely. Special thanks to Mr. H. Yuan, although you will never see these words, you are my most trusted friend in University of Tsukuba forever.

Finally, my deepest gratitude goes to my father Guoliang Liu, my mother Honghua Liu, my old sister Jundong Liu, and my wife Pingli Wu. Their never ending love and affection provide me strength and keep me strong to surpass all the hurdles. I will keep going on and do my best, I love you forever.